Molecular mechanics investigation of the transport mechanisms in the ClC-ec1 H^+/Cl^- exchanger and P-glycoprotein/Sav1866 ABC transporter

Inauguraldissertation
zur
Erlangung der Würde eines Doktors der Philosophie
vorgelegt der
Philosophisch-Naturwissenschaftlichen Fakultät
der Universität Basel

von

Yanyan Xu
von China

Basel, 2014

Genehmigt von der Philosophisch-Naturwissenschaftlichen Fakultät

Auf Antrag von

Torsten Schwede, Simon Bernèche, Anna Seelig

Basel, Sept. 16th, 2014

Prof. Dr. Jörg Schibler
The Dean of Faculty

Acknowledgement

It was a great experience to do my Ph.D here, in Bernèche group, in Biozentrum, in University of Basel, in Basel, in Switzerland, in Europe.

First I would like to thank my supervisor Professor Simon Bernèche. I feel very lucky to have him as my supervisor. He gave me a lot of freedom and always trusted me in my work as well as other things. He was always patient to explain to me concepts and ideas even to the details. Anytime I got anxious and confused about my work, he was always there to tell me with his gentle smile that everything so far is good and provide me with his opinions about the key issues at the moment and the ways to move on. When I have difficulty in coordinating my work and feelings in life, he shared with me his similar experience, which made me feel understood and supported.

I also would like to send my thanks to Professor Anna Seelig amd Timm Maier, who are in my Ph.D committee. Professor Anna Seelig, as one of our collaborators, was always enthusiastic about my data and initiated lots of discussion, motivating me in the Pgp/Sav project. Professor Timm Maier gave me detailed answers to my questions about structures and checked the publications himself to offer me advises about my work.

As our collaborators, Alessio Accardi and Daniel Basilio helped me a lot by discussion in driving the ClC-ec1 project. Meanwhile, the discussion with Professor Henning Stahlberg and Priyanka Abeyrathne improved my insights a lot on the ClC-ec1 system.

My colleagues were quite helpful. When I turned to them for help, they always stopped the stuff on hand and tried to help me immediately. Niklaus Johner and Florian Heer helped me a lot in familiarizing the basic techniques and working environment at the beginning. Wojtek helped me a lot in using iPMF as well as any other technical stuffs. Sefer Baday was always calm and told me patiently the solution to the details. Oliver was always happy to listen to me and learn about my work. Chungwen and I had a lot of discussion regarding the ClC-ec1 project, which drove me to think more deeply. Colleagues in other groups and IT guys were also very supportive and I am very grateful to all of them although they are not listed here. To point out, I used OPENSTRUCTURE to do structural analysis, in which I got a lot of support from people in Schwede group, especially Marco Biasini.

Of course, I would like to thank my parents and relatives, who were always there to support me especially when I was not in shape. I should also attribute my achievement to my good friends Shuo Wang, Ruifeng Zhou, Andrius Maslekovas, Shasha Yang, Langyu Gu, etc. They inspired me and supported me. Without them, I would not be as smart and optimistic as I am now ;-)

In a word, I love all the experience in the past four years. It would be very difficult to erase them from my memory...

Abstract

Although channels and transporters were thought to display completely different transport mechanisms, new findings have revealed that the boundaries between them might be more blurred. ABC family, which includes thousands of transporters, holds a channel member, CFTR (cystic fibrosis transmembrane conductance regulator). ClC-ec1, which was considered as a chloride ion channel as other members of the ClC family, was found to function as a Cl^-/H^+ exchanger. Since the proteins within the family have similar sequences and structures, it suggests that some small structural difference is enough to underlie the very different functions of channels and transporters. In order to identify this small but important difference and further understand mechanisms of channels and transporters, members from these two families were investigated by molecular dynamic simulations, P-glycoprotein/Sav1866 from ABC family and ClC-ec1 from ClC family.

In the investigation of P-glycoprotein/Sav1866 systems, unambiguous conformational changes in trans-membrane domains were demonstrated for the first time, which involve rotation of helices that potentially contributes to allocrites transport. Nucleotide-binding domains experience small changes in which the two domains never completely dissociate. Asymmetric nucleotide occupancy states were accompanied by an opening of the trans-membrane domain, while no cavity was seen in symmetric nucleotide occupancy states. Q-loop and X-loop were identified to be two essential motifs in the coupling between trans-membrane domains and nucleotide binding domains.

In ClC-ec1, an open intracellular gate was demonstrated for the first time and identified to be essential for ion permeation. It was further found that the interaction between Y445 and I402 at helix O, controlled by the conformation of helix O, is related to the opening of the intracellular gate. Furthermore, conformational changes of F357 were identified to be also essential for chloride ion permeation. Two conformations of F357 are correlated with inward facing and outward facing conformations of ClC-ec1, which constitute the alternating mechanism of chloride ion transport. The conformation of F357 is correlated to ion occupancy in the pore as well as the conformation of E148. The transport of ClC-ec1 was proposed to take a modified alternating mechanism, in which the protein transports chloride ions by alternating between the outward facing and inward facing conformations, while the binding of chloride ion in the pore triggers proton transport.

Contents

Figures

1 Introduction:

1.1 Blurred boundary between channels and transporters

1.1.1 Importance of channels and transporters

As we meet more and more living problems without keeping a balance with nature, a cell, as the unit of life, will also fail to work if its exchange of substances with the environment becomes problematic. In order to make sure of a proper environment a cell needs to survive, a healthy cell has a redundant system to protect itself while communicating with outer environment. These systems are notably composed of channels and transporters, which are responsible for the transport of small molecules in and out of the cell to meet different requirements, including the uptake of nutrients, elimination of waste products, protein secretion, energy generation and movement of signaling molecules.

These systems allow both bacteria and human to survive in the same world. Sometimes bacteria infect us and cause some diseases. We feel that we need to kill bacteria in order to cure these diseases and hence we started to design drugs. However, using transporters, bacteria could keep the drugs out of their cells, rendering drugs useless. Meanwhile, due to the malfunction of these systems in our bodies, we will be sick as well, suffering disease such as ion channel disease. Therefore, we become more and more curious about these systems and would like to know how these systems help us as well as bacteria.

1.1.2 General mechanisms and distinctions of channels and transporters

1.1.2.1 General mechanisms

Membrane transport mechanisms have been classified thermodynamically based on their ability to mediate either passive transport or active transport.

Passive transport moves a solute across the membrane from a side of high electrochemical potential to the other side that is of low electrochemical potential. Two types of membrane proteins, carrier proteins and channel proteins, transport substrates across the membrane passively. Carrier proteins transport substrates by undergoing conformational changes, which are induced by substrate binding on one side, exposing the substrate to the other side of the membrane. Alternatively, channel proteins contain an aqueous pore that allows diffusion of substrates down their gradient, which is much faster than carrier proteins, reaching rates of 10^6 and higher for ion channels.

Nevertheless, both passive processes dissipate the electrochemical gradient across the membrane built up by the action of an active transporter that coverts one form of energy to another. Contrary to passive transport mechanisms, an active transporter molecule can pump ions across the membrane against the electrochemical gradient with lower rates (10^3 ion/s). To do so, an input of free energy is required. For some transport molecules, such as Na^+-K^+-ATPase or

members of the ABC transporter family, ATP is hydrolyzed during the transport cycle and the energy harvested from ATP hydrolysis is used to do the work. Since the energy comes directly from ATP, this type of transport mechanism is called "primary active transport". Another class of transport proteins mediates a net transfer of one solute against its electrochemical gradient by using the energy derived from the electrochemical gradient of another solute and it is called "secondary active transport".

Two projects in this thesis involve primary active transport and secondary active transport separately. The proteins investigated, P-glycoprotein (primary active transport) and ClC-ec1 (secondary active transport), belongs to ABC (ATP-binding cassette) family and ClC family respectively, which are introduced in the following sections.

1.1.2.2 Distinction between channels and transporters

Although passive and active transport are defined thermodynamically, such definitions have an implication for the structure of the substrate-transport pathway. While an ion channel requires a water-filled pore for ion diffusion, such a pore is not allowed in an active transporter, because in that case, the substrate could move down its electrochemical gradient.

The successful operation of transporters requires elimination of short-circuits. In other words, given that an open pore would transport substrates much faster downhill than a transporter that works uphill, such leakage of accumulated substrates should be prevented. Otherwise, even just for a fleeting moment, it could quickly undo the transporter's hard work, rendering a transporter useless.

To prevent leakage, transporters should not allow the simultaneous opening of their gates. Given that many channels have more than one gate, the key difference between channels and transporters actually lies on the timing of the closure of the first gate with respect to the opening of the second gate, i.e. the coupling of the two gates. If the timing were not well controlled in transporters, leaving both gates simultaneously open, it would allow channel-like dissipative flow. Therefore, transporters usually experience an occluded state in which both gates are closed to occlude substrates, before the second gate opens to release them (Gadsby 2009).

1.1.3 Blurred boundary between Channels and transporters

Although the distinction between channels and transporters was thought to be clearly defined by the relative timing of the two gates, new findings have revealed that the boundaries between them might be more blurred than expected.

ClC-ec1, which was considered as chloride ion channels as other members in ClC family, was found to function as a Cl^-/H^+ transporter (Accardi, & Miller 2004). Similarly, ABC family, which includes thousands of transporters, holds a channel member, CFTR (cystic fibrosis transmembrane conductance regulator) (Riordan et al 1989). Since the proteins in the same family take similar sequences and structures, it seems that some small structural difference is enough to determine the very different functions of channels and transporters.

Though this is not addressed directly in this thesis, there are examples of proteins behaving both as channels and transporters. In vertebrate glutamate transporters and in their purified, reconstituted, prokaryotic homologues, Na-dependent transport is accompanied by a thermodynamically uncoupled electro-diffusive flow of chloride ions, which is not required for substrate transport. (Tzingounis, & Wadiche 2007; Fairman et al 1995; Wadiche, & Kavanaugh 1998; Vandenberg et al 2008; Ryan, & Mindell 2007)

As the coupling of the two gates is the key difference between channels and transporters, by intuition, the disruption of the coupling could convert a transporter into a channel. And this occurs in reality. The sophisticated marine toxin, palytoxin, binds specifically to extracellularly-exposed parts of the sodium-potassium transporter and thereby disrupts the tight communication between the gates, allowing both to sometimes be open at the same time, transforming the transporter into a cation channel (Redondo et al 1996; Scheiner-Bobis et al 1994; Hirsh, & Wu 1997).

1.2 ABC family

1.2.1 Distribution and classification

1.2.1.1 ABC family is a large family that exists in all kingdom of life.

ABC family is a large protein family present in organisms from all kingdoms of life, which couples hydrolysis of ATP to translocation of substrates across cellular membranes. In *E. coli*, ABC family constitute the largest protein family, including around 80 distinct systems that represent 5% of the genome {Linton 1998}, whereas 49 ABC proteins are present in humans (Dean et al 2001).

ABC proteins function as either importers, which bring nutrients and other molecules into cells, or as exporters, which pump toxins, drugs and lipids across membranes. Exporters are found in both eukaryotes and prokaryotes, importers seem to be present exclusively in prokaryotic organisms.

1.2.1.2 ABC proteins and human

ABC proteins play a plethora of important roles in different organs and tissues of human beings. Mutations of 17 human ABC protein genes underlie many genetic disorders, including Tangier disease (cardiovascular, ABCA1), persistent hyperinsulinemic hypoglycemia of infancy (pancreas, SUR1), Stargardt disease (eye, ABCA4), Wegener's granulomatosis (immune system, TAP), cystic fibrosis (lung and gut, CFTR) and Dubin-Johnson syndrome (liver, MRP2). Other ABC proteins protect cells from cytotoxins and can confer resistance to antibiotics, antifungals, and herbicides and, in man, anticancer drugs. Some important ABC proteins have been intensively studied, and are introduced here.

ABCB1 (P-glycoprotein, MDR1, Pgp) is the first identified eukaryotic ABC transporter, which involves multidrug resistance to cancer cells and lipid transport.

MsbA, a protein from *E. Coli* inner membrane, is an essential ABC protein in prokaryotes, conserved in all bacteria (Chang 2003). MsbA plays an important role in the transport of lipid A from the inner to the outer membrane of Gram-

negative bacteria. Lipid A, a hexa-acylated disaccharide of glucosamine unique to Gram-negative bacteria, is a major component of the outer membrane, representing the hydrophobic anchor of lipopolysaccharides on the outside of the outer membrane. When MsbA fails to function, lipid A and phospholipids in the inner membrane will be accumulated, which is lethal to *E. Coli* (Doerrler et al 2001; Zhou et al 1998) .

The chloride channel activity of cystic fibrosis transmembrane conductance regulator (CFTR) protein in the lung helps to protect from bacterial infections by maintaining hydration of the mucus layers lining the airways. The lack of chloride channel activity in cystic fibrosis patients leads to mucosal obstruction of a variety of ducts within organs such as the pancreas, liver, sweat glands, salivary glands and lungs. In particular, many cystic fibrosis patients have thick tenacious secretions in the lungs that obstruct distal airways and submucosal glands. These patients have chronic lung infections that cause a decline in respiratory function and eventual lung failure.

1.2.1.3 Classification of human ABC proteins

The 49 human ABC proteins have been divided into subfamilies depending on the arrangement of the domains and sequence homology in the NBD (nucleotide binding domains) and TMDs (trans-membrane domains) (Dean et al 2001; Klein et al 1999). The proteins from other organisms could be classified accordingly to these families with the same standards. Figure 1-1 (Loo, & Clarke 2008) shows the organization of the various domains and the number of human members in each superfamily.

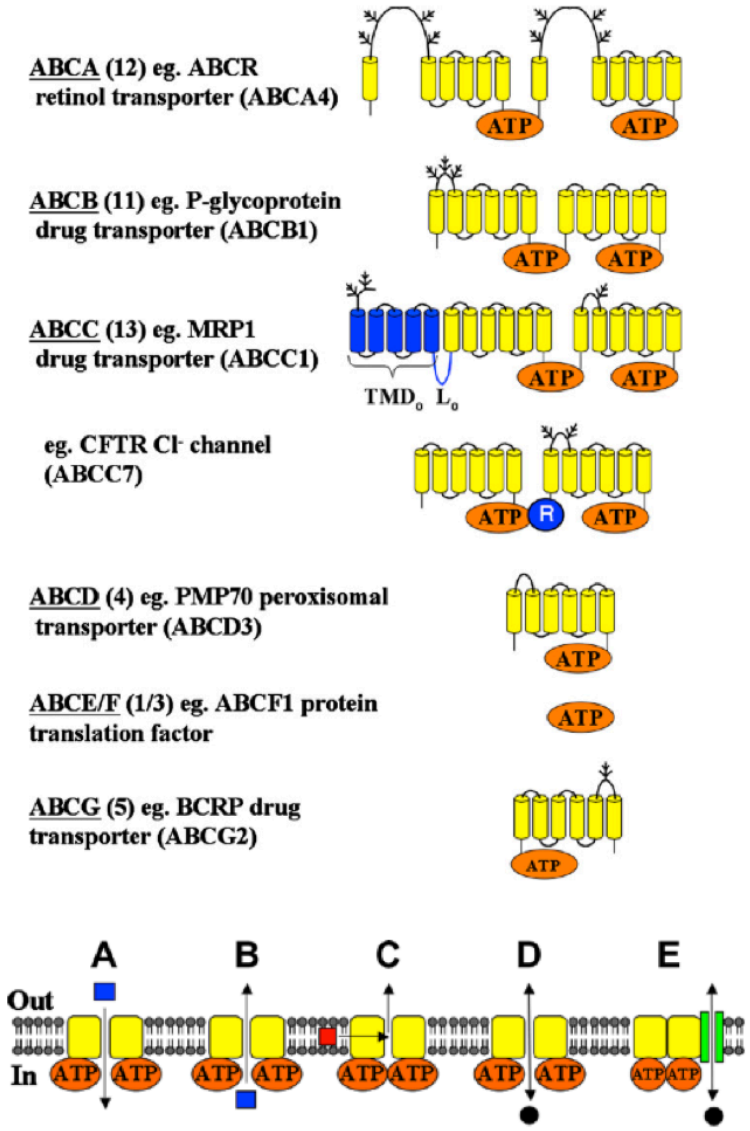

Figure 1-1: ATP-binding cassette(ABC) subfamilies

TMD: yellow, as well as blue cylinder in ABCC1; NBD: orange (Loo, & Clarke 2008).

Although protein members from the same subfamily are quite similar in sequence and structure, their function could be quite different due to small sequence variations. For example, Pgp (ABCB1, MDR1) has a surprisingly broad spectrum of amphiphilic substrates (Ford, & Hait 1990), while its family member ABCB4, which share 75% of its amino acid sequence (Klein et al 1999), is highly substrate specific, exclusively transporting PC (phosphatidylcholine) (van Helvoort et al 1996). In addition, MDR2 is about 80% identical to Pgp but functions as a PC transporter. The critical changes in the MDR1/MDR2 chimera were due to only 4 residues in the first cytopasmic loop. This is consistent to the fact that channels and transporters could belong to the same protein family.

1.2.2 ABC Structure architecture and function

1.2.2.1 Similarity and difference of ABC structure among different subfamilies

As illustrated in Figure 1-1, most ABC proteins comprise four core domains: two transmembrane domains (TMDs), which vary considerably between different ABC proteins, and two highly-conserved nucleotide-binding domains (NBDs) located at the cytosolic surface of the plasma membrane. Two TMDs, each of which consists of multiple membrane-spanning α-helices, form the pathway through which the transported substrate crosses the lipid bilayer, and define a specific binding site (or sites) for the substrates. NBDs undergo conformational changes induced by ATP binding, ATP hydrolysis and ADP release, which are coupled to the transport process to alternately expose the binding site to the extracellular and intracellular side of the transporter.

The organization of these four core domains differs in prokaryotes and eukaryotes. In prokaryotes, the subdomains are expressed generally as discrete polypeptide subunits. For example, Sav1866 is a homodimer, which has two identical subunits, each consisting of one TMD followed by one NBD. In eukaryotes, the transporter is generally expressed as a single polypeptide consisting of two homologous halves, each half comprising one TMD and one NBD. For example, Pgp is a monomer with a flexible linker to connect the two similar halves of molecules, each of which comprise one TMD and one NBD. Nevertheless, full-length Pgp and co-expressed half-molecules of Pgp devoid of the linker region share similar drug-stimulated ATPase activity (Loo, & Clarke 1994b), implying a trivial role of the linker in its function.

In the ABCC subfamily, several members contain extra domains. The TMD0 domain of MRP1 does not appear to be important for function because deletion of TMD0 was found to have no effect on either trafficking of the protein or its transport activity (Zhou et al 1998). However, L0 in CFTR has been found to be functionally important as it plays a role in regulating gating of the chloride channel (Naren et al 1999). In particular for CFTR, a R domain is inserted into two half-molecules, which contains multiple protein kinase A phosphorylation sites. An increase in the concentration of cAMP promotes phosphorylation of CFTR on domain R by protein kinase A, and promote channel opening (Cheng et al 1991; Berger et al 1991). Deletion of domain R did not affect trafficking but the channel remained constitutively open (Rich et al 1991).

1.2.2.2 Functional unit and essential questions

Since ABC transporters usually have two similar halves, it is possible that each half could act as a separate transporter. However, this is not the case. The cDNAs encoding the half-molecules of Pgp were expressed separately in cells and it was found that expression of either half-molecule alone was insufficient to mediate drug transport (Loo, & Clarke 1994b). Similarly, split molecules of CFTR showed little activity unless they were expressed in the same cell (Ostedgaard et al 1997). Therefore, interaction of the half-molecules is required to form a functional protein.

Since the interaction between the two half-molecules is indispensible, the four core domains should all be taken into account to deal with the essential question

for ABC transporter: how ABC transporter captures the energy of ATP hydrolysis to ensure the unidirectional transport of substrate across the membrane, often against a substantial concentration gradient?

1.2.3 Key domains and motifs

1.2.3.1 NBD and ATP hydrolysis

The NBDs of ABC proteins are quite conservative. There are several motifs, playing important roles in ATP binding and hydrolysis.

A functional ATP binding site is formed by the interaction of residues from both NBDs of the protein. As shown in Figure 1-2, the two NBDs form a nucleotide-sandwich dimer with ATP bound along the dimer interface. Each ATP lies between a helical domain (orange) from one NBD and a core domain (purple) from the other NBD. Interestingly, binding of ATP coincides with a rotation of the helical domain relative to the core domain. In structures of GlcV, compared to apo state, the helical domain is shown to move to meet the core domain from the other NBD in AMPPNP-Mg state (Verdon et al 2003). In the maltose transporter MalFGK2, addition of ATP together with MBP (periplasmic maltose-binding protein) will change the dynamics of the protein and experience a rotation on the helical domain (Orelle et al 2010). In apo/ATP simulations of Sav1866, the core domain in the absence of ATP (apo site) experiences a rotation, breaking ATP binding sites formed with the helical domain from the other NBD (Jones, & George 2011).

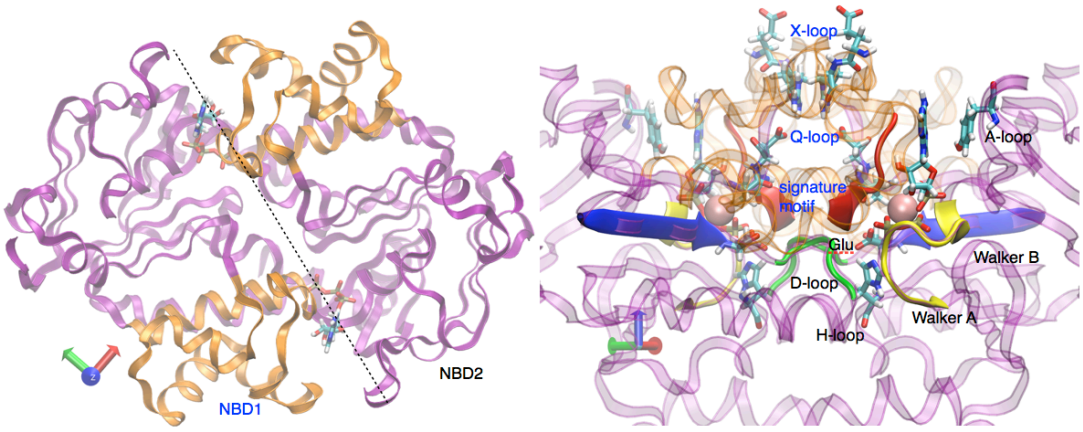

Figure 1-2: Structure and motifs of nucleotide binding sites

Purple, core domain; orange, helical domain; blue, Walker B; yellow, Walker A; green, D-loop; red, signature motif

Actually, such relative rotation between helical domain and core domain is used to bring the signature motif (red) into apposition with the Walker A (yellow) in the opposing subunit. The signature motif, also called C-loop, is the hallmark of ABC proteins with the sequence LSGGQ. Mutation studies on S, G, Q show that the signature motif is essential for ATP hydrolysis, but not for ATP binding (Tombline et al 2004a; Loo, & Clarke 2002; Bakos et al 1997). ATP binding is attributed to Walker A, which wraps around an ATP phosphate group in structure. Mutation on the highly conserved lysine residue (K380 in Sav1866) to either methionines or arginines in Pgp causes reducing of ATP binding and

abolishes ATP hydrolysis (Müller et al 1996; Azzaria et al 1989) , which implies the importance of this residue in anchoring the ATP in an appropriate position, ready for ATP hydrolysis (Azzaria et al 1989).

With the signature motif and Walker A anchoring the ATP by interacting with the phosphate group at one end of ATP, the A-loop, characterized by an aromatic residue located about 25 residues upstream of Walker A, puts ATP in a proper position by π-π stacking with the aromatic ring of ATP (Mao et al 2004). This residue is highly conserved within ABCB family and ABCC family. This is supported by detailed mutational studies showing that the conservative mutations (W/F) could maintain the transport function while non-conservative mutations (A/C) decrease or abolish nucleotide binding, hydrolysis and affect transport functions.

In addition to the motifs interacting directly with ATP, two sets of residues are commonly found in the active site to catalyze ATP hydrolysis: 1) a general base that promotes the attacking water; 2) a group that electrostatically stabilizes the phosphate oxygens (Matte et al 1998; Maegley et al 1996) . The residue that serves as the general base is ambiguous. Candidate residues include Glu503, which is adjacent to the Walker B motif, Gln422 from Q-loop and His534 in the H-motif region, which all cluster in the vincinity of the cleaved phosphate.

Although there is strong evidence in some systems that Glu adjacent to the Walker B motif is the crucial catalytic residue (Smith et al 2002; Geourjon et al 2001; Moody et al 2002) , this might not be universally true since mutation of Walker B glutamate in Pgp (Urbatsch et al 2000b; Tombline et al 2004c) , HlyB (Zaitseva et al 2005) and GlcV (Verdon et al 2003) retain some ATPase activity. Alternatively, the solution to organize the active-site residues is not unique.

Besides Walker B glutamate, an important role for the H-motif histidine has been observed in HlyB (Zaitseva et al 2005). In particular, drastic reduction of activity is observed in H662A, which could be crystallized with ATP. Therefore, it was proposed that both the His and Glu are essential for catalysis and function as a catalytic dyad (Zaitseva et al 2005). Here, the histidine acts as "linchpin" to hold the gamma-phosphate of ATP, the attacking water, Mg^{2+}, and other catalytically important amino acids together to support hydrolysis, while the role of glutamate is no longer a catalytic base, but to restrict the flexibility of histidine so that it adopts a catalytically competent conformation. (Ernst et al 2006; Oswald et al 2006; Zaitseva et al 2005)

The other motifs shown in Figure 1-2 include D-loop, X-loop and Q-loop. D-loop is thought to contribute to ATP binding and hydrolysis, since aspartate on the D-loop from one NBD could interact with Walker A from the other NBD, while D-loop move outward from the binding site in apo compared to Mg-ADP. Additionally, mutation of the Asp residue in Mouse Pgp (D509 in Sav) causes a decrease of ATP hydrolysis (Urbatsch et al 2000b).

X-loop and Q-loop are more related to coupling between NBD and TMD. As demonstrated in antigen ABC transport complex TAP, either substrate binding or translocation can be blocked by cross-linking the X-loop to coupling helix 1 or 2 (Oancea et al 2009), indicating that the X-loop plays an important role in coupling between NBD and TMD.

As for Q-loop, its function is still unknown. This loop lies between two sub-domains and stands out for its flexibility shown by NMR studies (Wang et al 2004). By superimposing structures with different nucleotide binding state, Q-loop from MJ1267 is shown to flip away from the binding site upon ADP binding (Karpowich et al 2001). By scrutinizing the position of Q-loop in X-ray structures, two possible functions were proposed. As shown in Sav1866 structure, Q-loop coordinates the cofactor Mg^{2+} which is essential for ATP hydrolysis and hence it may take part in preparation for ATP hydrolysis (Dawson, & Locher 2007). In HisP, Q-loop lies next to a water molecule that is thought to be the "attacking" water and hence it might be an activating residue for ATP hydrolysis (Hung et al 1998). However, Senior and coworkers have demonstrated in mouse Mdr3 that the Q-loop are involved neither in the activation of the attacking water for ATP hydrolysis, nor in the coordination of the essential Mg^{2+} cofactor, but rather in the interdomain signal communication (Urbatsch et al 2000a).

ATP hydrolysis model. The finding in Rad50cd that the dimerization ratio with ATP is higher than that with ADP or under conditions of apo state (Hopfner et al 2000) suggests that ATP facilitates dimerization of the two NBDs. However, do both of the two sandwich-like ATP binding sites hydrolyze? This is still a question in debate.

Whereas two ABC domains are always required for activity, only one functional ATPase site is enough to support transport activity in certain systems, e.g. His permease (Nikaido, & Ames 1999). This notion is supported by many examples of fully functional ABC transporters containing one degenerate nucleotide-binding site lacking Ser of D-loop, Gly of signature motif and Glu of Walker B (Procko et al 2009). This is consistent with an alternative catalytic mechanism, in which only one ATP hydrolyzes and drives the conformational change in the transport cycle. Such mechanism is supported by the observation that the ATPase activity is retained when one of the two ATP binding sites is inactivated by vanadate-trapping, mutation and chemical modification (Senior et al 1995).

However, this is not a universal property of ABC transporters. The substitution in a single site of the maltose transporter severely impaired both transport and ATPase activity, suggesting that hydrolysis at both sites is important for the function (Davidson, & Sharma 1997). Interestingly, even the glutamate substitutions that promote stable formation of the NBD dimer, when present in a single site, inactivate the intact P-glycoprotein transporter (Tombline et al 2004b). This could support another ATP hydrolysis mechanism, named processive clamp, proposed from three different dimeric intermediate states obtained by trapping and mutation, measured by photolabelling (Janas et al 2003). In this mechanism, both ATPs hydrolyze sequentially in the transport cycle.

1.2.3.2 Distribution of TMD and drug binding

Among the different ABC transporters, P-glycoprotein (Pgp) was most widely investigated. With the elucidation of the X-ray structure of Pgp and its homolog Sav1866, the large amount of biochemical data should be reviewed to get more insights on the mechanism of drug transport in Pgp.

1.2.3.2.1 TMD distribution

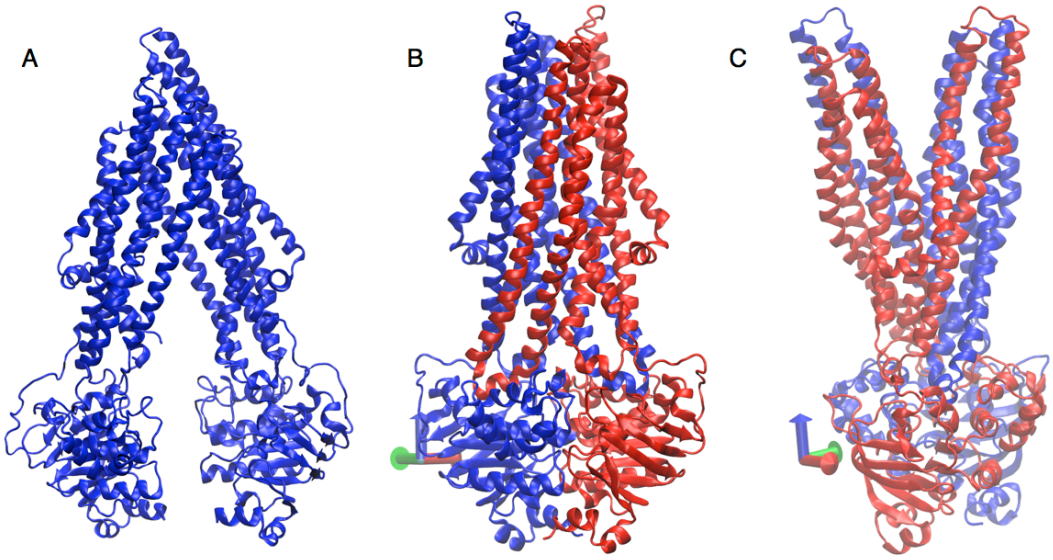

Figure 1-3: Crystal structure of P-glycoprotein and Sav1866

A. apo Pgp structure. B.C. Sav1866 structure with 2AMP-PNP. Blue and red, two identical subunits.

The structure of Pgp is in an apo state, with two NBDs clearly separated (Fig.1-3A), while in the X-ray structure of Sav1866 with 2AMP-PNP bound (Dawson, & Locher 2007), the NBD are closedly associated (Fig.1-3B). Interestingly, the individual helices of Sav are not simply aligned side by side as independent helical bundles. Rather, they embrace each other and have a significant twist. In addition, a central cavity facing outward is formed in the TMD. This cavity is relatively hydrophilic and was interpreted to represent an extrusion pocket, with little or no affinity for the hydrophobic substrates. Notably, this structure reflects the ATP-bound state (2AMP-PNP), but it is almost identical to that with 2ADP bound (Dawson, & Locher 2006).

1.2.3.2.2 Broad specificity and key interactions in Pgp

Pgp is unique in its ability to recognize and transport a plethora of diverse substrates, considerably different in chemical structure and pharmacological action, including many clinically important agents. In particular, Pgp substrates range in size from large complex molecules, such as paclitaxel and vinblastine, to smaller drugs such as daunorubicin and doxorubicin. Pgp also interacts with linear and cyclic peptides and ionophores, including gramicidin D, valinomycin, N-acetyl-leucyl-leucyl-norleucinal (ALLN), leupeptin, pepstatin A and several bioactive peptides (Sarkadi et al 1994; Sharom et al 1995) . With such broad specificity, K_d (dissociation constant) values for Pgp substrates cover a 1000-fold range (Sharom 1997).

In order to understand features of the seemingly dissimilar substrates, Seelig and coworkers screened a library of structurally diverse Pgp substrates for universal molecular features using 3D modeling. They found that the presence of hydrogen bond acceptors (or electron donors) moiety (carbonyl, ether, hydroxyl or tertiary amine groups) with a defined spatial separation was a key feature (Seelig 1998a; Seelig 1998b) . Two specific spatial separation patterns were

identified. Type I pattern consists of two electron-donor groups separated by 2.5±0.3Å, while Type II pattern is made up of two electron-donor groups with a spatial separation of 4.6±0.6Å. Type II may also be comprised of three electron donor groups with the outer two groups separated by 4.6±0.6Å.

The idea underlying such classification is that H-bonds are the main interaction between substrates and Pgp. Since the TM domains of Pgp contain a high fraction of amino acids with side chains capable of acting as hydrogen bond donors to interact with substrates, such idea is attractive. Later on, H-bonds were confirmed to be the main interaction by measuring the binding of typical substrates polyoxyethylene alkyl ethers. It showed that the lipid-water partitioning step was purely hydrophobic, increasing linearly with the number of methylene, and decreasing with the number of ethoxyl residues and therefore the substrate binding is purely electrostatic without any hydrophobic contribution (Li-Blatter, & Seelig 2010).

1.2.3.2.3 Drug binding sites in Pgp

A plethora of cross-linking studies have shown that more than one compound could occupy the drug-binding pocket simultaneously (Loo, & Clarke 2001b; Loo et al 2003b) . With such a large drug-binding pocket, do all drugs compete for one smart binding site capable of recognizing various drugs? Or, are there different binding sites tailored to diverse drugs? It was proposed from ATPase inhibition studies that drugs, peptides and modulators conformed to classical Michaelis-Menten competition for a common drug-binding site (Borgnia et al 1996). However, multiple sites for substrates binding were proposed in different methods. Photo-affinity labeling studies suggested that Pgp contained two separate drug-binding sites, one in each half of the protein (Dey et al 1997).

More importantly, two “functional” transport sites were demonstrated within Pgp, the H-site and R-site, named for its preference for Hoechst 33342(H33342) and rhodamine 123(R123) (Shapiro, & Ling 1997). The two sites interacted with each other allosterically, such that H-site and R-site drugs mutually stimulated each other’s transport. These two sites was mapping by fluorescence approach and showed that H-site lies within bilayer leaflet region of Pgp, whereas the R-site is in the cytosolic region (Lugo, & Sharom 2005b). Although it is reasonable to expect one binding site for one molecule, fluorescence approaches showed that R-site of Pgp is large enough to accommodate two compounds such as LDS-751 and R123 at the same time, which bind to Pgp in a non-competitive manner (Lugo, & Sharom 2005a).

Besides these two sites, a third drug-binding site on Pgp was identified and prazosin and progesterone binding to this side stimulate the transport activity of both the H and R sites (Shapiro et al 1999). Moreover, based on noncompetitive interactions, a minimum of four drug-binding sites on Pgp was determined in binding studies using radio-labeled drug. There are complex allosteric interactions between these binding sites, which could switch any site between high- and low- affinity conformations (Martin et al 2000).

All the above results demonstrate an exceptional chemical and structural flexibility of Pgp, offering many drug binding sites for interaction with different drugs. However, whether one specific drug could bind to different binding sites

is unclear. Chufan and coworkers found that one drug could adopt the alternative binding sites and modulate ATP hydrolysis when the primary binding site is mutated (Chufan et al 2013), demonstrating that each drug can bind to more than one site in the transport.

1.2.3.2.4 Drug recognition mechanism

Although there are multiple binding sites for Pgp, it is still difficult to understand how Pgp could recognize all such diverse substrates. Since binding of different substrates has been demonstrated to result in different conformations of the transmembrane helices based on MDR1 cross-linking experiments (Loo et al 2003c), an induced fit mechanism is proposed, which could explain the wide substrate specificity. However, the conformational selection theory, which is an alternative mechanism for molecular recognition, became the focus of research again in the last decade (Boehr et al 2009; Csermely et al 2010). According to this theory, all possible conformations of the protein are realized in the absence of substrates, even those conformations that are capable to bind substrates. The substrates select the favored conformations to bind to. This theory not only provides a good explanation for the recognition of an extremely wide set of drugs, but it could also explain the activation of ATPase upon drug binding. In particular, the presence of a drug would shift the conformational ensemble towards the binding competent conformations exhibiting the increased drug-stimulated ATPase activity.

1.2.3.3 NBD-TMD coupling

1.2.3.3.1 General mechanism and conservation

The TMD-NBD transmission interface features two coupling helices. Although they share little or no sequence similarity among the different transporters (Hollenstein et al 2007), the conservation in structure itself may offer a conserved mechanism of transport. Beside the conserved existence of these two coupling helices, the arrangement of the helices connected by one of the two coupling helices is also conserved. In particular, as shown in Sav1866, one of the two coupling helices from one half-molecule interacts with the NBD from the other half-molecule (Fig.1-3B). Although this is the only structure with such domain swap arrangement, the experimental cross-linking and genetic data for the eukaryotic drug exporters ABCB1 (Zolnerciks et al 2007), Yor1p (Pagant et al 2008) and the chloride channel CFTR (Serohijos et al 2008; He et al 2008) support a similar arrangement. Therefore, the general transport mechanism of ABC transporters should also be conserved.

Generally, it is accepted that ATP binding will cause dimerization of the two NBDs and the coupling helices will transmit this conformational change to the translocation pathway in TMD, from inward-facing (ADP-bound or nucleotide free) to outward-facing conformations (ATP bound) (Chen et al 2001). However, this is not always valid. For example, the structures of nucleotide-free BtuCD (Locher et al 2002) and ADP-bound Sav1866 (Dawson, & Locher 2006) adopt the outward-facing conformations, although they were both crystallized in the absence of ATP.

Apart from that, the additional periplasmic binding protein in ABC importer adds more complexity to the issue. Electron spin resonance spectroscopy studies that involve site-directed spin labeling indicate that ATP alone is insufficient to drive the closure of the maltose transporter NBDs. Rather, the presence of the maltose-binding protein is also required (Orelle et al 2008). Besides, the conformation of the outward-facing gate of BtuCD depends only on the docking of the binding protein and is insensitive to binding of AMPPNP (Goetz et al 2009). These studies suggest that there might be mechanistic distinctions between different families of ABC transporters and highlight the need for caution in generalization.

1.2.3.3.2 Model and questions

A model, shown in Figure 1-4, was proposed based on three different configurations of MsbA (Ward et al 2007). An open, nucleotide-free state was observed for the *E.coli* structure, in which the two NBDs are a significant distance apart (50 Å), as Pgp structure (Aller et al 2009). A second nucleotide-free state was observed for the *Vibrio cholera* MsbA in which the NBDs are closed. This 'closed apo' structure can be reached from the 'open apo' structure by a rigid body closure, centred on a hinge in the extracellular loop. To form the closed, nucleotide-bound structure observed in *Salmonella typhi* MsbA, a further pair of motions to align the NBDs is desirable to prepare the nucleotide sandwich dimer and generate an outward facing configuration in TMD which is similar to that observed in Sav1866 (Dawson, & Locher 2006).

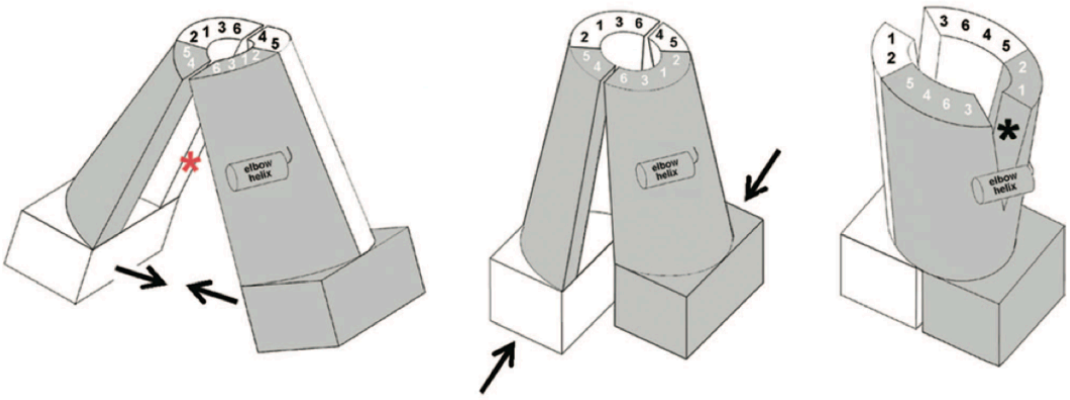

Figure 1-4: Model based on MsbA structures

Transporting model based on three MsbA structures, respectively in open apo, closed apo and nucleotide bound states (Ward et al 2007)

This model implies a state in which the two NBDs are completely separated. If this is the case, the association of NBD upon ATP binding could drive the conformational change in TMD, change the drug binding affinity and hence transport different drugs. On the other hand, if the two NBDs do not need to dissociate completely, ATP hydrolysis, instead of ATP binding, has to take the role of changing the conformation in TMD.

While the X-ray structure of apo Pgp is reported to have a large separation of NBD (Ward et al 2007) and EPR studies show similar magnitude of

conformational change in NBD (Borbat et al 2007), the requirement of dissociation of two NBDs is put into questions with different findings. EPR data in multiple configurations (Buchaklian, & Klug 2006) of MsbA shows that the LSGGQ motif is at least partially packed with the remaining structure throughout hydrolysis. Besides, when pairs of cysteines were introduced into the N- and C-terminal ends of NBD of Pgp, ensemble FRET demonstrates their close association during the catalytic cycle (Verhalen, & Wilkens 2011), while the corresponding residues are closed in the X-ray structure of Sav1866 and MsbA with nucleotides, but not in the structure of apo MsbA and apo Pgp with a huge separation of two NBDs. In addition, when NBD terminal ends of Pgp are linked closely together, not only the drug-stimulated ATPase activity is retained (Verhalen et al 2012), higher ATPase activity could be observed (Loo et al 2012). These functional results demonstrate that the dissociation of the two NBD might occur, but it is not an indispensible step in the drug-transport cycle.

1.2.3.3.3 Helix 6

How could a small change in NBD bring a big change in TMD? Based on the structures of the homologous bacterial ABC transporters MsbA and Sav1866, an outward-facing model of Pgp was obtained (Gutmann et al 2010). Compared with the inward-facing structures of Pgp, the helices in the outward-facing model have rotated along the length of their axis by up to 90 degrees. Since these helices constitute the drug-binding sites, drug affinity in TMD changes upon such rotation, enabling the dissociation of the substrate. Such rotation was proposed mainly in TM6 and a great deal of accumulated evidence indicates a pivotal role of TM6 in the drug translocation process.

The importance of TM6 has been implied by many investigations. Mutations on TM6 or TM12 (equivalence to TM6 in the second half-molecule) of Pgp, F335A and F978A in particular, drastically altered the drug resistance profile, suggesting that TM6/12 contributes to drug binding and/or translocation (Loo, & Clarke 1993). Mutations of human Pgp on V338, G341, A342 and S344 modulate the resistance activity and substrate specificity, implying the role of TM6 in drug-protein interaction and coupling of drug binding to ATPase activity (Loo, & Clarke 1994a). Apart from that, a Pgp mutant G338A/A339P within TM6 displays preferential resistance to actinomycine D and diminished resistence to colchicine and daunorubicin, implicating TM6 in the mechanism of Pgp drug recognition and efflux (Devine et al 1992; Ma et al 1997). Different substrate and nucleotide binding state favors different cross-linking involved in helix 6, implying helix 6 experience a conformational change in the transporting cycle (Loo, & Clarke 1997). By covalent modification of different part of TM6, it was found that the central segment is intransient, while the two ends experience conformational changes during ATP hydrolysis (Storm et al 2008).

More importantly, a possible rotation of helix 6 was proposed in different studies. Mutations on a series of residues in TM6 that cover different side of helix 6 could influence drug transport (Song, & Melera 2001). In the presence of ATP, cross-linking of mutant L339C (TM6)/ V982C (TM12) on human Pgp was decreased while that of F343C (TM6)/ V982C (TM12) was enhanced (Loo, & Clarke 2001a). Moreover, substitutions at the cytosolic end of TMs 6 and 12

cross-linked with three consecutive substitutions each, within TM4 and 10, respectively (Loo, & Clarke 2000).

Among diverse residues investigated, a single mutant F343C stands out for its capability of activating ATPase (Loo et al 2003a). Similar conclusion is obtained by fluorescence maleimide labeling of F343C (Rothnie et al 2004). Interestingly, labeling of I340C, which is on the same face of TM6 as F343, however, resulted in inhibition of ATPase activity. This opens the possibility that substrates of Pgp could bind in more than one orientation in the common drug-binding pocket, but only some orientations could induce conformational changes in Pgp.

1.3 ClC family

1.3.1 Distribution and mammalian subfamilies

1.3.1.1 Distribution

The ClC family encompasses members widely distributed in various species from bacteria to humans. These protein molecules play a variety of biological roles, including maintenance of membrane potential, regulation of trans-epithelial Cl- transport, and control of intravesicular pH.

Although the amino acid identity between the bacterial ClCs and those of the mammalian ClC is only 20%, studies of mammalian ClC channels have shown that they should adopt an overall similar structural architecture (Ramjeesingh et al 2006; Lin, & Chen 2003; Estévez et al 2003; Engh, & Maduke 2005) . The high-resolution crystal structures from bacterial ClCs provide a useful framework to understand functional data of both bacterial and mammalian ClCs.

1.3.1.2 Classification of mammalian subfamilies

The first member of the ClC gene family, ClC-0, was identified and cloned from the electric organ of *Torpedo ray* (O'Neill et al 1991; Jentsch et al 1990) . Homology cloning efforts in the 1990s identified nine members in mammalian species (ClC-1 to ClC-7, ClC-Ka, ClC-Kb), constituting three subfamilies (Maduke et al 2000; Jentsch et al 1999) .

ClC-0 and its mammalian homologs, ClC-1, ClC-2, ClC-Ka and ClC-Kb form one subfamily. These members are Cl- channels, and they are all present on the cell membrane to control Cl- flux and membrane potential.

The second branch of the family includes ClC-3, ClC-4 and ClC-5. These proteins are located on the membrane of intracellular vesicles and are thought to be important in maintaining the pH of these vesicles (Stobrawa et al 2001; Mohammad-Panah et al 2003; Günther et al 2003) , consistent with their functional properties as Cl-/H+ antiporters.

The third branch of the family contains ClC-6 and ClC-7, which are expressed in various tissues. These two proteins cannot be functionally expressed in heterologous expression systems (Brandt, & Jentsch 1995). It has been reported that they may be present also in the intracellular organelles to regulate the vesicular pH (Kornak et al 2001).

While the first branch is chloride ion channel, the latter two branches are both chloride/proton antiporters. Given that they belong to the same family, the structural difference is naturally small, implying small difference in function, although channels and transporters are considered quite different. Not only the proton gradients are important in gating of ClC channels, they actually transport protons, as supported by the pH changes close to the extracellular surface of ClC-1 channels during gating (Picollo, & Pusch 2005), and that non-equilibrium gating of ClC-0 channels depends on the proton electrochemical potential gradient (Lísal, & Maduke 2008). Therefore, the difference between ClC channels and transporters is very small. It is not the presence of proton transport, but whether the proton transport is coupled to chloride ion transport.

1.3.2 Architecture, chloride ion binding sites and ion pathways

1.3.2.1 Architecture

The high-resolution crystal structure of *E. coli* ClC molecule ClC-ec1 (Dutzler et al 2002) provides a lot of insight about the structure and function of prokaryotic and mammalian ClC proteins. Several mutational studies as well as experiments using substituted cysteine accessibility method (SCAM) have indicated that the overall structure of the pore-lining portion of CLC-0 should be similar to the anion transport pathway of bacterial CLC proteins (Engh, & Maduke 2005; Lin, & Chen 2000; Lin, & Chen 2003).

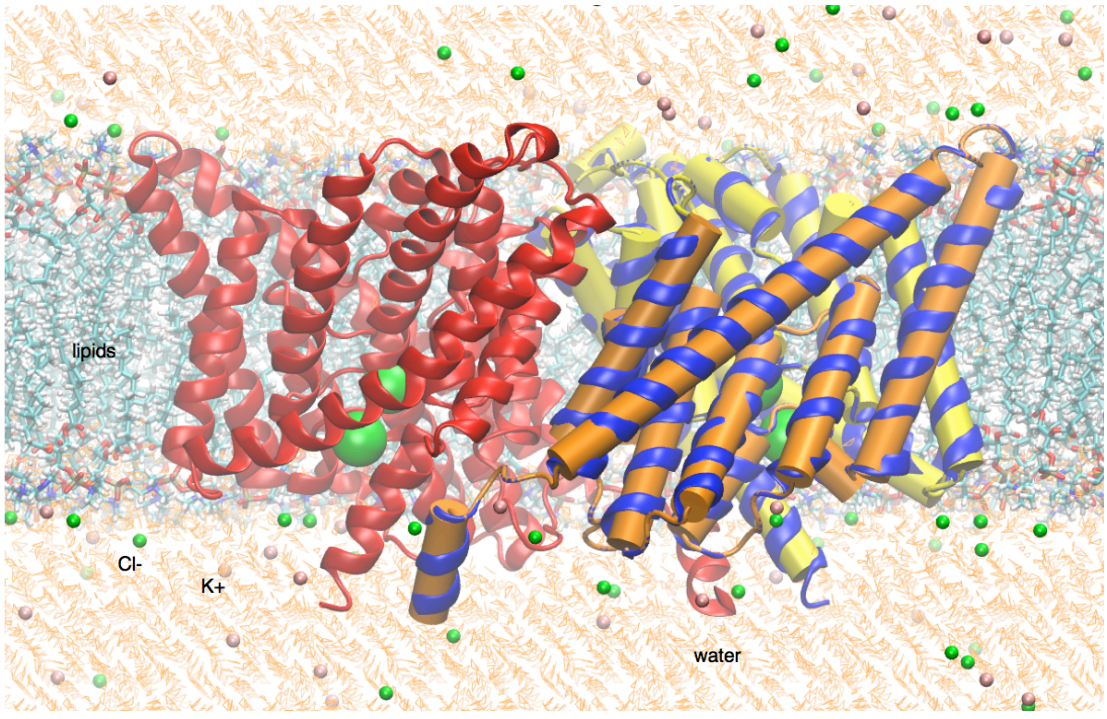

Figure 1-5: Structure of ClC-ec1

Blue and red helices, two subunits; yellow and orange cylinder, two sudo-symmetric domains which constitutes one subunit; green balls, chloride ions; pink balls, potassium ions; orange line, water molecules.

The structure of ClC-ec1 shows two identical subunits, highlighted in blue and red in Fig.1-5, which are in a two-fold symmetry with the normal of the

membrane as the axis. Within each subunit the protein is made of 18 α-helices, named helix A to R, from NH2 to COOH terminus of the protein. The distribution of helices constitutes two antiparallel domains, which are sudo-symmetric (yellow and orange in Fig1-5). Notably, some of these helices run halfway through the lipid membrane, with the positively charged end of the helix dipole coordinating Cl^- in the middle of the cell membrane (Dutzler et al 2002; Dutzler et al 2003).

1.3.2.2 Chloride ion binding sites

Four Cl^- binding sites were determined and proposed to form the Cl^- ion permeation pathway (Fig.1-6). Among them, two binding sites, Scen and Sint, are implied by the two chloride ions in the wild type ClC-ec1 structure (Dutzler et al 2002), while the E148A and E148Q mutant structures show a third Cl- ion close to the extracellular side, named Sext (Dutzler et al 2003). In addition, binding energy calculation based on the structure of ClC-ec1 indicated a fourth binding site, which is closer to extracellular side than Sext and hence is called Sext*. According to the pseudo-symmetry of the two domains constituting one subunit, Sext* lies at a position vaguely symmetric to Sint (Faraldo-Gómez, & Roux 2004).

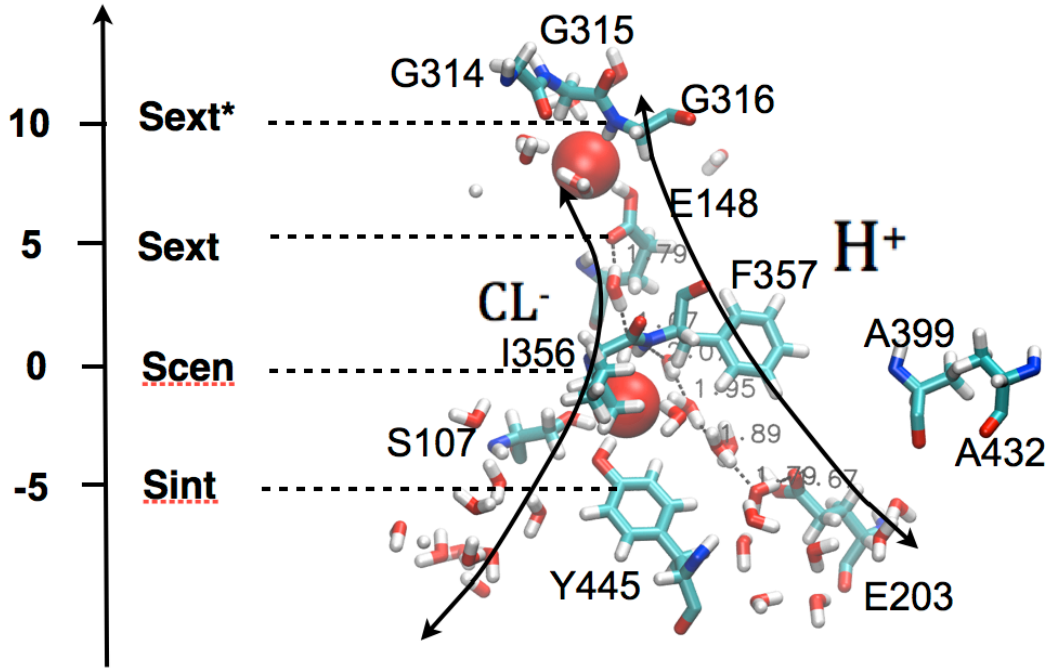

Figure 1-6: Divergent routes for chloride ions and protons

1.3.2.3 Proton transport and pathway

In the study of proton transport, E148 and E203 are considered important, as either E148A or E203A blocks proton transport. A water chain between these residues could facilitate proton transport. Given that E203 is far from chloride ion pathway, chloride ions and protons were proposed to follow different pathways, diverging at E148 (Accardi, & Miller 2004).

1.3.3 Fast gating and slow gating in channels

1.3.3.1 Gating properties of ClC-0: fast gating and slow gating

1.3.3.1.1 Timescales distinguish fast gating and slow gating

Gating is an essential feature of channel function. Among different ClC channels, only the gating function of ClC-0 has been studied extensively. The potentially related transporter functions, i.e. the regulation of gating by chloride ion and proton, have been well documented as well. Based on the kinetics of the channel opening, the gating of ClC-0 includes "fast" and "slow" gating, which operate in the time scale of milliseconds and seconds, respectively. Shown in Fig.1-7 is the single-channel recording trace of ClC-0. The long, non-conducting states between bursts of channel activities (indicated by arrows in Fig.1-7, from ref (Chen, & Hwang 2008)) represent the closure of the slow gate. When the slow-gate is open, a burst of channel activity appears, and the three current levels (the non-conducting level, the middle level, and the fully open level) can be observed. The current fluctuation within a burst is called fast gating because the gating mechanism operates at a much faster time scale (milliseconds) than that of slow-gating (seconds to minutes).

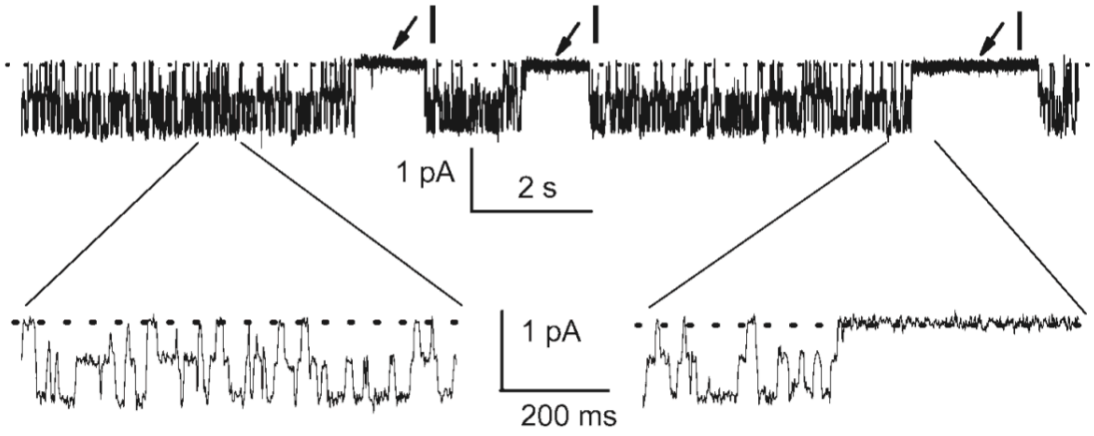

Figure 1-7: Gating of ClC-0

Gating of ClC channels is comprised of fast gating and slow gating which operate in different timescales. The arrows mark the non-conducting state with both fast gate and slow gate closed (Chen, & Hwang 2008)

1.3.3.1.2 Asymmetry of gating

Channel-gating process is not at thermodynamic equilibrium. The closure of the slow-gate predominantly succeeds from a state in which one of the two fast-gates is open, while the slow-gate opens to a state in which the fast-gates of both pores are open. This non-equilibrium gating is more prominent with a larger chloride ion gradient across the channel pore imposed by the membrane voltage (Richard, & Miller 1990). However, the chloride gradient was found not to be sufficient to drive the asymmetry, and proton gradient across the cell membrane provide the energy for the non-equilibrium gating cycle (Lísal, & Maduke 2008).

1.3.3.2 Fast gating

There are generally two models to explain the fast gating. They both consider chloride ion channel as a ligand-gated channel, but the ligands for the two models are different. One is the chloride ion gated model, in which the binding of chloride ion is proposed to activate the channel, opening the fast gate. The other model considers the channel as a degraded transporter and takes the proton as the ligand, in which the protonation of Glu166 (conrresponding to Glu148 in ClC-ec1) is considered as the essential step that opens the fast gate of ClC-0. Both models describe some aspect of the fast-gating process, but fall short in explaining other gating properties.

The chloride ion gated model fits well with the observation that the chloride ion and various permeable anions at the extracellular side facilitate the opening of the ClC-0 fast gate (Pusch et al 1995). In addition, the computational study using metadynamic methodology indicates that the main barrier of chloride ion translocation near Glu_{ex} was reduced by an ion-push-ion effect (Gervasio et al 2006). Another computational study also shows that the external chloride ion can push the side chain of Glu into a more central position where, pressed against the channel wall, it does not impede the motion of chloride ions (Bisset et al 2005).

However, single-channel studies in ClC-0 have suggested that the competition between chloride ions and the side-chain of the glutamate residue may be used to explain the effect of internal ion on the closure of fast gate. In particular, fast-gate closure of ClC-0 is reduced by an increase of internal chloride ion concentration while the opening rate of the fast gate is kept intact (Chen 2003; Chen, & Miller 1996; Chen et al 2003; Cheng et al 2007) .

If this is the case, it could not be used to explain opening of the fast gate, because the internal and external chloride ion effects on fast gating of ClC-0 were demonstrated to be very different. For example, altering concentration of external chloride mainly affects the opening rate, while changing concentration of internal chloride ion alters the closing rate but has little effect on the opening rate of the fast gate (Chen et al 2003; Chen, & Miller 1996) . The apparent chloride ion affinities in modulating the opening rate and the closing rate by concentration of external and internal chloride ion, respectively, differ by 20-fold, suggesting that the chloride-binding sites involved in the opening and closing mechanisms may be different (Chen et al 2003; Chen, & Miller 1996) . In addition, the fast-gating opening and closing mechanisms are differentially affected by point mutations. For mutations at the external pore entrance of ClC-0, K165, the effect is on the opening rate but not the closing rate. On the other hand, a mutation at the intracellular pore entrance of ClC-0, K519, influences more on the closing rate but not the opening rate (Chen et al 2003). Taken together, these results strongly suggest that these two aspects of the fast-gating mechanism, the opening and closing process, may not be reversible processes of each other (Lin, & Chen 2000).

The degraded transporter model could explain the complicated fast gating by the protonation of Glu_{ext}. Nevertheless, there are several problems of this model. First, the proton and chloride ion transport should not be tightly coupled. Second, binding of anion at Scen is critical for proton transfer from Glu_{in} to Glu_{ex}

(Nguitragool, & Miller 2006). However, Scen is intracellular to the side chain of Glu_{ex}. When the gate is closed, how does a chloride ion in the extracellular medium reach Scen? Third, where is the intracellular protonation site since the position where Glu_{in} lies in the transporter is a valine in channels?

1.3.3.3 Slow gating

The mechanism of slow gating is unknown, but there are several studies implicating that it involves a large conformational change. Manipulations that disrupt the COOH-terminal on the intracellular side have been shown to affect the kinetics of slow-gating, suggesting that, in addition to the membrane-spanning part of the protein, the COOH-terminal half of the channel is also important for slow-gating (Wu et al 2006; He et al 2006) . Fluorophores labeled at helix R of ClC-ec1 displayed chloride ion and pH dependent fluorescence change (Bell et al 2006), suggesting that the movement of COOH-terminal domains may be transduced to the permeation pore through helix R.

1.3.4 Important residues related to coupling between proton and chloride ion transport in anti-porters

1.3.4.1 E148

E148 is a residue lying on both the proton and chloride ion pathways, which plays an important role in transport of both ions. In respect to chloride ion permeation, E148 acts as external gate, as it binds to the pore, notably at Sext, thus blocking permeation. This is further supported by the fact that the E148A and E148Q mutant structures include a Cl- ion at Sext (Dutzler et al 2003). On the other hand, E148 plays a role in proton transport and gets involved in the coupling mechanism. In E148A, proton is hardly transported, and the reversal potential follows the equilibrium of potential of chloride ion calculated from the Nernst equation. Thus the mutant protein becomes an uncoupled chloride ion channel (Accardi, & Miller 2004).

1.3.4.2 E203

Generally, glutamate at this position is strictly conserved in all known ClCs of the transporter subclass, while a valine is always found here in ClC channels. Therefore, it appears that E203 is essential for proton transport. This is supported by the mutant E203Q, which has a similar structure as wild-type protein but fail to permeate protons. Among diverse mutants, E203 is found to be the unique internally facing carboxylate to block proton permeation completely and hence is desirable for proton transport (Accardi et al 2005).

In a detailed study on the role of E203, it is found that the residue at this position does not have to be a glutamate for proton transport, but a protonatable amino acid is essential. By examining structural and functional properties of mutants at this position, certain dissociable side chains (E, D, H, K, R but not C and Y) retain proton/chloride exchanger activity to varying degrees, while other mutations (V, I, or C) abolish proton coupling and severely inhibit Cl- flux. Moreover, substitutions by other non-protonatable side chains (Q, S, and A) show highly impaired proton transport with substantial Cl- transport (Lim, & Miller 2009).

However, an unusual ClC homolog, ClC-ck2, functions as a chloride/proton anti-porter but contains an isoleucine at the Glu_{in} position. Introduction of a glutamate at the Glu_{in} site in ClC-ck2 does not increase proton flux (Phillips et al 2012). This surprising finding would imply that a residue at this position does not even have to be protonatable. In other words, E203 may play a role in proton transport, but not an indispensable one. Alternatively, ClC-ck2 has a different mechanism.

1.3.4.3 Y445

Y445 is the residue that directly coordinates a Cl^- at Scen and forms the intracellular gate with S107. It seems important to have this bulky and hydrophobic residue because substitution by F or W preserves WT transport behavior, while substitution by A, E, or H, produces uncoupled Cl^- transport with greatly impaired movement of proton. In addition, the intermediate mutant Y445L exchanges protons for chloride ions but at a reduced proton/chloride ion ratio. Moreover, the uncoupling observed in different mutants is correlated to the ratio of ion binding at Scen and Sint, implying that Y445 accounts for ion binding and that the ion binding to Scen somehow facilitates the movement of proton (Accardi et al 2006).

Consistent with these observations, further studies have shown that mutation at this position leads to uncoupling in a way that proton/chloride ion transport ratio decreases roughly with the volume of the substituted side chain and the uncoupled mutants transport chloride ion at the similar rate as WT (Walden et al 2007).

An independent experiment, in which the coupled transport of proton with various anions in the wild-type ClC-ec1 was measured, also revealed a similar correlation between the anion occupancy at Scen and the coupled transport (Nguitragool, & Miller 2006).

Such correlation is supported by a theoretical study in which anion occupancy in ClC-ec1 was demonstrated to cause more negative intrinsic potential of Scen, a condition that may be required for proton to pass the energy barrier in the transport pathway (Yin et al 2004).

1.4 Motivation of my dissertation

The thesis makes full use of high-resolution crystal structures of Sav1866 and ClC-ec1 to perform simulations to understand the molecular mechanism of the two systems. In particular, what kind of conformational transitions does the protein experience in the transport cycle? How do nucleotide binding and ATP hydrolysis drive the conformational of Sav1866? What is the role of protons in the transport of chloride ions in ClC-ec1? In this way, hopefully we can get some new insights on the functions of these proteins and move one step more on the way to find out the key molecular elements that define the blurred boundaries between channels and transporters.

2 Small changes in the nucleotide-binding domain of ABC transporters could trigger large conformational changes of their trans-membrane domain

2.1 Introduction

2.1.1 Role and importance of Pgp/Sav

ABC family is a large protein family present in organisms from all kindoms of life, which couples hydrolysis of ATP to translocation of substrate across cellular membranes. In *E. coli*, ABC transporters constitute the largest protein family, including around 80 distinct systems that represent 5% of the genome {Linton 1998}, whereas 49 ABC transporters are present in humans (Dean et al 2001). Among all the ABC transporter members, P-glycoprotein (Pgp) is investigated most extensively.

Pgp is unique in its ability to recognize and transport a plethora of diverse allocrites. This broad specificity determines its important physiological role in protecting the organisms against toxins by exporting them into the bile, urine, or gut. Additionally, different lipids such as short-chain PC (phosphatidylcholine) PAF (platelet activating factor) and GlcCer (glucosylceramide) could be Pgp allocrites as well and hence Pgp was proposed to be also involved in lipid transport (Pohl et al 2005).

Consistent with the role it plays in protecting cells, Pgp is one of the three ABC family members that express in tumor cells, giving rise to multidrug resistance (MDR) and causing failure of cancer chemotherapy treatment (Litman et al 2001). To overcome such failure, Pgp modulators are designed to increase drug penetration through biologically important protective barriers. However, this brings out a series of side effects, including the inhibition of the enzymes that metabolized drugs and the resulting toxicity of the typical drug dose (Tan et al 2000). Therefore, it's clinically important to selectively block the action of Pgp by using proper modulator. Only when a proper-designed modulator is combined with drugs, could cancer cells be killed.

In order to properly design modulators, the mechanisms regarding how Pgp works in multidrug resistance is worth investigating. Recently, X-ray structure of mouse Pgp was obtained (Aller et al 2009; Jin et al 2012) , bringing the possibility to investigate the mechanism at the atomistic level. However, there is no nucleotide bound in the ATP binding sites. Complementary to these structures in apo state, a bacteria homolog of Pgp, Sav1866 (Sav), has its structure with nucleotides published (Dawson, & Locher 2006; Dawson, & Locher 2007). Sav has been shown to confer resistance to Hoechst 33342, a Pgp allocrite. In addition, Sav-mediated resistance and transport of Hoechst 33342 is inhibited by Pgp modulator verapamil. Both demonstrate that Sav could serve as a model for studies on the MDR mechanisms displayed by Pgp (Velamakanni et al 2008).

2.1.2 Architecture and general mechanisms

The X-ray structure of Sav includes four core domains, two nucleotide-binding domains (NBD) and two trans-membrane domains (TMD). The two NBD form two ATP binding sites at their interface (Fig.1-2). Each binding site could accommodate one ATP, sandwiched by a signature motif from one NBD and a Walker A from the other NBD. By recruiting ATP, the NBD could trigger ATP hydrolysis at the binding site, which in turn could drive conformational changes in the TMD. Such conformational changes are required for drug transport, because the drug-binding sites, which are formed by the two TMD, 12 trans-membrane helices in total, should alternate between high affinity and low affinity to recruit and release drugs. Notably, the long intracellular loop of TMD2 in Sav contacts NBD1 (Fig.1-3). Such domain arrangement is consistent to Pgp apo structure and it was supported by cystein mutagenesis and chemical cross-linking experiment in Pgp (Zolnerciks et al 2007).

2.1.3 Coupling issue between TMD and NBD

The desirable variation of drug affinity in TMD implies at least two conformations in the transporting cycle. It was generally considered that different ATP binding states in NBD were coupled to either inward facing or outward facing conformation of the TMD (Chen et al 2001). In particular, the inward facing conformation is correlated to ADP bound or nucleotide free states, while the outward facing one corresponds to the ATP bound state.

By comparing three different X-ray structures of MsbA, a bacterial ABC transporter, a model (Fig.1-4) was proposed in which binding of the nucleotide causes a packing rearrangement of trans-membrane helices and turns the conformation from inward facing to outward facing (Ward et al 2007). Another model proposed based on the comparison between the Sav and apo Pgp structures (Aller et al 2009) indicates the same relation between inward/outward facing conformations and nucleotide binding states.

However, this is not always valid, such as ADP-bound Sav1866, which adopts the outward facing conformations. Moreover, the two models include a state in which two NBDs are completely separate, which was questioned by different findings. For example, EPR data in multiple configurations (Buchaklian, & Klug 2006) of MsbA shows that the LSGGQ motif maintains extensively contacts with the rest of protein throughout hydrolysis. Besides, when pairs of cysteines were introduced to cross-link the equivalent residues of the two NBD, ensemble FRET demonstrate their close association during the catalytic cycle (Verhalen et al 2012). When the central regions of the two NBD in Pgp are linked closely together, not only the drug-stimulated ATPase activity is retained (Verhalen, & Wilkens 2011), even higher ATPase activity could be observed (Loo et al 2012).

Another correlated question is whether ATP binding alone is enough for drug transport or is ATP hydrolysis required? Based on variation of drug binding affinity (Vergani et al 2003; Aleksandrov et al 2000; Martin et al 2001; Martin et al 2000; Rosenberg et al 2001) and TMD conformational change observed in 2D crystals (Rosenberg et al 2001) upon ATP binding, it has been proposed that ATP binding rather than hydrolysis provides the energy input required for substrate transport (Higgins, & Linton 2004). However, there is no molecular

insight of the conformational change induced by ATP binding. Thus, the question remains unanswered.

2.1.4 Our work

To understand whether the two NBDs will dissociate completely when no ATP is bound in the binding sites (apo state), simulations of apo Pgp and Sav were performed. The result shows that the complete dissociation of the two NBD is unlikely. To investigate if ATP bound could trigger conformational change in TMD from inward facing to outward facing, different nucleotide binding states of Sav were set up to perform molecular simulations and explore the conformational changes. Two different conformations of TMD, open and closed, were seen in the simulations, while NBD does not change much in all the cases. Our work demonstrates that the NBDs only change in a small scale, but this seems enough to bring TMD to a different conformation, switching it from high drug-binding affinity to low drug-binding affinity. Helix 1 and helix 6 experience the largest conformational change in TMD, resulting from the conformational change in Q-loop and X-loop at the ATP binding site upon ATP hydrolysis. A network among helix 1, helix 3, helix 4 and helix 6 seems to be involved in the signal transmission.

2.2 Results:

2.2.1 Conformational changes in the NBD are small

Seven different nucleotide-accompany states were set up based on the X-ray structure of Sav1866 to explore the range of possible conformational changes. Among them, 2apo states were applied to test if the X-ray structure of Pgp and MsbA is reasonable. Whether the ATP hydrolysis takes place according to the alternative catalytic mechanism (Senior et al 1995) or the processive clamp (Janas et al 2003) is still under debate, and therefore states for both mechanisms were considered. A 2ADP state was introduced to mimic the situation when hydrolysis at both ATP binding sites is required according to the processive clamp mechanism, while ADPA_ATPB/apoA_ATPB and ATPA_ADPB/ATPA_apoB represent the states with only one binding site hydrolyzed as postulated by the alternative catalytic mechanism.

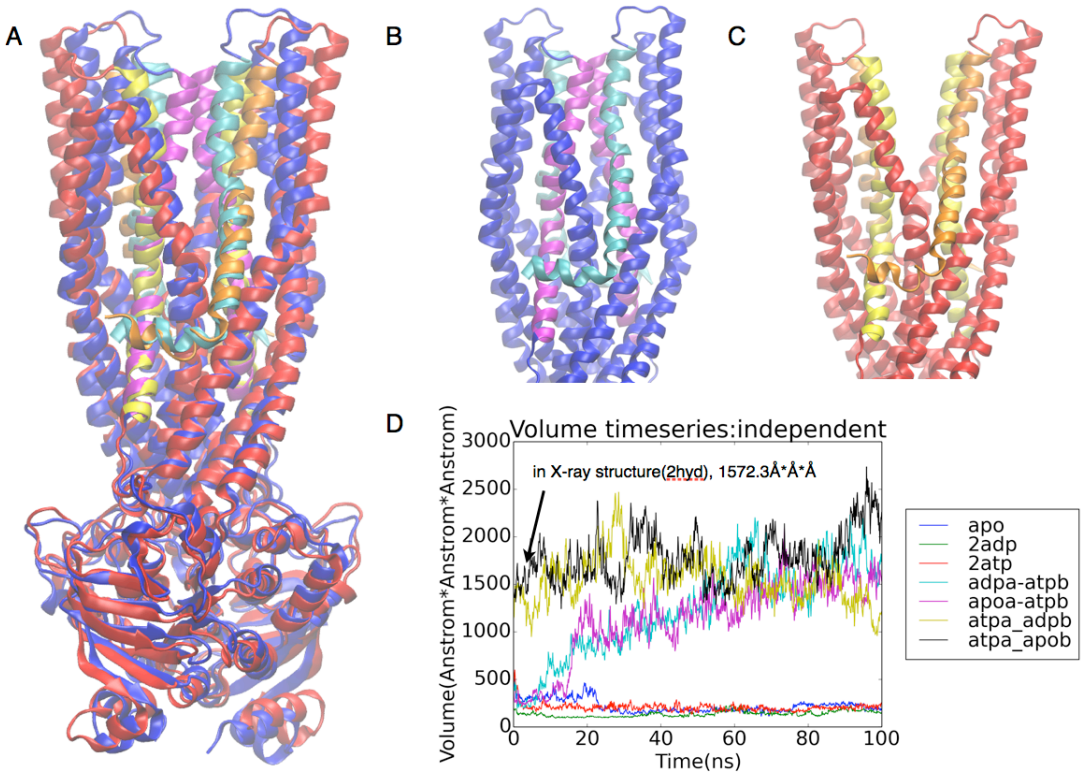

Figure 2-1: Open and closed TMD in Sav1866

A. Superposition of snapshots at the end of simulations with 2ATP and ADPA_ATPB, shown separately of TMD in B and C. Helix 1 is separately highlighted in cyan and orange, helix 6 in purple and yellow, other parts of protein in blue and red. D. Timeseries of the volume of the opening of TMD at the level of extracellular leaflet lipids. Different cases listed in legends are in corresponding small letters.

Simulations show two associated NBDs of Sav in all the states investigated (Fig2-1A). In other words, not a single case with dissociated NBD as in the X-ray structure of apo Pgp (Aller et al 2009) was observed. To characterize the ATP binding sites at the NBD interface, the distance between the signature motif from one subunit and Walker A from the other subunit (binding distance) was measured along the 100ns simulations of the seven systems. Different fluctuations are seen for different nucleotide occupancy states, and the distance variation ranges between 7 to 14 Å (Fig2-2, A-B). Both the largest and the smallest distances are observed in the 2apo state, implying its flexibility. The 2ATP occupancy state seems to be the most stable one with a distance around 9.5 Å. The original state of the X-ray structure, 2ADP, is also stable, with only some minor fluctuations between 9 Å and 10.5 Å.

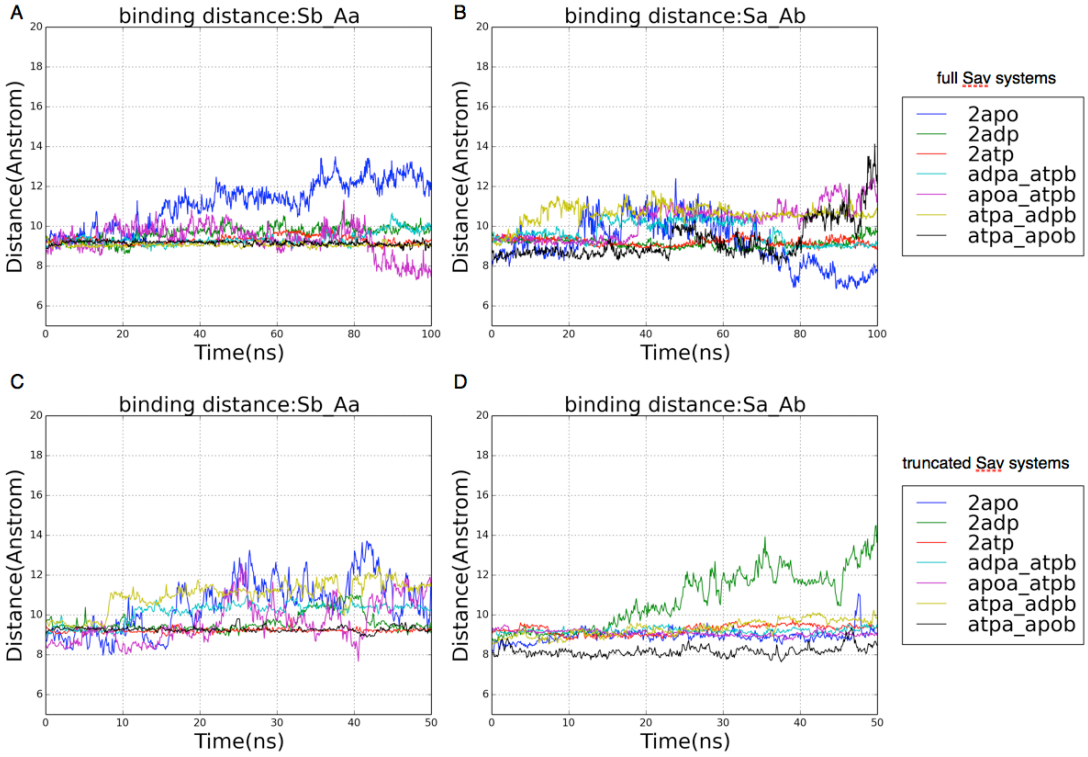

Figure 2-2: Binding distance of Sav1866 in different nucleotide occupancy

Binding distance is the distance between center of mass of signature motif (S) and Walker A (A). a, PROA; b, PROB.

Truncated systems containing only the solvated NBDs and the intracellular parts of the TMDs were also set up and simulated for 50ns. As shown in Fig2-2, C-D, the scale of fluctuations does not change much, confirming the small conformational changes in NBDs. In addition, simulations of Pgp starting from the crystal structure with two separate NBDs were performed and one of the two binding distance reached a magnitude similar to that in Sav (around 13 Å) within 5ns (Fig2-3).

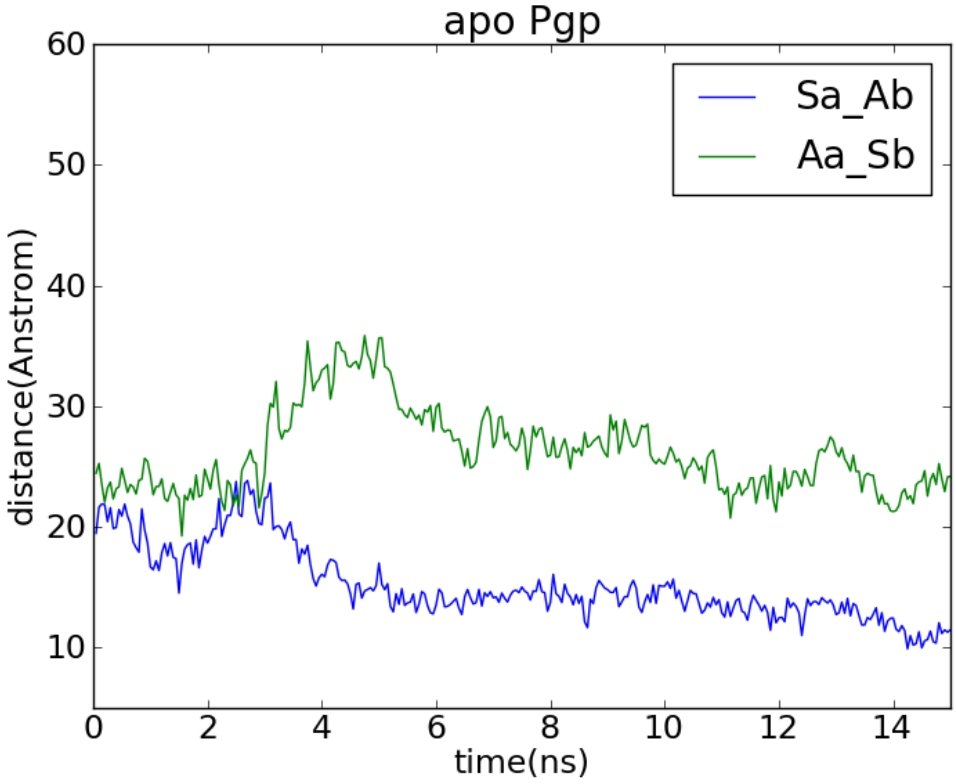

Figure 2-3: Binding distance of apo P-glycoprotein

Labels are the same as that in Fig.2-2.

2.2.2 TMD shows two clearly different conformations

Different from NBD, TMD shows two clearly different conformations, with and without a cavity facing outward, called open and closed conformations (Fig.2-1, B-C). To distinguish these two conformations, volumes of the cavity lying at the level of outer leaflet were calculated (Fig.2-1D). When the nucleotide occupancy states at the two ATP binding sites are the same, i.e. 2apo, 2ATP, 2ADP (symmetric cases), the volume remains small, indicating that they take the closed conformation, shown in Fig.2-1B. On the other hand, when the two ATP binding sites are in different nucleotide occupancy states (asymmetric cases), larger volumes are seen, demonstrating the open conformation as in Fig.2-1C.

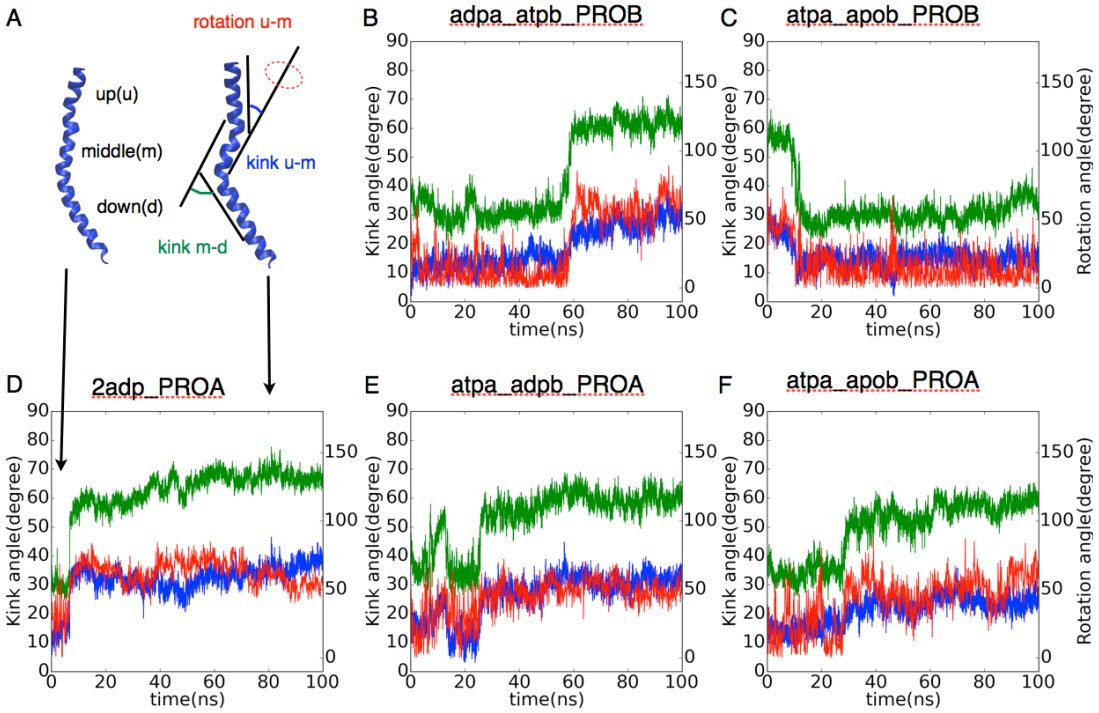

Figure 2-4: Correlation of kink angle and rotation angle of helix6 in Sav1866 simulations

The largest conformational change that distinguishes the open and closed conformations lies in helix 1 and helix 6, as shown in Fig.2-1. Helix 6 can be divided into three parts, up (u), middle (m) and down (d) (Fig.2-4A). As shown in Fig.2-1A, part u seems to experience a rotation around the axis of part m. To further characterize the conformational change in helix 6, kink angle between neighboring parts, u-m and m-d, were calculated. Meanwhile, rotation of part u around the axis of part m was calculated relative to the orientation of X-ray structure. It is called rotation angle u-m. And the rotation angle m-d is obtained in an analogous manner.

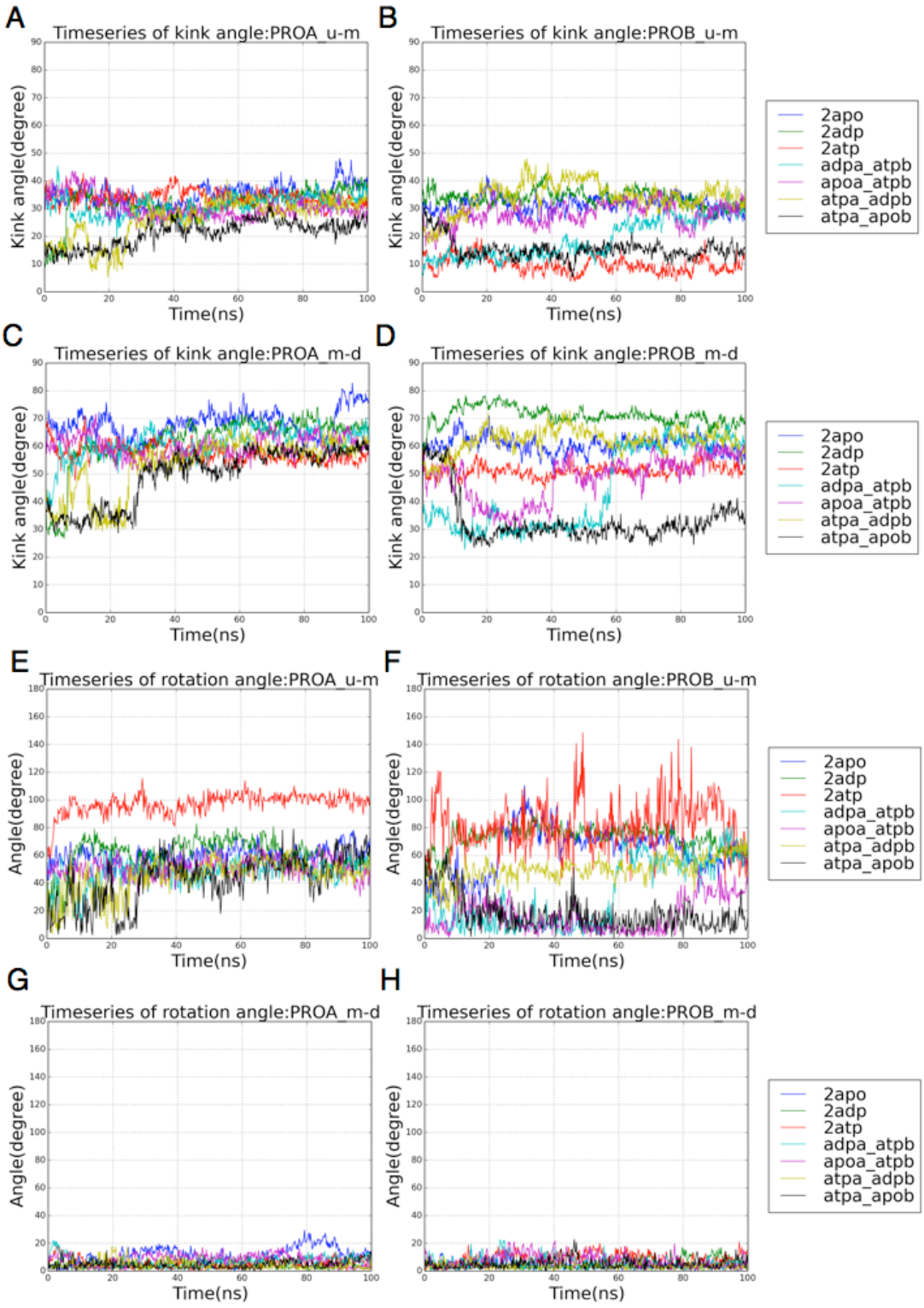

Figure 2-5: Timeseries of kink angle and rotation angle of helix 6 in Sav1866 simulations

As shown in Fig.2-5, the rotation angle m-d does not deviate much from the X-ray structure value for all the cases, while rotation angle u-m and two kink angles vary significantly. Interestingly, the latter three properties change

simultaneously in some cases (Fig.2-4). Such correlation is seen in five cases out of the seven cases, showing similar transition of the two kink angles and rotation

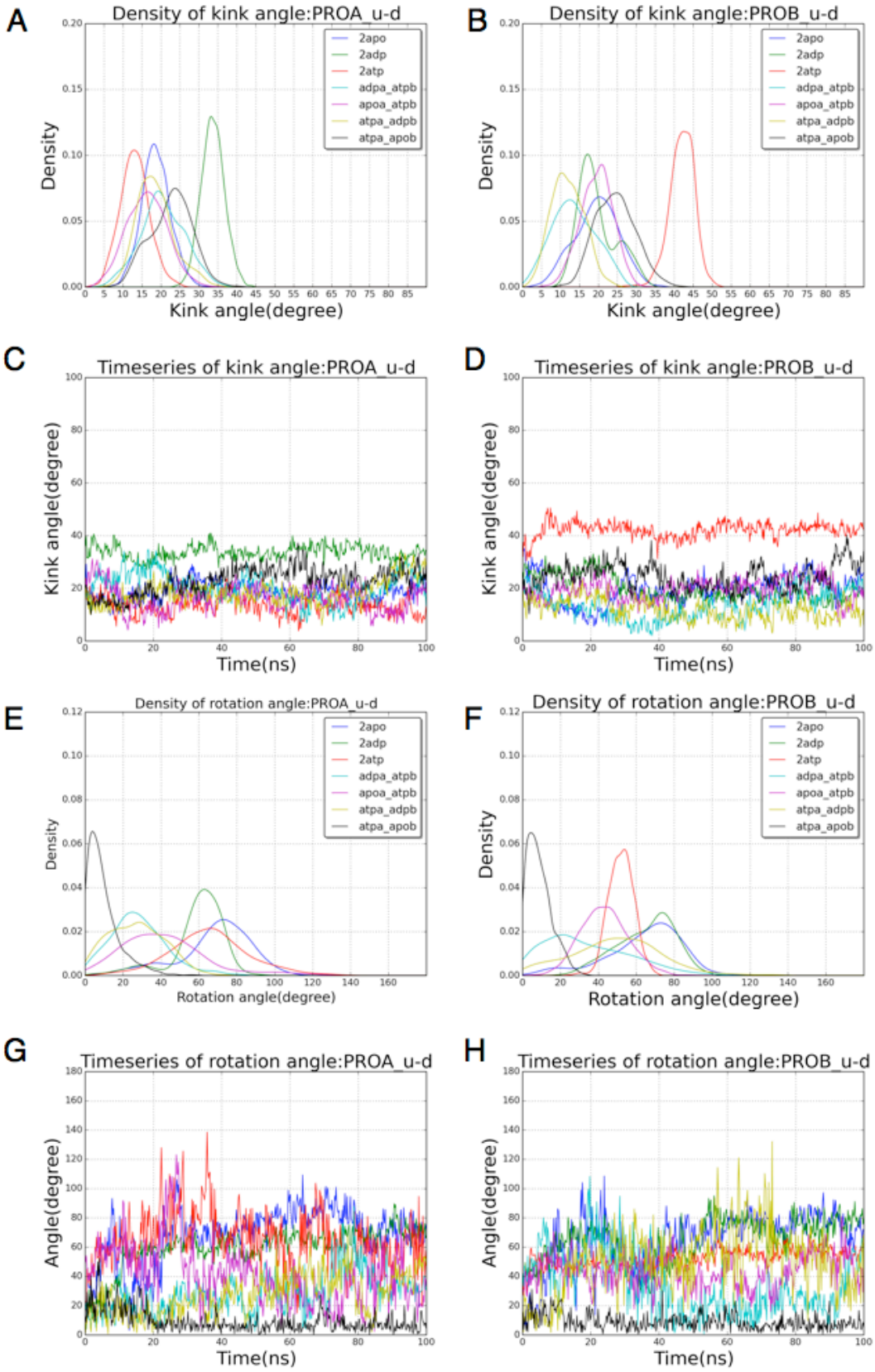

Figure 2-6: Kink angle and rotation angle of helix 1 in Sav1866 simulations

angles m-d. Structurally, helix 6 kinks and rotates part u around the axis of part m at the same time.

Therefore, rotation of helix 6, which appears to be responsible for the transition between open and closed conformations Fig.2-1A is confirmed and characterized. In addition, symmetric cases, especially in PROB (Fig.2-5F), have a bigger rotation angle u-m than asymmetric cases, which accounts for the closed conformation in TMD.

Apart from helix 6 that fills the centre of the TMD, helix 1 also apparently experience a big conformational change to gather around helix 6 that arrives at the centre. Helix 1 could be divided into two parts, upper part (u) and lower part (d) and similar analysis was performed on helix 1. As shown in Fig.2-6, helix 1 in PROB clearly has a high kink angle in the case with two ATPs bound. So does the same kink angle in PROA for the case with two ADPs bound. As for the rotation angle, higher values are seen in the symmetric cases (2ATP, 2ADP, 2apo), while the asymmetric cases (ADPA_ATPB, apoA_ATPB, ATPA_ADPB, ATPA_apoB) take relatively small values. These differences are consistent to the volume variation, which shows graphically that asymmetric cases have an open TMD while symmetric cases have a closed TMD.

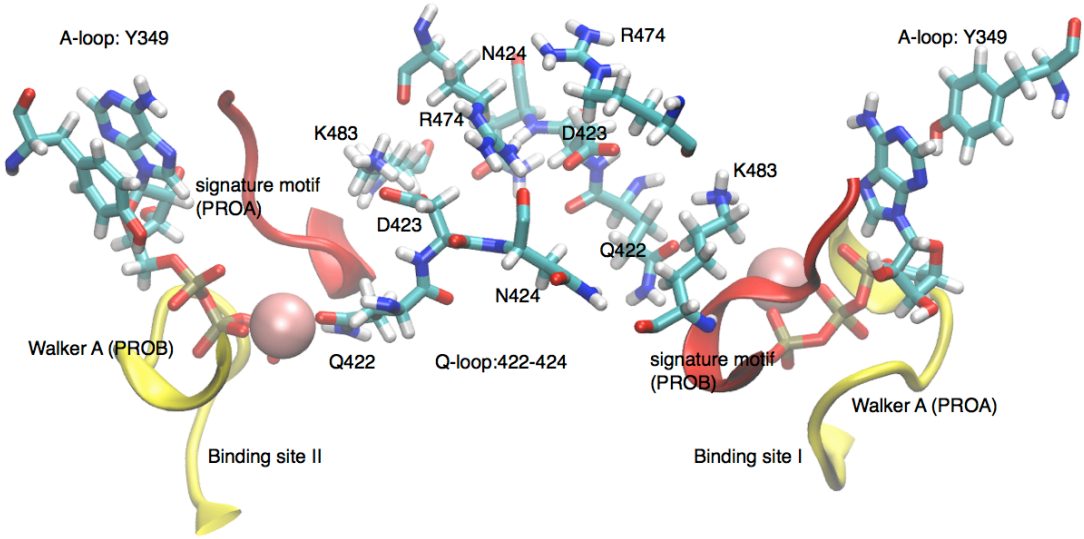

Figure 2-7: Two binding sites of Sav1866 in different configurations

A snapshot at the end of 100ns Sav simulation with 2ATP. In binding site I, Q422 coordinates with the Mg ion, D423 interacts with K483 and N424 interacts with R474. These interactions are not seen in binding site II.

2.2.3 ATP hydrolysis on only one side has a special influence on helix 3 and 4

In order to understand how the small conformational change in NBD could drive a large conformational change in TMD, we scrutinized the structure of NBD. It was found that in the case with two ATP bound, in the binding site with Walker A from PROB (binding site II), there are a series of interactions (Fig.2-7), which are not seen in the other binding site (binding site I). This is consistent with the observation that only in the binding site II, A-loop is well aligned with aromatic ring of ATP. Since the environment of binding site II is more organized than that

of binding site I when ATP is bound, the organized state is taken as a typical ATP bound state.

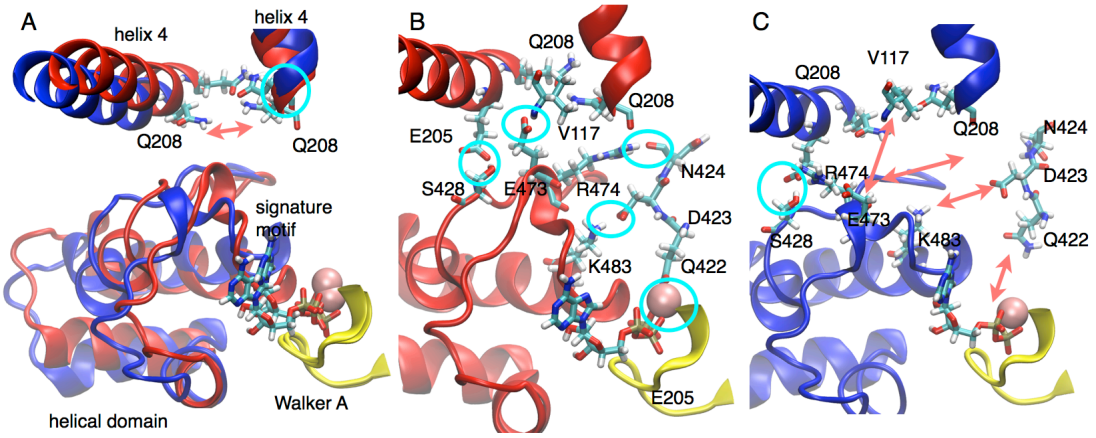

Figure 2-8: Rotation of helical domain upon ATP hydrolysis

Snapshots of binding site II at the end of 100ns simulations. Red, 2ATP; blue, ATPA_ADPB

Among these interactions, three residues in Q-loop are involved: 1) Q422 coordinates the catalytic cofactor magnesium ion; 2) D423 forms a salt-bridge with K483, which follows the end of signature motif; 3) N424 forms a H-bond with R474, which belongs to X-loop. Besides R474, another residue from X-loop, E473, forms a H-bond with main chain of V117 in helix3.

To learn about the conformational changes resulting from variations of the nucleotides, we superimposed the snapshots from simulations of systems in different nucleotide binding states. Given that binding site I does not reach a stable state when ATP is bound, cases with different nucleotides bound at the organized binding site II were compared. It was found that when binding site II is occupied by ADP instead of ATP, while keeping ATP at the other binding site, the helical sub-domain, one of the two sub-domains constituting NBD, experiences a rotation (Fig.2-8A). It suggests that the binding site may response in the same way upon ATP hydrolysis. Scrutiny of the structures reveals that all the interactions in the organized ATP bound state mentioned above are lost (Fig.2-8, B-C), while the H-bond between E205 and S428 next to them exists in both cases. Thus, the breakage of some interactions and the remaining interactions together cause the rotation.

To identify how the rotation and the breakage of these interactions play a role in the coupling between NBD and TMD, it was noticed that the signature motif, which sandwiches an ATP with Walker A, lies close to K483. In other words, K483 could respond to the variation of nucleotide binding site in the ATP hydrolysis cycle. Furthermore, as seen in Fig.2-7, V117 belongs to helix 3, and the two residues Q208 from helix 4 are more separated with ADP in binding site II than that with ATP. Thus, V117 and Q208 constitute the interface between NBD and TMD. Therefore, these interactions form a signaling route from ATP binding sites of NBD to helix 3 and helix 4 of TMD.

In order to understand if the separation for Q208 is important in coupling between the conformational changes in NBD and TMD, we calculate the distance between two nitrogen atoms. Interestingly, 2apo, ATPA_ADPB, and ADPA_ATPB stand out with a large 208-208 separation (Fig.2-9), while the others remain in a small separation. Given the flexibility of the 2apo state is seen in the binding distance, it is reasonable to have a larger 208-208 separation. For the other two states, both include one ATP at one binding site and one ADP at the other, corresponding to the state in which the breakage of some interactions and a rotation of helical domain are seen. If the rotation of the helical domain is taken as an important conformational change upon ATP hydrolysis that contribute to the coupling between TMD and NBD, the 208-208 separations may be also an important element in coupling. In particular, a larger 208-208 separation seems to correlate with the opening of the TMD. However, this is not the case. In the other two asymmetric cases, apoA_ATPB and ATPA_apoB, although their TMDs take open conformations, the 208-208 separations remain small. Moreover, the closed TMD in 2apo comes with a large 208-208 separation. This indicates that a large 208-208 separation could contribute to the opening of the TMD, but is not an indispensible element. The flexibility of the apo state in at least one of the two binding sites may render this element unrelated to the opening of the TMD. Some other elements instead of the 208-208 separation should be responsible for the opening of TMD when one or two binding sites are in apo state.

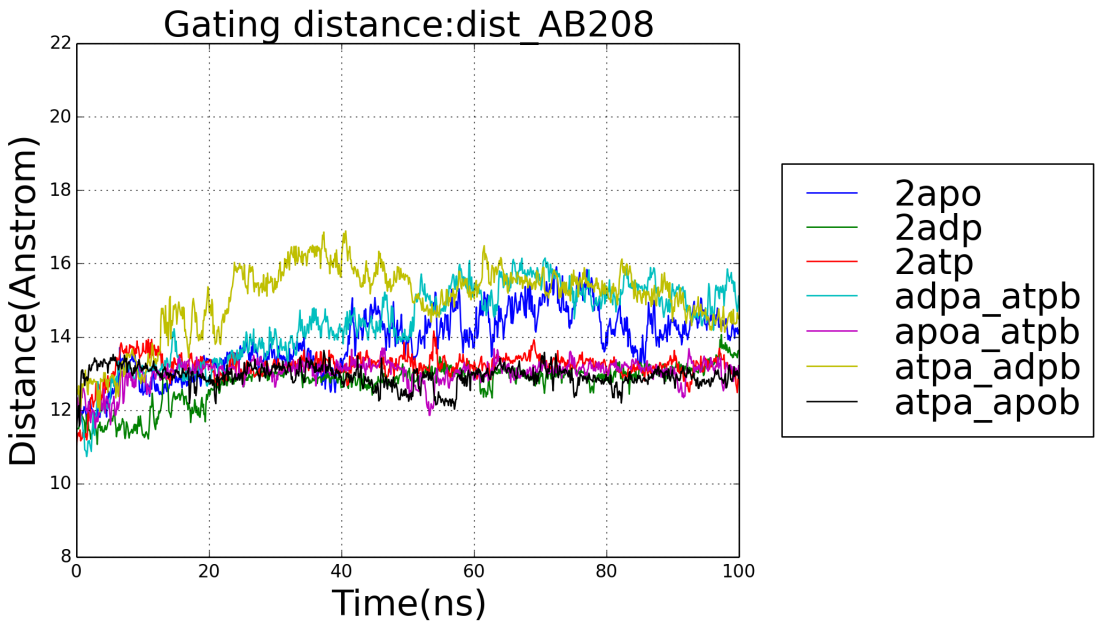

Figure 2-9: Distance between two 208 residues

2.2.4 A network formed by helix 1, helix 3, helix 4 and helix 6

Based on the breakage of the H-bond between V117 and E473 and the larger separation between Q208 from helix 4 found in the states with one ATP and one ADP bound, it implies that the small change in NBD upon ATP hydrolysis could bring some conformational change in helix 3 and helix 4 of TMD. However, the key conformational change in TMD identified above is helix 1 and helix 6. How

do helix 1 and helix 6 change the conformation during ATP hydrolysis? Is it caused directly by the conformational change in NBD, or is it influenced by helix 3 and/or helix 4, which experience variation upon ATP hydrolysis?

The conformation with two ATPs bound shows no direct network between helix 6 and NBD except that the NBD connects to the end of helix 6, which is far away from the ATP binding sites (Fig.2-10A). Therefore, the conformational change in helix 6 might depend on a network formed by helix 3, helix 4 and helix 6. Such a network was found in the region where they cross each other. As shown in Fig.2-10C, R186 and R190 from helix 4 both form salt-bridges with D312 from helix 6, while D127 and R123 from helix3 form salt-bridges with R313 and Q316 from helix6 separately. With such network, conformational changes at Q208 and E205 of helix 4 and V117 of helix 3 could be transmitted to helix 6 and hence justify the identified conformational change of helix 6.

As regards to the rotation of helix 1 (Fig.2-10B), two parts of interactions with helix 6 may be related. It seems that the top two polar residues of helix 6, Thr276 and Thr279, attract the charged residue on the top of helix 1, Lys38 and Asp42. In addition, Arg4 could move with Asp319 due to the salt-bridge between them. Thus, a network formed by helix 1, helix 3, helix 4 and helix 6 could transmit the signals from the bottom of helix 3 and helix 4 to helix 1 and helix 6, causing different conformations in TMD.

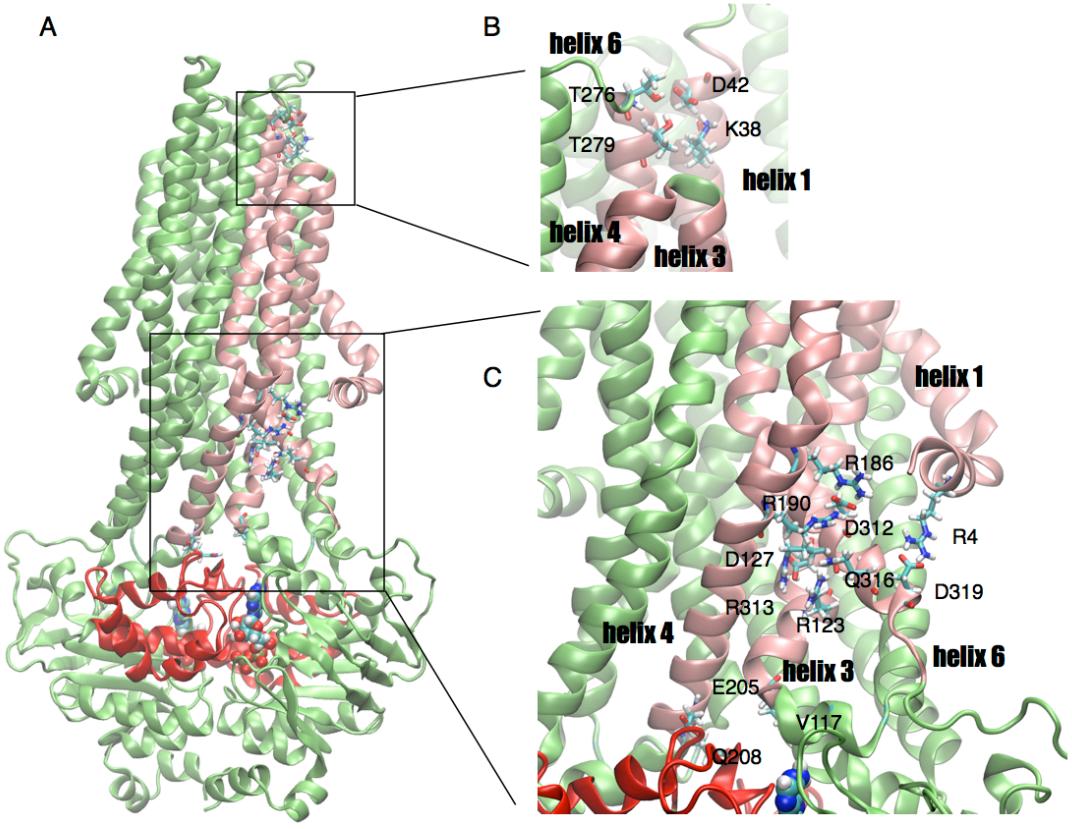

Figure 2-10: Network among helix 1, helix 3, helix 4 and helix 6

Snapshot at the end of 100ns' simulations with 2ATP. Red, helical domain (residue 426-494); cyan, IC; pink, helix1 (residue 1 to 45), helix 3 (residue 116 to 158), helix 4 (residue 161 to 208), helix 6 (residue 277 to 322).

2.3 Discussion:

2.3.1 Smart small changes in NBD instead of the dissociation of NBD trigger the transport cycle

The issue whether NBD will completely dissociate or not in ABC transporters has not been solved yet. X-ray structures of MsbA (Ward et al 2007) and Pgp (Aller et al 2009) show a big separation between two NBD, while that of ABCB10 (Shintre et al 2013) and T287/288 (Hohl et al 2012) display an associated state.

Two X-ray structures for apo MsbA with different NBD separations, a closed state and an open state have implied the flexibility of the apo state. It was consistent with flexible binding distances and the 208-208 distances observed in our simulations of the apo state. However, the separations of the two NBD in the simulations of apo Sav and Pgp are much smaller than that displayed by the X-ray structure of MsbA with the two NBDs largely separated. This indicates that although dissociation of NBD could be caught in crystal structures of apo ABC transporters such as MsbA and Pgp, it does not seem to be a stable state.

In addition, since X-link in the terminal ends of two NBDs of Pgp does not interfere with transport (Verhalen et al 2012), but could even activate it (Loo et al 2012), it demonstrates that the dissociation of NBD is not required for the transporting cycle. More importantly, it is demonstrated by target molecular dynamic simulations of Sav (St-Pierre et al 2012) that the large conformational change in NBD obtained by pulling apart the two NBD could not change the conformation of TMD. Instead, as shown in our simulations, some small changes could lead to large conformational changes in TMD, potentially revealing a more efficient mechanism.

2.3.2 ATP hydrolysis on a single side is sufficient to trigger conformational changes in NBD and TMD

Another controversial issue is whether ATP binding or ATP hydrolysis drives the conformational changes of TMD. Based on the finding that ATP binding promotes the association of NBD, it was argued that ATP binding instead of ATP hydrolysis is the driving force of the transport cycle (Smith et al 2002). Despite that the complete association/dissociation of the two NBDs is not essential in the transport cycle, it remains that such mechanism could still apply but involves smaller changes of conformation.

Since the variation observed in 2D crystal structures of AMP-PNP-bound Pgp revealed large conformational changes while the subsequent ATP hydrolysis introduced more limited changes (Rosenberg et al 2001), such a big change upon ATP binding instead of ATP hydrolysis was proposed to be the driving force. Similar conclusion was drawn from the variation of drug-binding affinity upon ATP binding (Vergani et al 2003; Aleksandrov et al 2000; Martin et al 2001; Martin et al 2000; Rosenberg et al 2001) . Given the apo state is flexible as seen in apo MsbA structures, larger conformational change could be expected. However, a large change does not imply that it is essential for transport.

As shown in the snapshots from the simulations of the 2apo state and 2ATP bound states, they both hold a closed TMD, implying that ATP binding itself is not enough to drive conformational changes in TMD. However, in all asymmetric

cases, an open TMD is seen, indicating that hydrolysis of ATP on one binding site while keeping the other with ATP bound is required for conformational change in TMD. The 208-208 separation seems essential to the coupling between the NBD and TMD. Since the 208-208 separation is seen only in the state with one ATP and one ADP bound, ATP hydrolysis instead of ATP binding on one binding site is desirable for coupling. Additionally, binding of the "next" ATP to take place of ADP or fill the apo binding site could close the cavity in TMD by a similar coupling, which is also essential in the transport cycle.

2.3.3 Rotation of helix 6

Helix 6 has been proposed by different mutation studies to be central in the transport mechanism. Simple mutations on some residues of helix lead to varied drug resistance profile, indicating its role in drug binding and/or translocation6 (Loo, & Clarke 1993; Loo, & Clarke 1994a; Devine et al 1992; Ma et al 1997) . This is consistent with the observation in our simulations that helix 6 constitutes the main difference between the open and closed TMD conformations.

More importantly, mutations on a series of residues in TM6 of Pgp that cover different side of helix 6 mediate Pgp function, implying a possible rotation of TM6 (Song, & Melera 2001). Such rotation is strongly supported by some cross-linking studies. In particular, helix 6 is able to crosslink with three consecutive residues in helix 4 and helix10 (Loo, & Clarke 2000). Meanwhile, in the presence of ATP, crosslinking of mutant L339C (TM6)/ V982C (TM12) on human Pgp was decreased while that of F343C (TM6)/ V982C (TM12) was enhanced (Loo, & Clarke 2001a). Although the sequence identity of helix 6 is as low as the entire TMD, the common existence of helix 6 and conservation of helix6 rotation demonstrate a similar role of this helix. Interestingly, such rotation was demonstrated in our simulations. Specially, the rotation occurs on the upper part of helix 6, and is correlated with the variation of a kink angle in helix 6.

Such rotation could be also applicable and important for transporters to generate different conformations of TMD to recruit and release the allocrites. It was already seen in another ABC transporter, Maltose transporter. By comparison of the inward-facing and outward-facing structure of Maltose transporter, it was identified that rotation of helices defines the transition of the two conformations (Khare et al 2009).

2.3.4 Q-loop and X-loop in coupling between NBD and TMD

In the investigation of the coupling between NBD and TMD, Q-loop and X-loop have been proposed to transmit the conformational change. These two loops are highly conserved in ABC transporters (Seeger, & van Veen 2009), but their functions are still unclear.

Q-loop links two sub-domains, the helical domain and the core domain. Since the helical domain is seen to rotate upon ATP binding in different studies (Verdon et al 2003; Orelle et al 2010; Jones, & George 2011), Q-loop is expected to experience some conformational change as well, which was shown by the flexibility displayed in NMR studies (Wang et al 2004). By scrutinizing the position of Q-loop in X-ray structures, two possible functions were proposed. As shown in the Sav1866 structure (Dawson, & Locher 2007), Q-loop coordinates

the cofactor Mg^{2+}, which is essential for ATP hydrolysis and hence it may take part in preparation for ATP hydrolysis. In HisP, Q-loop lies next to a water molecule that is thought to be the "attacking" water and hence it might be an activating residue for ATP hydrolysis (Hung et al 1998).

However, Senior and coworkers found that mutation on Q-loop of mouse Mdr3 does not influence Mg-ATP binding, reaction chemistry or interaction with Mg ion, but reduces stimulation of ATPase activity by drugs. They proposed that the Q-loop is involved neither in the activation of the attacking water for ATP hydrolysis, nor in the coordination of the essential Mg^{2+} cofactor, but the interdomain signal communication (Urbatsch et al 2000a). On the other hand, based on reduced binding affinity of Mg-ATP for MRP1 and the fact that Mg-ATP dependent LTC4 transport remains with an increased K_m and V_{max} values, Yang and coworkers argued that the Q-loop plays a role in Mg-ATP binding, not in ATP hydrolysis and inter-domain communications between NBD and TMDs (Yang et al 2011). Nevertheless, since Vmax of drug transport is modified in the latter case, Q-loop should be also involved in coupling between NBD and TMDs. Regarding the difference in Mg-ATP binding in these two cases, given that MRP1 belongs to ABCC subfamily while Pgp belongs to ABCB family, it may have something to do with the structural and functional difference for particular proteins. In addition, if Q-loop plays a role in Mg-ATP binding in preparation for ATP hydrolysis, given that the environment for Mg-ATP binding measurement is different from that of the real hydrolysis, Q-loop mutants do not have to change the Mg-ATP binding affinity measured in experiments.

According to our observations, Q-loop could coordinate the cofactor Mg ion, seen in the organized binding site. With such coordination, the residues nearby were properly placed to interact with the X-loop from the other subunits. Regarding to the X-loop, it was shown in our simulations to interact with the bottom residues of helix 3 and helix 4. This is consistent with the finding in antigen ABC transport complex TAP that either substrate binding or translocation can be blocked by cross-linking the X-loop to coupling helix 1 or 2 (Oancea et al 2009), which lies at the bottom of helix 3 and helix 4 separately. Therefore, the Q-loop and X-loop collaborate to transmit the conformational changes of TMD and NBD. The role of Q-loop in ATP-Mg binding and coupling between TMD and NBD could not be separated.

2.4 Conclusion

Our work for the first time demonstrates unambiguous conformational change in trans-membrane helices. The TMD could take two different conformations, open conformation and closed conformation. Symmetric nucleotide occupancy states adopt the closed conformation while the open conformation is seen in asymmetric nucleotide occupancy states. Although the TMDs adpot different conformations, conformational variation in the NBDs is small. The situation with two completely dissociated NBDs was not observed, even in the absence of nucleotides.

Q-loop and X-loop were identified to be two essential motifs in the coupling between TMD and NBD. In addition, the distance of the two Q208 could also be essential in coupling and used to investigate the signaling route. Since it failed to drive the transition of the conformation in TMD by controlling the distance

between two Q208 residues only (data not shown), some other elements should be combined to test the conformational change in TMD.

2.5 Method

2.5.1 System preparations

In order to explore the conformational changes of the Pgp and Sav structures, different molecular systems were set up using the CHARMM-GUI web service. A system with apo Pgp based on the crystal structure (PDB ID: 3g5u) was set up for 100ns simulation. Based on the Sav structure with 2 ADP bound (PDB ID: 2hyd), 7 different systems of Sav with different nucleotide binding states were set up, 2apo, 2ADP, 2ATP, ADPA-ATPB, apoA-ATPB, ATPA-ADPB, ATPA-apoB, labeled in small letters in the figure legends. Here, the first three labels represent symmetric nucleotide binding states in two sites, both apo, both ADP, or both ATP, while the two binding sites of the latter four cases are in different states, described separately in a similar way before and after "-". The binding site constituted by Walker A from PROA is called binding site I, while the one constituted by Walker A from PROB is called binding site II. "ADPA-ATPB" means one ADP is bound at binding site I while one ATP is bound at binding site II. Analogous descriptions are given for the other labels. In all the systems with nucleotides bound, a magnesium ion is always included next to the nucleotide. ADP coordinates are directly taken from the Sav structure. The position of Mg and ATP is determined by alignment of NBD with MJ0796 (PDB: 1l2t). The latter includes ATP and a sodium ion. The sodium ion lies at the position where Mg ion should be found. Accordingly, after alignment of NBD of MJ0796 to the Sav structure, ATP and Na coordinates were taken as the initial position of ATP and Mg ion in the systems of Sav for 100 ns simulations.

Truncated Sav systems were set up by using only the intracellular part of the protein, including NBD as well as the portion of the trans-membrane helices that lie at the cytosolic side of the membrane, i.e., residue 151 to 165, 369 to 626, and 894 to 915. The simulations last 50ns.

All the systems were set up under periodic boundary conditions in a NPT ensemble with a temperature of 323.15K and a pressure of 1atm. The rectangular periodic system box for the Pgp and full Sav systems contains two bilayers composed of around 190 1-palmitoyl-2-oleoyl-sn-glycero-3-phosphocholine (POPC) surrounding the Pgp or Sav at the level of their TMDs. The membrane is positioned according to OPM (Orientation of proteins in membrane database). Both the full and truncated systems were solvated by water molecules on the top and the bottom of the protein (around 24300 for full systems, 21550 for truncated systems), and potassium/chloride ions were added to neutralize the systems and imitate a 150 mM KCl solution. The timestep of all the simulations is 2 fs.

2.5.2 Molecular simulations

Simulations were carried out using NAMD ({Phillips 2005}) with the following parameters. The cutoff for both the Lennard-Jones and Coulomb interactions was set to 12 Å. The switching function begins to take effect at 10 Å. The non-bonded pair list is updated every 10 steps, which includes all the pairs within 16 Å. The

non-bonded forces were calculated every step. Long-ranged electrostatic interactions were treated every step by Particle Mesh Ewald (PME) method with the interpolation order of 6. Langevin dynamics was used on non-hydrogen atoms to control the temperature with a damping coefficient of 1/ps while constant pressure was controlled by a Langevin piston Nosé-Hoover method with the oscillation period of 50 fs and the oscillation decay time of 25 fs. All bonds involving hydrogen atoms are constrained to the normal length in the parameter file with SHAKE algorithm.

2.5.3 Structural analysis

OpenStructure (Biasini et al 2010) was the main tool used for the analysis of the conformational changes along the simulation trajectories. The distance between the signature motif (center of mass of residue 478 to 482) from one NBD and Walker A (center of mass of residue 374 to 381) from the other NBD is calculated for simulations of truncated Sav systems, full Sav systems and the Pgp system, named as "binding distance". The label "Sa_Ab" indicates the distance between the signature motif of PROA and Walker A of PROB. Apart from the binding distance, the distance between the two 208 residues was also calculated for simulations of full Sav systems.

Helix 6 is divided into 3 parts, residues 277 to 290, 291 to 300 and 301 to 319. According to their position, they were labeled as part u (upper), m (middle), and d (down). Kink angles were calculated between u and m or m and d by determining their vectors and the angles between the two vectors. Rotation angles u-m and m-d are the rotating angles relative to X-ray structure around axis m and d. Rotation angle u-m were determined as follows: 1) align part m and two residues before and after part m of snapshots to the X-ray structure; 2) calculate the projections of the u upon the surface with m as the normal vector for snapshots in the simulations as well as X-ray structure; 3) calculate the angles between such projections of any snapshot and that of X-ray structures. For rotation angle m-d, similar procedures were followed.

A similar analysis was performed on helix1. Helix1 is divided into two parts with a kink at residue 26. The two parts, residue 12 to 26 and 27 to 45, are labeled as part d (down) and u (up). The kink angle between u and d was calculated by determining the angle between the vectors of part u and d. Rotation angle of part u around d was calculated as in helix 6.

Besides OpenStructure, HOLE (Smart et al 1996) was used to calculate the radius along the cavity of the TMD after the snapshots were aligned to X-ray structure with VMD (Humphrey et al 1996). With the data of radius, volumes of the cavity of the TMD were calculated by Python. Only the volume at the level of extracellular leaflet is included.

3 Conformational changes required for chloride ion permeation in ClC-ec1 exchanger

3.1 Introduction

Members of the ClC family transport chloride (Cl^-) , nitrate ($NO3^-$), bromide (Br^-), iodide (I^-) or thiocyanate (SCN^-) ion across cell membranes and assist in many crucial cellular functions in both prokaryotic and eukaryotic cells (Iyer et al 2002; Miller 2006) . Mutations in these proteins cause many hereditary diseases, including myotonia congenita, Dent's disease, Bartter's syndrome, osteopetrosis, Neuronal Ceroid Lipofusciosis and idiopathic epilepsy (Hübner, & Jentsch 2002). Interestingly, ClC family is comprised of both channels and antiporters, which are traditionally considered to be structurally distinct. The study of ClC family proteins could provide insights on the boundary between channels and transporters, to understand how these proteins work in vivo, and to create a basis for the development of more efficient drugs to treat related diseases.

In 2002, Dutzler and coworkers resolved the high-resolution X-ray structure of a prokaryotic ClC protein (Dutzler et al 2002), ClC-ec1, which promotes the cell expulsion of protons in response to extreme acid conditions, conferring acid resistance to the bacteria. Due to the availability of the structure and the similarity to other ClC family members, ClC-ec1 is often taken as a model protein to investigate ClC transport mechanisms.

ClC-ec1 is a membrane-embedded homodimer. Each subunit allows the exchange of two Cl^- for one proton (H^+) (Robertson et al 2010), while the two subunits are coupled by a slow gating process. Going through the protein, Cl- and H+ follow different pathways (Accardi et al 2005). Four Cl- binding sites were determined and are likely to constitute the Cl- permeation pathway (Fig.3-1A). Among them, two binding sites, Scen and Sint, are observed in the wild type ClC-ec1 structure, while the E148A and E148Q mutant structures show a third binding site close to the extracellular bulk, which was named Sext (Dutzler et al 2003). In addition, binding energy calculation based on the structure of ClC-ec1 indicated a fourth binding site, which is on the extracellular side of Sext and hence is called Sext* (Faraldo-Gómez, & Roux 2004). According to the pseudo-symmetry of the two domains constituting one subunit, Sext* lies at a position symmetric to Sint. Different from the clear binding sites and pathway for chloride ion transport, the pathway for proton transport is still obscure. E148 and E203 are considered important, as either E148A or E203A blocks proton transport. However, the pathway between E148 and E203 is still unclear.

Apart from the side chain movement of a conserved Glu at Sext (Glu148 in ClC-ec1), it remains unclear whether ClC channels and antiporters have to undergo additional conformational changes to sustain ion transport. The apparently different affinities in the open and closed states in the ClC channel, ClC-K (Gradogna et al 2010) and ClC-0 (Accardi, & Pusch 2003) have implied some conformational change, while many other studies demonstrated conformational changes in the interface between the two subunits and at the C-terminus.

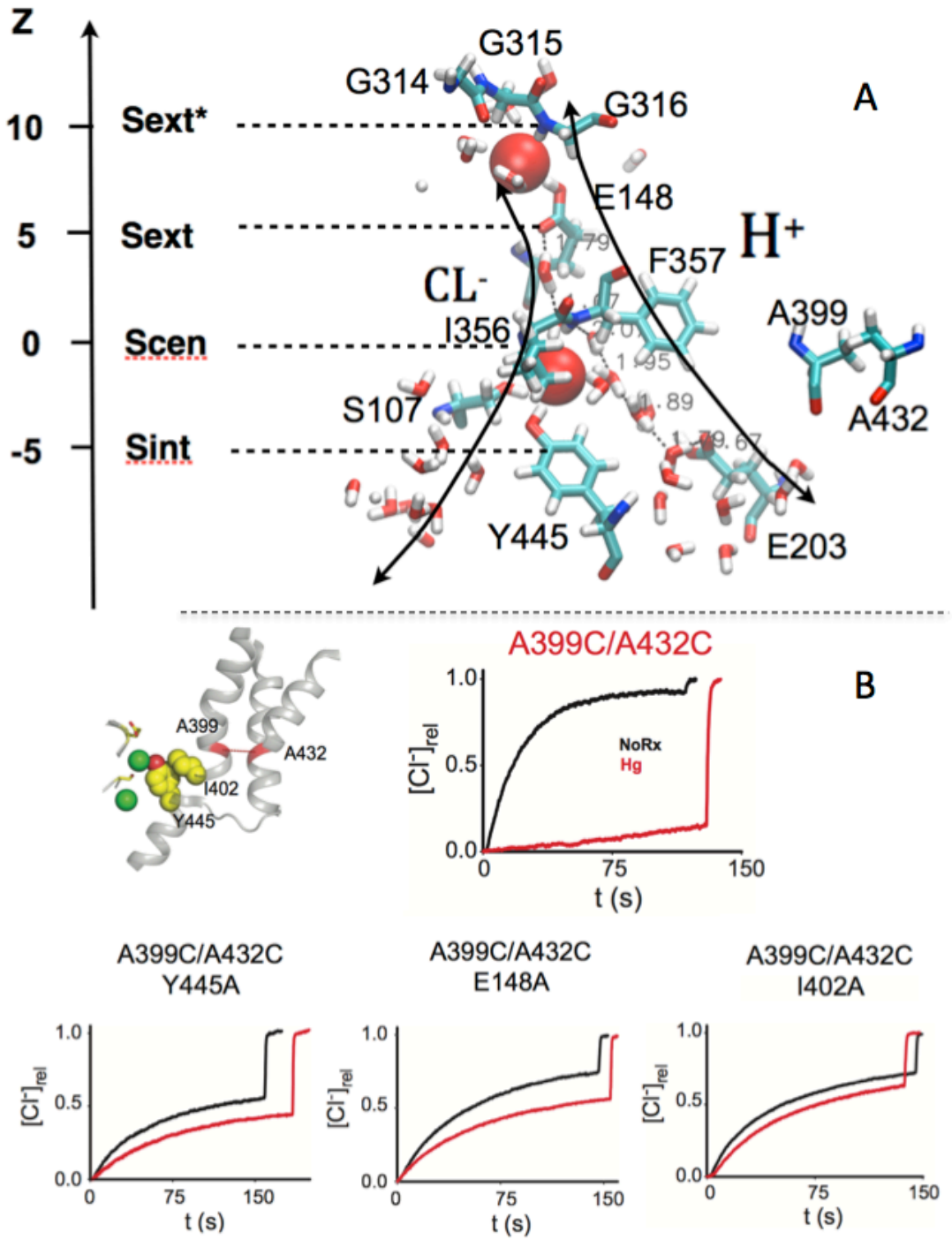

Figure 3-1: Structure of ClC and X-link experiment

The subunit interface was claimed to undergo changes by Elvington and coworkers (Elvington et al 2009). They utilized solution-state 19F-NMR to pinpoint regions of conformational change in ClC-ec1 and showed signal change on not only the chloride ion permeation pathway (Y445) but also at the subunit interface (Y419) upon changing pH or chloride ion concentration. Normal mode analysis of ClC-ec1 suggests that the alternating exposure of both ClC pores to both sides of the membrane is accompanied by conformational changes at the interface (Miloshevsky et al 2010).

Conformational changes of labelled C-termini in ClC-0 were suggested by the different FRET signals seen in the open and closed states (Bykova et al 2006). As a response to the variation of the C-termini, helix R could also experience some conformational changes. With the environment-sensitive fluorophore in ClC-ec1, the change of helix R has been measured, showing varied fluorescence changes upon acidification and change of chloride ion concentration (Bell et al 2006). While Picollo and coworkers have shown that chloride ion uptake mediated by E148 is almost pH-independent (Picollo et al 2012), this pH-dependent fluorescence change remains when E148 is substituted by alanine.

Although the conformational changes at the subunit interface and C-terminal ends were usually found separately, they correlate somehow to each other and may be coupled. For example, point mutation at the C-termini of ClC-5 impedes its function because the mutation abrogates ATP binding and hence prevents the dimerization of the two subunits (Wellhauser et al 2011). Additionally, the common gate of CLH-3b, a ClC-1/2/Ka/Kb channel homolog, which is activated by GCK-3 kinase-mediated phosphorylation on the cytoplasmic C-terminus, opens with conformational changes at the subunit interface (Yamada et al 2013).

With the above investigation, it seems clear that there exists some conformational changes, at least at the subunit interface, C-terminus and helix R, but how these conformational changes relate to the ion transport cycle is still obscure. Interestingly, in efflux assay, a crosslink (X-link) between residue 399 and 432, which is at a distance from the permeation pathway, prevents ion permeation, implying again conformational changes beyond the pathway (Fig3-1). In addition, this X-link effect is removed partly in E148A and mostly in mutants Y445A and I402A, indicating that these residues may be involved in the conformational change that is restrained by X-link.

In order to understand why the X-link inhibit the ion permeation in the efflux assay, and further uncover the mystery of the conformational change required in the transporting cycle, we set up molecular dynamic systems with and without the X-link and performed simulations. Structural and free energy analyses demonstrate that the opening of the intracellular gate is required for chloride ion permeation in ClC-ec1 and is controlled by the interaction of the bottom of helix O with Y445.

3.2 Results

3.2.1 Chloride ion permeation requires an open intracellular gate

Among the three Cl- binding sites identified by X-ray crystallography, Scen has the highest affinity (K_d=0.72mM) while Sint has the lowest affinity (K_d>20mM) in the single ion binding state (Picollo et al 2009). Consistent with this fact, in most of our simulations starting from the wild type ClC-ec1 X-ray structure with one ion at Scen and one ion at Sint, the ion from Sint leaves the binding site within 1 ns and usually reaches the bulk within 5 ns, while the ion at Scen remains stable at its original position. The stability of the ion at Scen can be attributed to the constriction region formed by S107 and Y445 (Fig. 3-1A). This constriction acts as a gate and prevents the ion from reaching the intracellular binding site and hence is called "intracellular gate". Therefore, conformational changes at the intracellular gate are essential for chloride ion permeation.

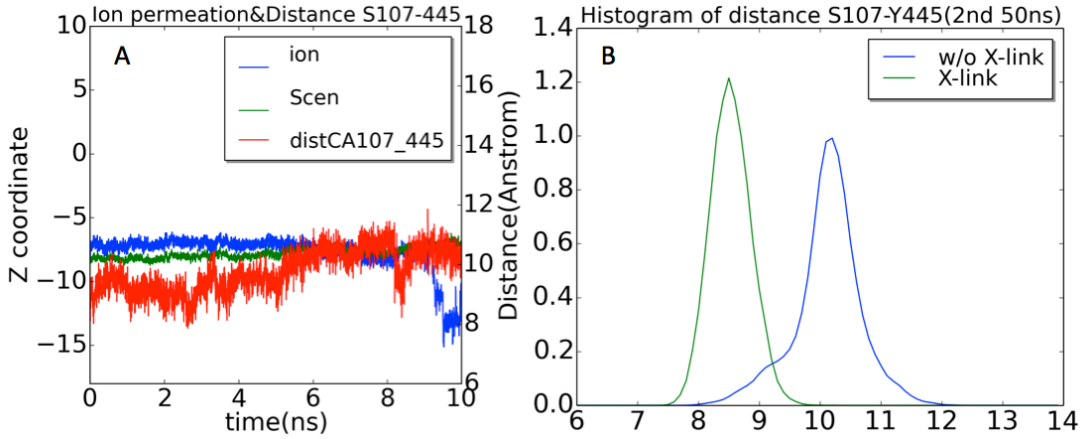

Figure 3-2: Ion permeation and size of the intracellular gate

A. Timeseries of z coordinate of ion, Scen and distance between CA atoms of S107 and Y445. B. Histogram of the distance between CA atoms of S107 and Y445 of the 2nd 50ns out of 100ns simulations

Despite this constriction, ion translocation is observed in our WT simulations, in which the ion from Scen reaches Sint and further leaves the pore (Fig.3-2, blue and green). This event provides us with the opportunity to investigate how the permeation occurs. Given that the intracellular gate is believed to regulate ion permeation, the size of the intracellular gate is measured, characterized by the distance between CA of S107 and Y445. The simulations show that before the ion transition, the intracellular gate starts to fluctuate around bigger values (10.5Å) than before (9Å) (Fig.3-2A, red). This suggests that the transport of chloride ions needs an opening of the intracellular gate.

In the 100ns simulations, the intracellular gate remains open, as further shown by the histogram of Fig.3-2B (blue), revealing a peak around 10.2Å. When the X-link is applied, the histogram shows a peak around 8.5Å, clearly smaller than that without the X-link. This smaller intracellular gate is consistent with unfavorable permeation in the X-link experiment.

3.2.2 The opening of the intracellular gate is restrained by the X-link resulting in higher free energy barriers for permeation

In order to get a complete picture of the X-link effect on ion permeation and further examine the importance of the size of the intracellular gate, free energy calculations for the ion permeation were performed.

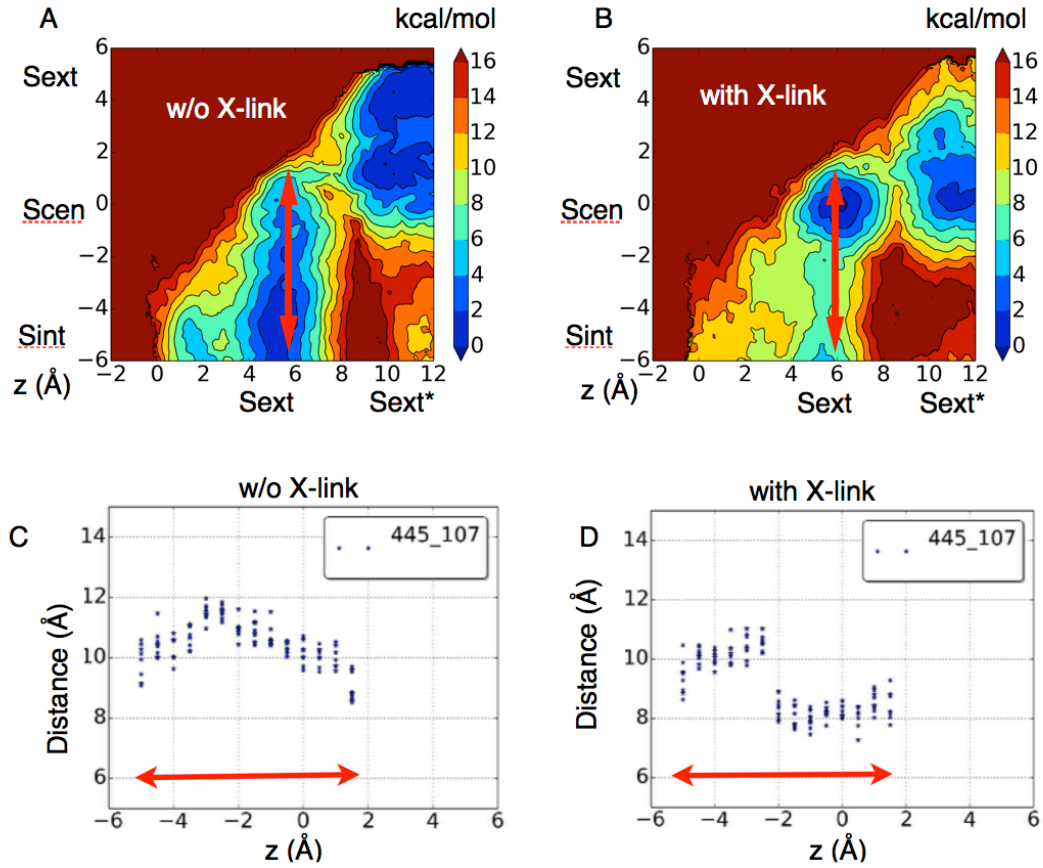

Figure 3-3: Free energy calculation of ion permeation and variation of the intracellular gate

Free energy calculations with the z positions of two ions in the pore relative to Scen as the reaction coordinates. Without X-link, A; with X-link, B. The variation of the distance between CA atoms of S107 and Y445 when the lower ion passes the intracellular gate with the top ion at Sext. Without X-link, C; with-Xlink, D.

Given that multi-ion occupancy states were identified notably by X-ray crystallography, two ions were included in the system for free energy calculations and their position along the z direction constitute the two reaction coordinates. Specifically, the red arrows in Fig.3-3A and Fig.3-3B correspond to the movement of an ion between Scen and Sint, while the other ion stays in Sext. Fig.3A shows a low permeation free energy barrier (on the order of 2 to 4 kcal/mol) in the absence of X-link. When X-link is applied, an apparently bigger energy barrier is seen (8 to 10 kcal/mol). Hence, the X-link effect in the efflux essay experiment is solidly justified by the difference in the ion permeation free energy barrier.

In order to understand if this barrier difference is related to the size of the intracellular gate, the distance between CA of S107 and Y445 is measured along the red arrow. In wild type, when the ion goes from Scen to Sint, the size of the gate grows gradually, implying that the gate is flexible and easy to open. In the

case with X-link, however, the gate looks quite rigid, which shows a jump of -3 Å. Therefore, it is demonstrated that the X-link prevents ion permeation by limiting the opening of the gate and hence creating a bigger ion permeation free energy barrier.

3.2.3 The opening of the intracellular gate is related to the interaction between I402 and Y445

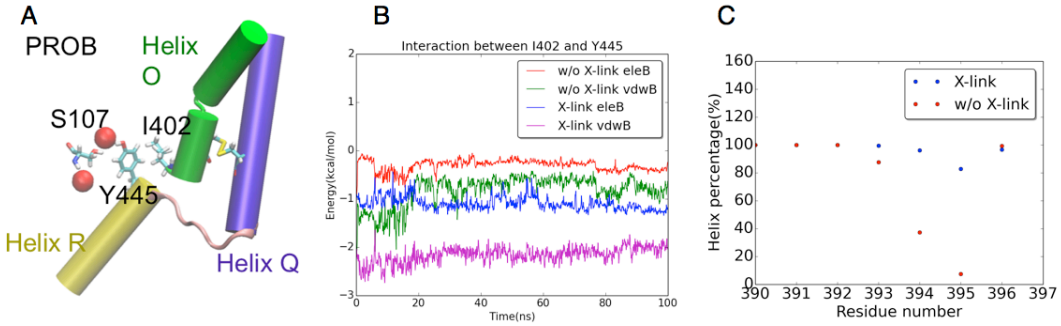

Figure 3-4: Interaction of I402 and Y445 and kink of helix O

A. X-ray structure with kink helix O in PROB; B. Interaction energy between I402 and Y445 in PROB; C. The probability to find a residue in a helical domain along the simulations with and without X-link.

In order to understand in detail how the X-link limits the opening of the intracellular gate and to get insights on the conditions allowing the intracellular gate to open for ion permeation, the structure near the intracellular gate was scrutinized. The interaction between I402 at the bottom of helix O and Y445 seems to correlate with the opening of the gate. Specifically, as shown in the structure of Fig.3-4A, I402 may prevent the opening of the intracellular gate by limiting the movement of Y445.

In our simulations, the ion permeation event occurs only in PROB, not in PROA. According to our hypothesis, this should be attributed to different interaction between I402 and Y445. Interaction energy calculations on the X-ray structure, i.e. the starting conformation of the simulations, demonstrated larger interaction in PROA than PROB (Fig.3-5), supporting our hypothesis.

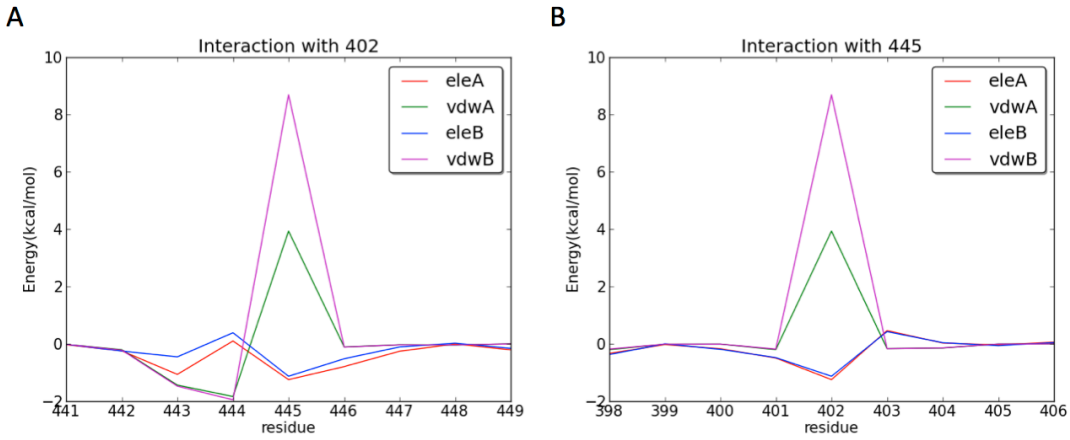

Figure 3-5: Interaction energies between residues close to I402 and Y445

ele, electrostatic energy; vdw, Van der Wall energy; A, PROA, B, PROB

To further verify this hypothesis, the X-link effect on this interaction energy was further examined in PROB. It was found that the X-link augments the electrostatic and Van der Waal interactions (Fig.3-4B), which is consistent with the smaller intracellular gate in the presence of the X-link (Fig.3-2B). In other words, in the absence of X-link, smaller interaction between I402 and Y445 favors the opening of the intracellular gate. In addition, as shown by the interaction energy in the X-ray (Fig.3-5), the interaction energy represents most of the interaction in this region. Therefore, a small interaction between I402 and Y445 is desirable in the opening of the intracellular gate.

To understand the cause of the different interaction energies, we projected on the XY plane the position of I402 (Obottom, i.e. the bottom residue of helix O), S107 and Y445 (Fig3-6). In the case with X-link, I402 is closer to Y445 in average and sits in a line with Y445 and S107, which may hinder the fluctuation of Y445 and contribute to the smaller probability of the opening of the intracellular gate.

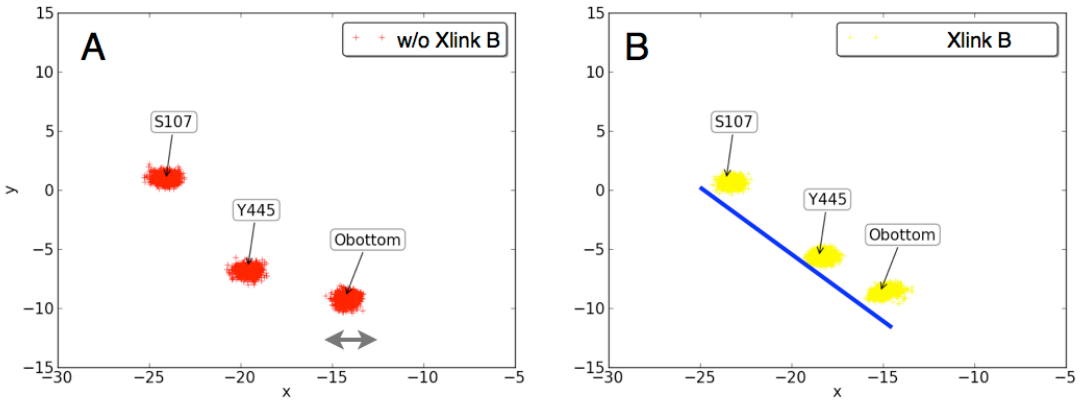

Figure 3-6: Projection on the X-Y plane of S107, Y445 and I402 at the bottom of helix O

Obottom, I402

3.2.4 The opening of the gate is favored by a kinked helix O

In order to further understand the reason for the bigger interaction between I402 and Y445 in the case with X-link, the secondary structure of helix O, to which I402 belongs, is analyzed. Fig.3-4C presents the probability of finding each of the seven residues (390-396) of helix O in a helical conformation in the simulations. As a result, in the absence of the X-link, helix O is kinked at residue positions 393 to 395, while the X-link brings the kinked PROB to a straight conformation.

Therefore, the fact that X-link prevents ion permeation in the experiment could be attributed to the straight conformation of helix O, which leads to larger interaction between I402 and Y445, and hence hinders the opening of the intracellular gate and increases the ion permeation free energy barrier.

Taken together, the molecular mechanics and electrophysiology data show that the opening of the intracellular gate is required for ion permeation and controlled by the interaction between the bottom of helix O and Y445, which is related to the conformation of helix O.

3.3 Discussion

3.3.1 The opening of the intracellular gate is seen

In WT structure, the dehydrated chloride ion at Scen appears to be cut off from both the extracellular and intracellular solutions. The carboxyl group of E148 blocks access to the extracellular side, and the Y445 side chain appears to do the same on the inside. The structure reflects an occluded state in the transporting cycle in which both gates are closed around a substrate chloride ion. Whereas an outward-open state has been observed crystallographically in E148Q or E148A mutants (Dutzler et al 2003), no inward-open state has been reported with an unblocked cytoplasmic pathway.

Given the radius of the chloride ion is bigger than the constriction between S107 and Y445, an opening of the intracellular gate is required for ion permeation to take place. In the occluded state, thermal fluctuations do not seem to provide sufficient access to a conducting state. The state with an open intracellular gate was captured in our simulations, characterized by the distance between CA atoms of S107 and Y445. Thus, it suggests that the opening of the intracellular gate is possible and may contribute to ion permeation.

3.3.2 The opening of the intracellular gate requires conformational changes beyond the pore

Given that the permeation pathway and the intracellular gate are so narrow with residues well packed around, it is not possible to open the intracellular gate without moving neighboring residues. Therefore, it is reasonable to see that the intracellular gate opens with the conformational change beyond the pore as shown in the simulations, in agreement with different studies (Elvington et al 2009; Bell et al 2006; Bykova et al 2006).

The conformational change in our simulations lies on the side of Y445, indicating that Y445 does restrain ion permeation with its bulky side chain, which is consistent with the observation that E148A/Y445A mutant speeds up

permeation rates compared to E148A (Jayaram et al 2008). Notably, although S107 could be seen to form the intracellular gate with Y445, no apparent conformational change was seen on the side of S107. In other words, S107 could not restrain the ion permeation with its side chain, which is consistent with the observation that S107G on top of E148A/Y445G cannot increase chloride flux beyond the double mutants (Jayaram et al 2008).

Moreover, the conformational change observed in the simulations involves helix O, which includes I402. By X-linking residue 399 and 432, helix O is restrained to be straight, preventing movement of I402 and hence hindering the opening of the intracellular gate.

3.3.3 Hydrophobic interaction determines the conformational change on the side of Y445

It has been demonstrated that the residue type at the position 445 influences the ion binding affinity and a huge hydrophobic residue is required to guarantee the coupling between Cl^- and H^+ transport (Accardi et al 2006). Our finding that the interaction between I402 and Y445 is essential for regulating the gate could explain the reason behind such observation. If the amino acid at position 445 is small like leucine, the interaction between I402 and 445 is not big enough to stop the ion at Scen, more chloride ions permeate, and coupling is undermined. On the other hand, if the amino acid at position 445 is a charged histidine, water molecules would gather around this position. Thus, the interaction between I402 and 405 is diminished and the coupling is impaired.

3.3.4 Intracellular gate in transporters and slow gating in channels

The intracellular gate Y445 is conserved in both ClC channels and transporters. Notably, S107 is also conserved through channels and transporters, implying a similar constriction in the ClC channel structures as in ClC-ec1. Given that the chloride ion is not small enough to pass through the constriction, the movement of Y445 seen here could also occur in ClC channels.

ClC channels have complicated gating mechanisms, fast gating and slow gating. Fast gating mainly relies on Glu_{ext}, similar as the extracellular gate in ClC exchangers. On the other hand, slow gating was demonstrated to be involved in conformational change in the C terminus (Bykova et al 2006; Fong et al 1998; Wu et al 2006; He et al 2006) . As Y445 lies at the helix R, the last helix connecting to the C terminus, the conformational change at the intracellular gate may synchronize with the conformational change at the C terminus. Hence, the intracellular gate in ClC transporters may be related to slow gating in channels.

Notably, it has been demonstrated that mutation at the corresponding residue of Y445 has minimal effects on single-channel conductance (Chen, & Chen 2003; Accardi, & Pusch 2003) , implying some differences between the intracellular gate of ClC transporters and slow gating in ClC channels. One should be cautious in correlating them, but comparison of studies on both is highly desirable, because this may underlie the small but important difference between ClC channels and transporters.

3.4 Conclusion

This work, for the first time, showed the ClC conformation with an open intracellular gate, implying the necessity to open the intracellular gate for ion permeation. For ions to pass through the intracellular gate, the hydrophobic interaction on the side of Y445, especially the interaction between I402 and Y445, needs to be reduced, which is correlated to the conformation of helix O. The opening of the intracellular gate demonstrated here in the ClC transporters could be helpful in unveiling the slow gating mechanism of the ClC channels, while the comparison between them could help understand the distinction between channels and transporters in ClC family.

3.5 Method

3.5.1 System preparation

In order to explore the conformational change of the ClC structure that is restrained by X-link, two systems mimicking the experimental conditions were set up for simulations. Default protonation states of all residues are used. The molecular systems were assembled using the CHARMM-GUI web service. The crystal structure of CLC-ec1(PDB: 1ots) from OPM(Orientation of Proteins in Membranes database) was used for simulations under periodic boundary conditions in a NPT ensemble with a temperature of 323.15 K and a pressure of 1 atm. The rectangular periodic system box contained two layers of bilayers composed of dimystoylphosphatidylcholine (DMPC) lipid molecules around a ClC-ec1 dimer, water molecules 10 Å above and below the protein, and potassium/chloride ions to neutralize the systems and reproduce a 150 mM KCl solution.

3.5.2 Molecular Dynamic simulations

Simulations were carried out using CHARMM36 forcefield by NAMD {Phillips 2005}. The cutoff for both the Lennard-Jones and Coulomb interactions was 12 Å, with a switching function beginning at 10 Å. Non-bonded forces were calculated every timestep. Non-bonded pair list is updated every 10 steps, which includes all the pairs within 16 Å. Long-ranged electrostatic interactions were treated every step by Particle Mesh Ewald (PME) method with the interpolation order of 6. Langevin dynamics was used on non-hydrogen atoms to maintain the temperature constant with damping coefficient of 1/ps while constant pressure was controlled by Langevin piston Nosé-Hoover method with the oscillation period of 50 fs and the oscilallation decay time of 25 fs. All bonds involving hydrogen atoms were constrained to the nominal length in the parameter file using the SHAKE algorithm. The simulations last 100 ns each with a timestep of 2 fs.

3.5.3 Free energy calculations

In order to understand the X-link effect on ion permeation, monomer systems with and without X-link were set up for free energy calculations. In both systems, two ions were placed in the pore, and their z coordinates relative to Scen were used as two reaction coordinates. Starting with one ion at Sext and the other at Scen, 2D free energy landscapes were calcultated using iPMF (Wojtas-Niziurski

et al 2013). A total of 813 (w/o X-link) and 807 (with X-link) simulation windows were created and simulated for 300 ps each.

3.5.4 Interaction energy calculations

By scrutinizing the structure, I402 seems to interact with Y445, hindering the opening of the intracellular gate. To verify this hypothesis, the electrostatic and Van der Wall interaction energies between residue I402 and Y445 are calculated by namd energy module in VMD (Humphrey et al 1996) along the simulations with and without X-link. To confirm that the interaction between I402 and Y445 is bigger than interactions of other pairs around this region, the interaction between I402 and each residue of 441 to 449, and that between Y445 and each residue of 398 to 406 in the X-ray structure, are calculated in the same way.

3.5.5 Structure and energy analysis

OpenStructure (Biasini et al 2010) is used to characterize the ion permeation and the conformational changes observed in the different systems, including: 1) z coordinates of the ion in the pore and Scen, defined as the center of mass of residue 356, 357, 107, 445; 2) Timeseries and histograms of the distance between CA atoms of S107 and Y445; 3) Probability of finding each residue of 390 to 396 in a helical conformation. 4) Projection of CA atoms of S107, Y445 and I402 on XY plane.

4 Different conformations of F357 are correlated to the conformations of ClC-ec1 to recruit and release chloride ions

4.1 Introduction:

Alternating models for transporters are commonly seen in diverse systems (Khare et al 2009; Kaback et al 2011; Arkin et al 2007) . In the lactose permease (LacY) symporter, ligand binding tests on various cysteine mutants suggest an alternating mechanism, controlled by ligand binding (Kaback et al 2011). Molecular dynamic simulations on the antiporter Na^+/H^+ demonstrates that a single residue D163, which could alternate between protonated and deprotonated state, controls the alternating accessibility of the sodium binding states to the cytoplasm or periplasm (Arkin et al 2007). In maltose transporter, an ABC transporter, the resting states of the transporter with or without ATP bound takes the inward-facing conformation, while outward-facing structure is seen in the presense of maltose as well as maltose-binding protein (MBP). Comparison of the two structures shows rotation of different helix bundles in TMD (Khare et al 2009). In the latter two cases, the ligand binding is also required, since protonation of D163 is an essential step in the alternating mechanism of Na^+/H^+ exchanger, while outward-facing structure of maltose transporter is seen at the presence of maltose. The alternating systems could respond to the signal that a ligand is bound in different ways to generate the alternate states, such as protonation of a residue and rotation of some helix bundles.

It has been demonstrated that the inverted topology repeats encode the structural information required for the generation of the two alternate states in neurotransmitter sodium symporter, excitatory amino acid transporter (EAAT) and major facilitator superfamily (MFS) (Crisman et al 2009; Forrest et al 2008; Radestock, & Forrest 2011) . Similar rules could be applied to ClC-ec1. The X-ray structure of ClC-ec1 shows that the protein consists of two subunits while each subunit has its chloride ion permeation pore, formed by two domains in a 2-fold sudo-symmetry, which is the same as the so-called inverted topology (Dutzler et al 2003).

ClC-ec1 belongs to a family expressed in species from bacteria to human. Mammals express nine ClC isoforms that differ in tissue distribution and subcellular localization. Human diseases and knockout mouse models have yielded important insights into their physiology and pathology. Phenotypes and diseases include myotonia, renal salt wasting, kidney stones, deafness, blindness, male infertility, leukodystrophy, osteopetrosis, lysosomal storage disease and defective endocytosis (Jentsch 2008).

Apart from the various diseases to which it is related, the ClC family attracts attention because it comprises channels and transporters. The sequence and structure similarities between channels and transporters challenge the traditional clear distinction between these classes of proteins. It is thought that the study of the ClC family could provide new insights on the boundary between

channels and transporters at the molecular level. Given the inverted topology of ClC structures, ClC transporters should be able to generate alternate states and fit the alternating mechanism. However, its alternating feature is still awaiting experimental conformation.

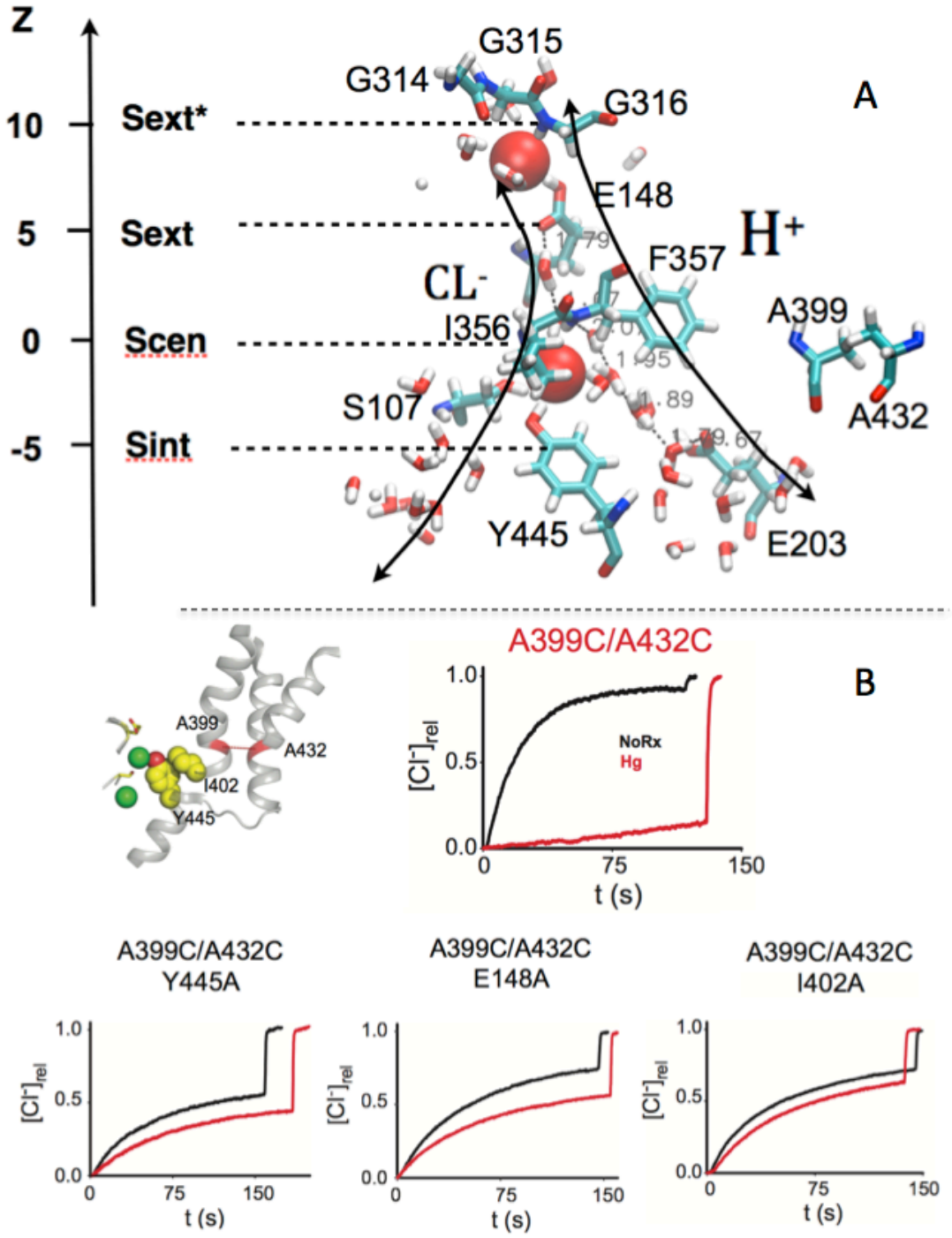

Figure 4-1: Chloride binding sites, pathways of protons and chlorides in ClC-ec1 and X-link experiment

Interestingly, an experiment seems to provide insights on the alternating features of ClC-ec1. In efflux assay, a crosslink (X-link) between residue 399 and 432, at distance from the permeation pathway, prevents ion permeation (Fig.4-1). More importantly, substitution of either E148 or Y445 by Ala, i.e. removal of

either the extracellular gate or intracellular gate (Picollo et al 2009), could abolish the X-link effect. This implies that the X-link may influence the interaction between the two gates. If the two gates are correlated to allow the opening of only one of them, such interaction may be the key to manipulate the alternating process if it exists.

Previous work has identified the interaction between Y445 and I402 is important for the opening of the intracellular gate (Chapter 3). However, if the X-link influences the intracellular gate only, E148A should not remove the X-link effect as seen in the experiment. Therefore, the X-link may have an impact on the extracellular gate as well. By scrutinizing the snapshots in the simulations with and without X-link, the conformational change of F357 was identified to be essential for ion permeation and it was hypothesized that the X-link could prevent such conformational change. By restraining F357 to one of two stable conformations, the protein was locked in one of two conformations identified in the simulations. The inward facing conformation favors ion permeation through the open intracellular gate while the outward facing conformation facilitates the movement of chloride ions between Sext and the extracellular bulk.

4.2 Results:

4.2.1 F357chi1 changes conformation for ion permeation

In order to uncover the molecular mechanism behind the X-link effect, we perform molecular dynamic simulations with and without the X-link. The ion from Scen is released in one subunit (PROB) in the simulations performed without the X-link. As seen in Fig.4-2A, an ion leaves the central binding site (Scen), reaches the intracellular binding site (Sint) and leaves the pore.

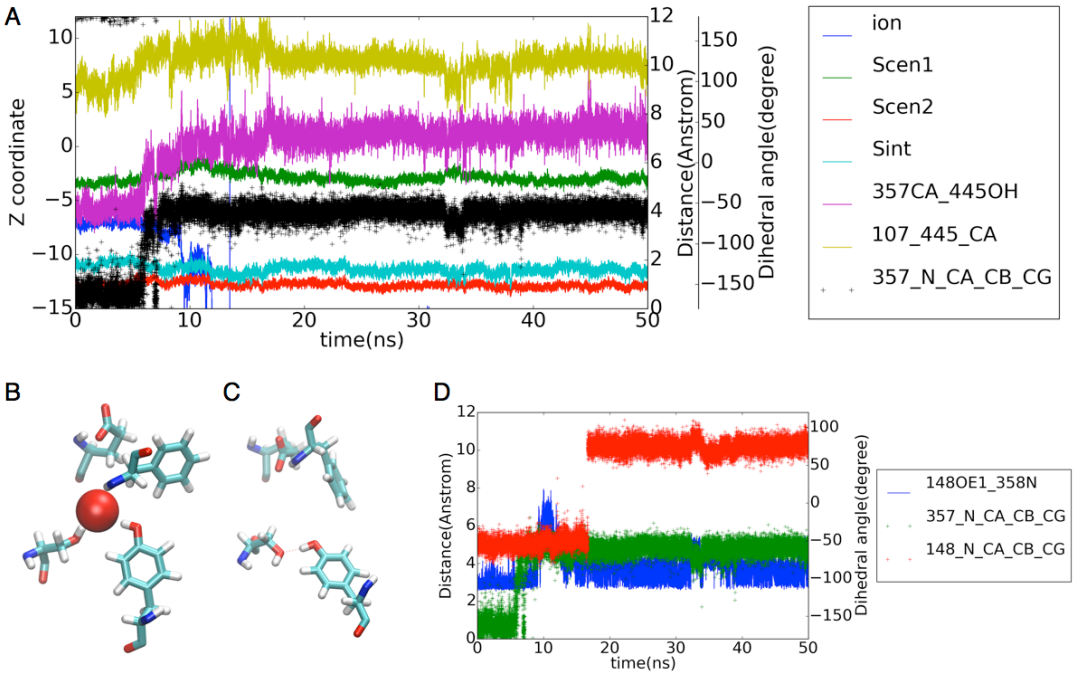

Figure 4-2: Ion permeation event

A. Timeseries of ion position along z axis(ion), central binding site (Scen1, center of mass of 356 and 357, Scen2, center of mass of 107 and 445), intracellular binding site (Sint, center of mass of 107 and 108), distance between CA atoms of 107 and 445(107_445_CA), between CA of 357 and OH of 445(357CA_445OH), and dihedral angles 357chi1(357_N_CA_CB_CG); B. Snapshots at the end of 2ns simulations. C. Snapshots at the end of 22ns simulations. D. Timeseries of distance between OE1 atom of E148 and N atom of A358 (148OE1_358N), 357chi1 (357_N_CA_CB_CG) and 148chi1 (148_N_CA_CB_CG).

To understand how the ion passed the intracellular gate between Scen and Sint, the structure nearby was scrutinized and the conformational change of F357 was found to correlate with the conformational change of the intracellular gate and ion permeation. As shown in Fig.4-2A, the intracellular gate defined by the distance between CA atoms of S107 and Y445 increased, which is followed by the variation of 357chi1 and ion permeation. The two conformations of F357, called sideway and down conformations with chi1 around -160 and -70 respectively, are shown before and after the transition (Fig.4-2B, C). The correlation between the intracellular gate and F357 could be illustrated by the distance between the CA atom of F357 and hydroxyl oxygen atom of Y445, which increases with the conformational change of F357. In other words, conformational changes of F357 directly influence Y445 since they both include an aromatic ring and repulse each other.

Apart from that, conformational changes of F357 are also correlated to the external gate formed by E148 and A358. As seen in Fig.4-2D, the distance between OE1 atom of E148 and N atom of A358 increases after the conformational change of 357, followed by the variation of E148chi1.

In order to understand whether the X-link is correlated to F357, dihedral angles of F357 chi1/chi2 were analyzed. F357 of both subunits in WT simulations take both sideway and down conformations (Fig.4-3A, B). The X-link in PROA locks F357 to be in its down conformation (Fig.4-3C) while the X-link in PROB locks

F357 to be in the sideway conformations (Fig.4-3D). This indicates that the X-link prevent the conformational change of F357.

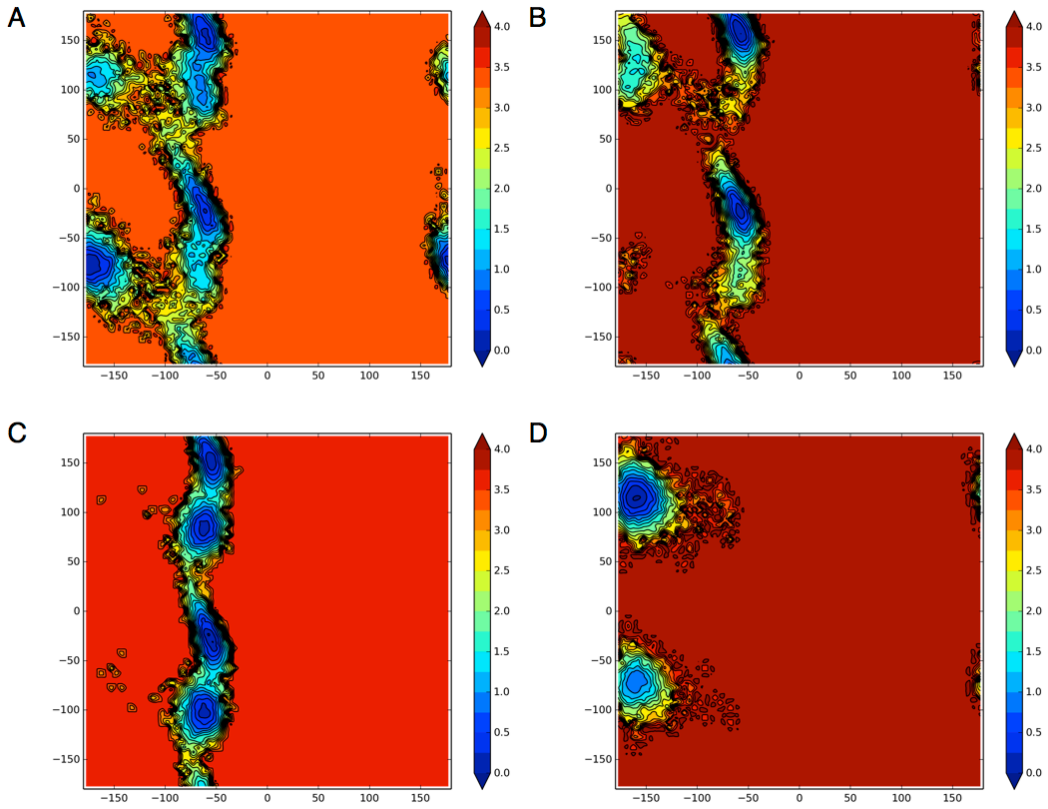

Figure 4-3: X-link influences F357chi1-chi2 distribution

x=F357chi1, y=F357chi2. A. w/o X-link, PROA; B. w/o X-link, PROB; C. X-link, PROA; D. X-link, PROB

To confirm the correlation of the ion permeation and the conformational changes, we performed free energy calculations for the system without the X-link (PMF1) and with the X-link (PMF2). The reaction coordinates are defined in Table 1. The results show an increase of the free energy barriers when the X-link is applied, notably for the lower ion (y-axis) to move between Scen (0.0) and Sint (-5.0), and the higher ion (x-axis) to move between Sext (5.0) and Sext* (10.0) (Fig.4-4A, D, red arrow). Chi1 of 357 is analyzed for sampling conformations in the free energy calculations. As shown in Fig.4-4B, with the lower ion at Scen (along y=0), F357 changes from sideway conformation (chi1=-160) to down conformation (chi1=-70) when the higher ion leaves Sext. Similar change occurs when the lower ion leaves the Scen with the higher ion at Sext (along x=5.5), seen in Fig.4-4C. This demonstrates that F357 experiences a conformational change when the ion enters and leaves the pore.

When the X-link is applied, the similar conformational change is seen, but there is a clear gap between the two favorable F357chi1 (-160 and -70), suggesting that it hinders the conformational change of F357. Therefore, ion permeation requires the conformational change in F357 while the X-link between 399 and 432 prevents it.

No.	Condition	Reaction coordinate(s)	Results
1	w/o X-link	$x=z_{ion\_relative(upper\ ion)}$ $y=z_{ion\_relative(lower\ ion)}$	Fig.4-4A
2	X-link		Fig.4-4D
3	No ions	x=357chi1	Fig.4-5A, B
4	One ion at Scen		Fig.4-5C, D
5	One ion at Sext		Fig.4-5E, F
6	One ion at Scen One ion at Sext		Fig.4-5G, H
7	357chi1=-70	$x=z_{ion\_relative(upper\ ion)}$ $y=z_{ion\_relative(lower\ ion)}$	Fig.4-7A
8	357chi1=-160		Fig.4-7B

Table 1: list of free energy calculations (potential of mean force, PMF)

$z_{ion\_relative} = z_{ion\_relative} - z_{scen}$

Scen: x=0.0, center of mass of backbone of I356, F357, S107, Y445

Sext: x=5.0

4.2.2 F357 could be sideway when the ion fills the pore

Since F357 experiences conformational changes when ion permeation is taking place, different ion binding states of the transport cycle should be related to different F357 conformations. In order to confirm such implication, we performed free energy calculation of F357chi1 in four systems with different ion occupancy (no ions (PMF3), one ion at Scen (PMF4), one ion at Sext (PMF5), two ions at Scen and Sext separately (PMF6)).

A deep free energy well is seen at -70 (down) in the system without ions (Fig.4-5A, B) as well as that with an ion at Sext (Fig.4-5E, F). In the case with one ion at Scen (Fig.4-5C, D) and two ions in the pore, PROB shows a different well at -160 in PROB. This indicates that ion binding could promote F357 to take the sideway conformation.

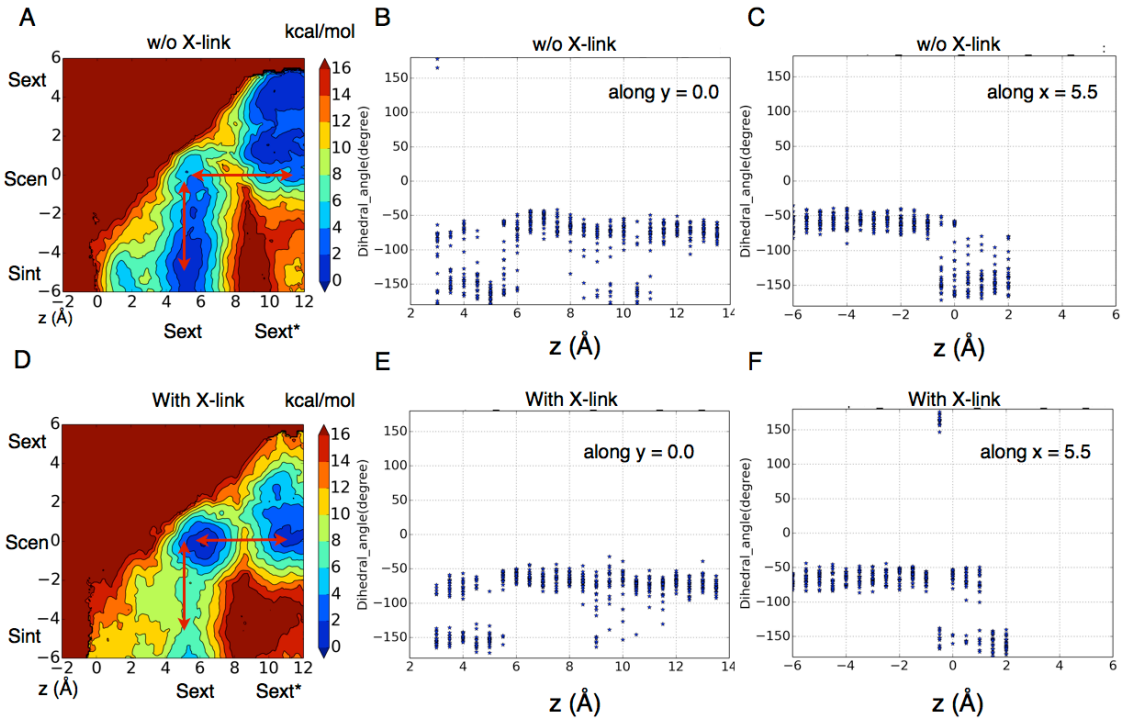

Figure 4-4: Conformational changes of F357 during ion permeation

Free energy landscape of ion permeation(kcal/mol): A, without X-link; D, with X-link. F357chi1 when the lower ion is at Scen(0.0) with the higher ion at different positions (window_z, Å) in the samplings of the free energy calculations: B, without X-link; D, with X-link. F357chi1 when the higher ion is at Sext(5.5) with the lower ion at different positions in the sampling of the free energy calculations: C, without X-link; F, with X-link.

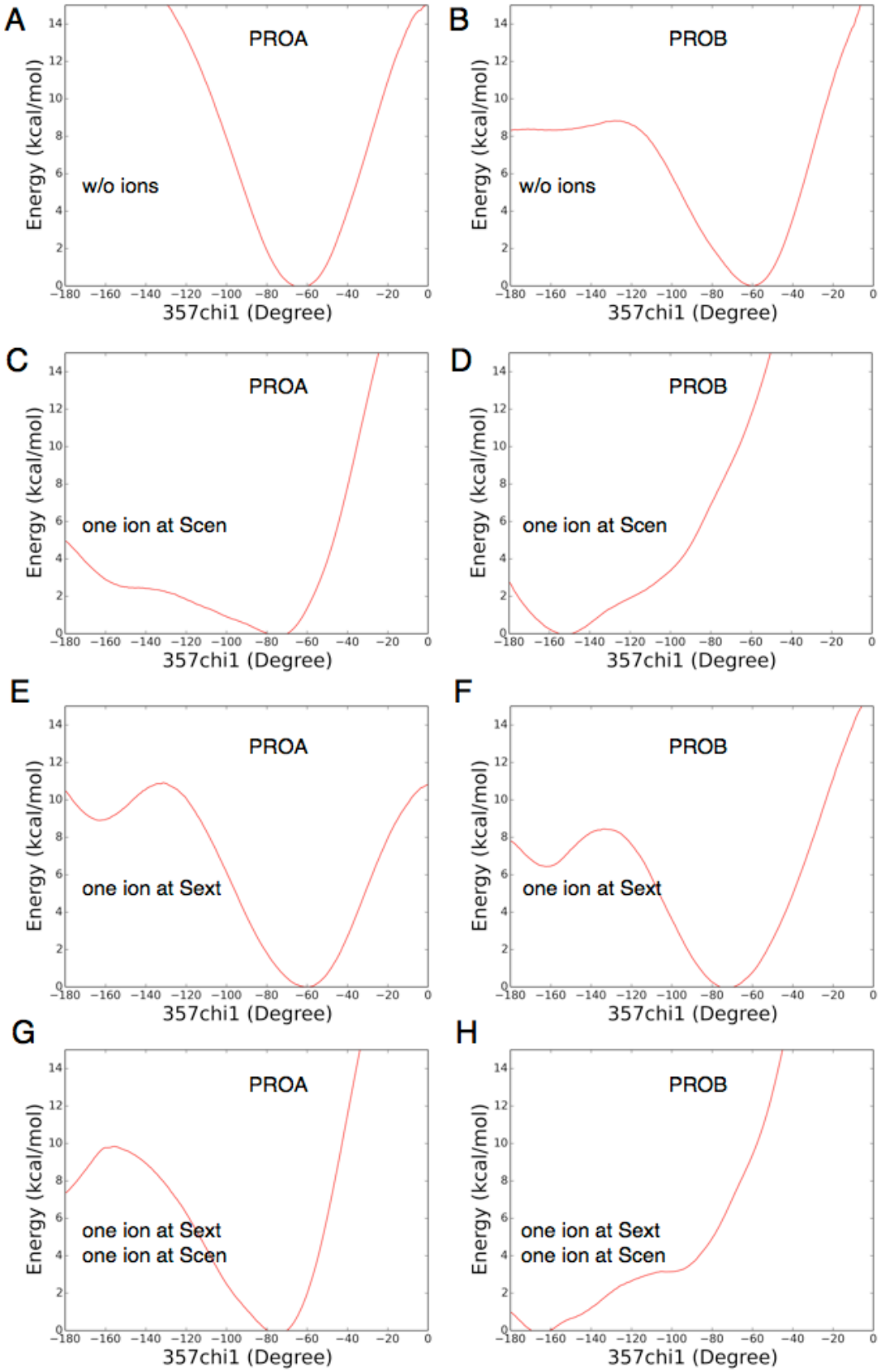

Figure 4-5: Free energy calculations of F357chi1 with different ion occupancy

Without ions, PROA, A; PROB, B. With one ion at Scen, PROA, C; PROB, D. With one ion at Sext, PROA, E; PROB, F. With two ions, one at Sext, one at Scen, PROA, G; PROB, H.

In the case with one ion at Scen, the two subunits are different in the preference of the well (Fig.4-5C, D). In particular, in PROA, the well at -70 (down) is energetically favorable, while it is at -160 (sideway) for PROB. In order to understand such discrepancy, conformations of sampling structures were scrutinized. As shown in Fig.4-6A, B, the ion is more packed in PROB than in PROA. In particular, G149 coordinates the ion at Scen in PROB, while such coordination does not exist in PROA.

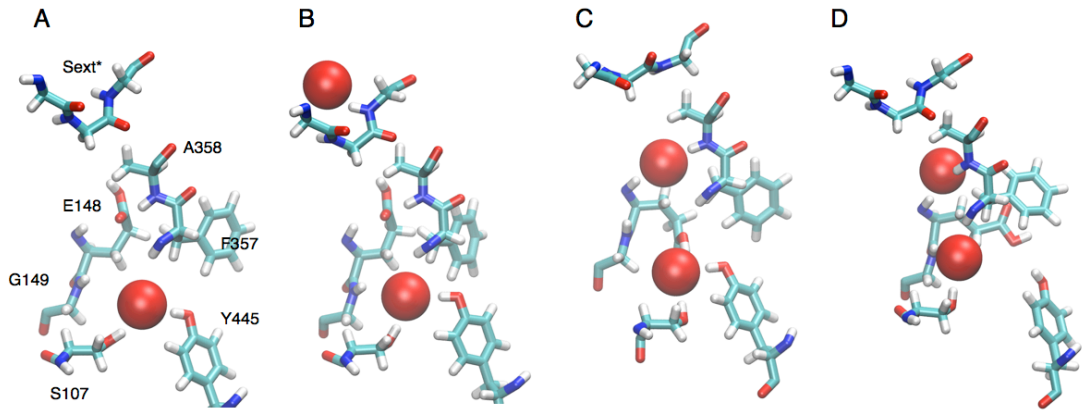

Figure 4-6: Ion binding and conformation of F357

All the four snapshots are taken from the sampling of pmf calculations of F357 when F357chi1=-160 (sideway). One ion at Scen: PROA, A; PROB, B. One ion at Scen, one ion at Sext: PROA, C; PROB, D.

Notably, PROB recruits another ion at Sext*(Fig.4-6B), which remains there when F357 is sideway (data not shown). This implies relatively high ion binding affinity at Sext* in PROB. In other words, the conformation with higher ion binding affinity at Sext* may favor F357 to be sideway.

In the case of two ions in the pore (Fig.4-5G, H), the two subunits also prefer different conformations of F357, which could be attributed to different conformations of the pore. The main difference lies in the conformation of E148. In PROA (Fig.4-6C), E148 goes down to coordinate the ion at Scen, while E148 from PROB stands sideway (Fig.4-6D). It suggests that the protonated E148 could move sideway and further down to Scen. Moreover the down conformation of E148 would prevent F357 from taking its sideway conformation, favoring the down conformation although two ions are bound in the pore.

4.2.3 Two conformations of F357 represent different states in the transport cycle

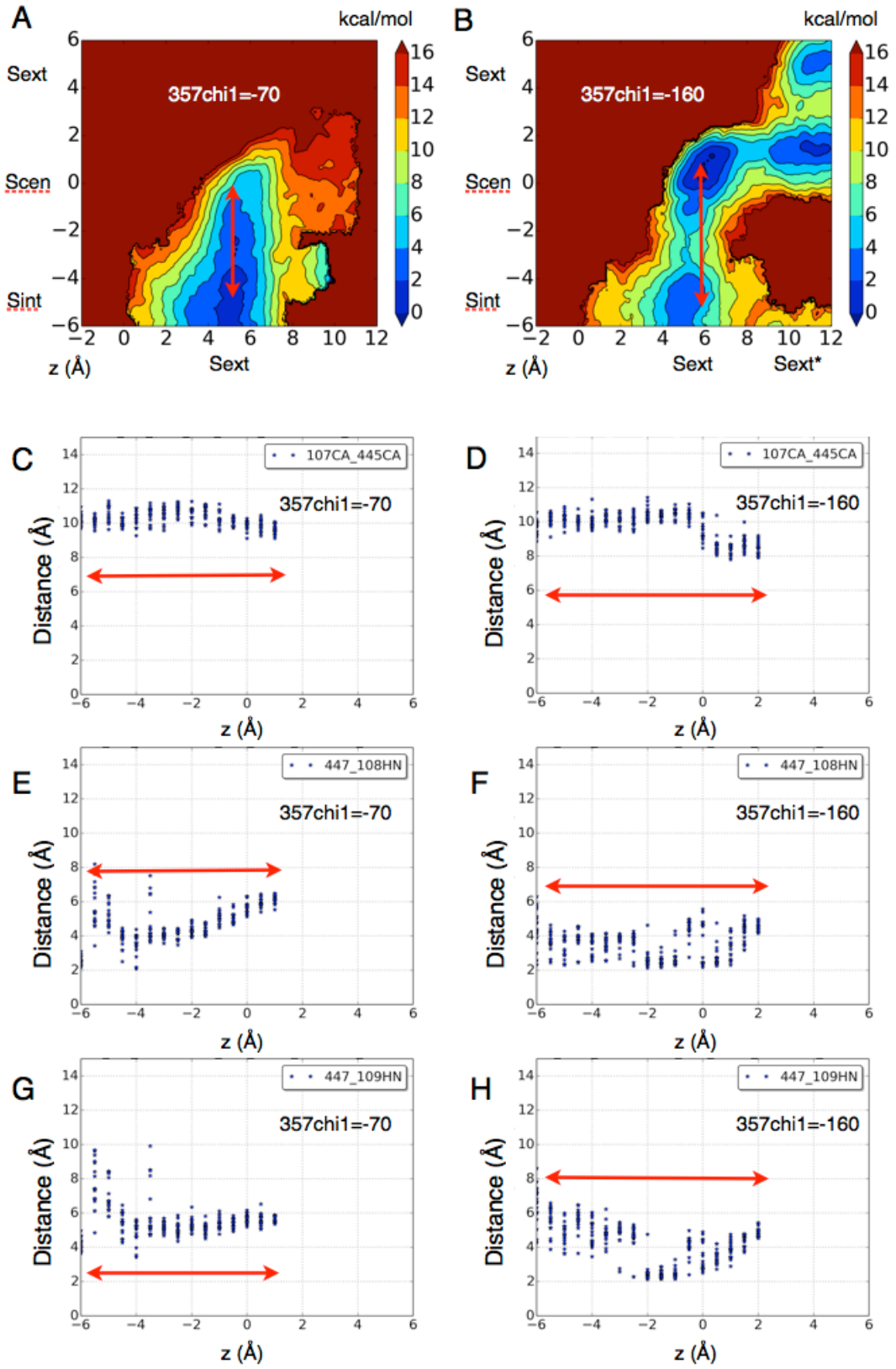

Figure 4-7: Free energy calculations of ion permeation with restrained 357chi1 and structural analysis

Free energy landscape: 357chi1=-70, A; 357chi1=-160, B. Distance analysis when lower ion goes through the intracellular gate with the higher ion at Sext: between CA atoms between S107 and Y445, 357chi1=-70, C; 357chi1=-

160, D; between the lower ion and 108HN, 357chi1=-70, E; 357chi1=-160; between the lower ion and 109HN, 357chi1=-70, G; 357chi1=-160, H.

In order to confirm the correlation between F357 and ion binding affinity in the transport cycle, we perform free energy calculations with two ions in the pore in which F357 is restrained to different conformations (Fig.4-7A, B). The results show quite different free energy landscapes. In particular, when F357 is at down conformation (chi1=-70), 1) the well with the upper ion at Sext (x=5.0) and the lower ion at Scen (y=0.0) does not exist as the other case; 2) the barrier to go through the intracellular gate is clearly smaller; 3) it is very difficult for the upper ion to move from Sext (y=5.0) to Sext* (y=10.0). Taken together, this conformation appears to favor ion permeation through the intracellular gate, but not the extracellular gate. On the other hand, when F357 is in a sideway conformation (CHI1=-160), 1) the well with one ion at Sext and another at Scen is stabilized; 2) the barrier to go through the intracellular gate is relatively bigger; 3) the transition between Sext (y=5.0) and Sext*(y=10.0) becomes easier. Hence, this appears to be the state to recruit the ion and occlude the ion in the pore.

In order to understand the conformational difference behind the free energy difference, we analyzed the two gates and ion coordination in the sampling structures in the free energy calculations. There is no big difference in the external gate as described by the distance between the main chain nitrogen atoms of E148 and A358 (data not shown). However, the intracellular gate, defined with the distance between the main CA atoms of S107 and Y445, shows clear difference (Fig.4-7C, D). When F357 is in its down conformation, the intracellular gate remains at around 10 Å. When F357 takes the sideway conformation, the intracellular gate varies. When the lower ion starts to leave the intracellular gate, the gate distance turns from 8 Å to 10 Å. In other words, the down conformation of F357 keeps the intracellular gate open, which is not true in the sideway conformation.

The two conformations of F357 lead to different ion coordination schemes in Scen. As shown by the distance between the lower ion and the nitrogen atoms of residues 108 and 109 (Fig.4-7E, F, G, H), when F357 is in its down conformation, the lower ion is not coordinated by residues 108 and 109 which could favor ion permeation. When F357 takes a sideway conformation, the lower ion interacts with residues 108 and 109, preventing ion permeation.

Therefore, the two conformations of F357 are related to different ion coordination schemes and intracellular gate states, respectively corresponding to ion release and ion recruitment.

4.2.4 A possible network justifying the correlation between the conformation of F357 and the states of the transporter

It has been shown in restrained free energy calculation that different conformations of F357 are correlated with different conformations of the pore. But how could they be correlated? By scrutinizing the residues around the chloride ions in the permeation pathway, we found a network that could describe the correlation between the conformation of F357 and the two gates.

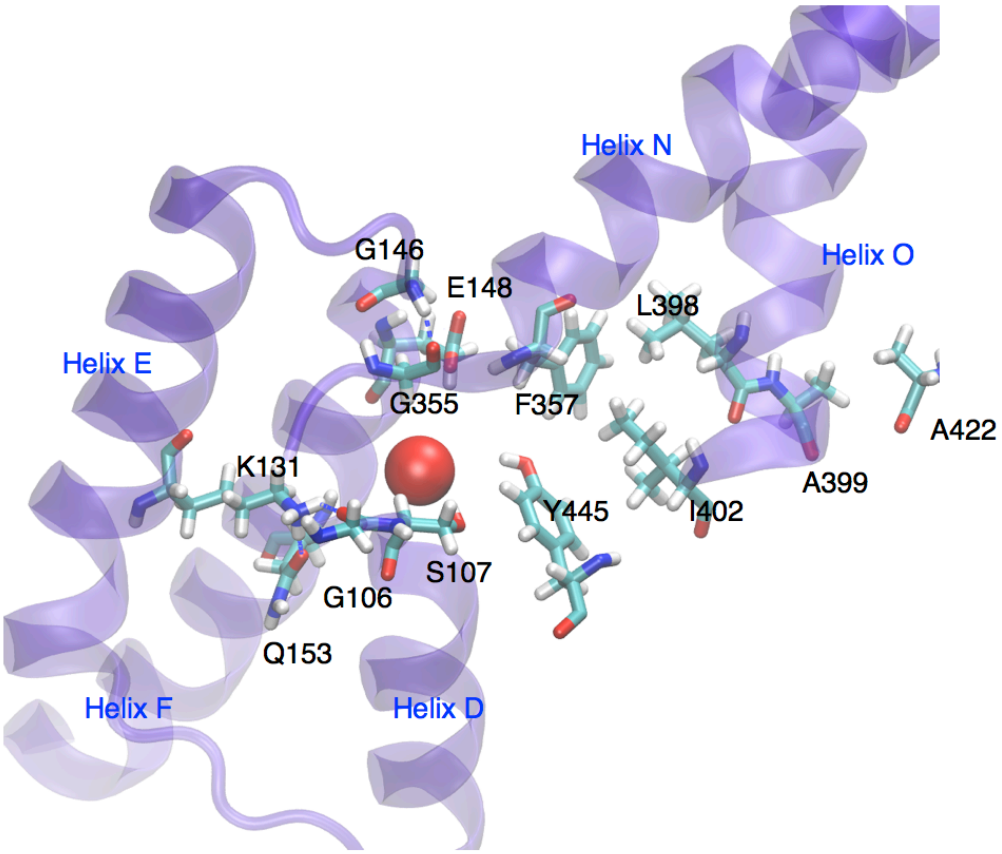

Figure 4-8: A network near the chloride ion permeation pathway

There are different residues and interactions surrounding the pore. As seen in Fig.4-8, on the left side, charged interactions dominate, while hydrophobic interactions constitute the main interactions on the right side. Conformational changes of F357 directly modify the conformation and dynamics of helix N. The H-bond between G146 and G355 could contribute to the transfer of the movement in helix N to helix F, which includes E148. Therefore, through such pathway, F357 could influence the extracellular gate. Moreover, conformational changes in helix F could be transferred to helix E by H-bond between Q153 and K131 and hence to helix D by H-bond between K131 and G106. In this way, F357 could also influence the position and conformation of S107, one of the two residues that form the intracellular gate. The right hand side feature hydrophobic interactions among F357, Y445, I402 and L398. Thus, conformational change of F357 could influence that of Y445, the other residue that form the intracellular gate. Therefore, F357 could influence both gates.

Notably, such network describes the possible molecular correlation between the two gates, making sure that only one gate is open at a given time. Besides, it could also explain the X-link effect. Since L398 and I402 both belong to helix O where A399 is, a X-link between A399 and A432 could reduce the flexibility of L398 and I402. Due to the hydrophobic interaction and limited space available in this region, the movement of aromatic ring of F357 would become difficult.

4.3 Discussion:

4.3.1 Ion binding and conformation of F357

F357 is highly conserved in both ClC channels and transporters. This suggests that F357 could be important in the transport mechanism in both channels and transporters. The amino acid of ClC-1 corresponding to F357 of ClC-ec1 is F484. F484C and F484A of ClC-1 significantly reduce affinity of the inhibitor 9-anthracene carboxylic acid (9-AC) (Estévez et al 2003), implying the role of F484 in ion binding affinity of ClC-1. Our simulations showed the correlation between ion binding in ClC-ec1 and the conformation of F357. In particular, F357 is intrinsically found in its down conformation (357chi1=-70), while ion binding at Scen favors the sideway conformation of F357 (357chi1=-160).

Different Y445 mutants have implied different chloride ion binding affinity, as deduced from ion occupancy in X-ray structures (Accardi et al 2006). Mutants Y445F and Y445W have ion occupancy at Scen similar to that of in WT, while Y445L, Y445A, Y445H and Y445E display reduced ion occupancy at Scen. ITC measurements later confirmed the extremely low chloride ion binding affinity at Scen in Y445A and Y445H, and intermediate for Y445L (Picollo et al 2009). This implies that the aromatic ring is essential at this position for chloride ion binding. Similar to Y445, F357 has an aromatic ring and lines around the chloride ion permeation pore. Furthermore, F357 is just above Y445. When F357 is in its sideway conformation, Y445 is less constraint. When F357 is in its down conformation, Y445 could be repulsed and has to move to a lower position. Such interaction may be important for ion binding at Scen.

The ion binding at Scen was also demonstrated to be indispensible for proton transport and coupling (Accardi et al 2006; Nguitragool, & Miller 2006) . Since our simulations indicate a correlation between ion binding and F357, F357 may also be involved in the mechanism of proton transport. Such correlation is implied in an investigation of the hydration pathways for proton transport (Han et al 2014). It was found that for the formation of water wires, the chloride ion at Scen is required and I109 has to move away from the hydrophobic region formed with F199, F357 and Y445 through side-chain rotation. As seen in our free energy calculations with restrained F357chi1, I109 would coordinate with chloride ion at Scen when F357chi1=-160, implying the conformational correlation between F357 and I109. Therefore, the conformation of F357 seems to be correlated with the water wire formation as well, especially that the distribution of the conformation of F357 is shown to be different in the sampling snapshots with and without water wires (Han et al 2014).

4.3.2 Two conformations in the transport cycle

Our simulations suggest that the two conformations of F357 could represent different states of the transport cycle of ClC-ec1. When F357 is in a sideway conformation, the protein is inclined to recruit the ion with the external gate open and the intracellular gate closed. This is generally called outward facing conformation. When F357 is in a down conformation, the protein is likely to release the ion, with the external gate closed and the intracellular gate open. And it is the inward facing conformation. Accordingly, alternating of the conformation seems to be essential in the transport mechanism while the X-link between 399

and 432 prevents conformational change in F357 and hence restrains the protein to be in one of the two alternating conformations.

The X-ray structure of E148Q demonstrates an outward facing conformation with an open extracellular gate and closed intracellular gate. In this conformation, F357 is in its sideway conformation, which is consistent with our implication that an outward facing protein comes with a sideway F357. Although no X-ray structure has been reported to represent the inward facing conformation of ClC-ec1, given that alternating between the inward facing and outward facing conformations is essential in different transporters, it should also apply to ClC transporters. However, it should be different from the classical alternating mechanism. First, instead of one pathway for both substrates, the chloride ions and protons take different pathways (Accardi et al 2005). Second, the rule of one substrate bound at a time does not apply, but rather simultaneous substrates binding is required (Picollo et al 2012). Comparison of the X-ray structure between WT and E148Q demonstrates that the extracellular gate could open by moving the side-chain of E148 away from the pore without influencing the intracellular gate. Taking E148Q as a surrogate for the E148 protonated state, the transport mechanism in ClC-ec1 could be seen as the combination of the protonation of E148 and alternating conformations for chloride ion transport. Nevertheless, in which conformation protonation of E148 occurs is still mysterious.

4.3.3 Interaction between intracellular gate and extracellular gate

Although it is still not clear how protonation of E148 occurs, the conformation of E357, which was proposed to mediate the alternating mechanism, is correlated with that of E148. In our free energy calculations of F357chi1 with two ions in the pore, when the protonated E148 is sideway, F357 is likely to take the sideway conformation, which corresponds to a closed intracellular gate. However, when the protonated E148 takes the down conformation to coordinate the ion at Scen, F357 favors down conformation, which is corresponding to the conformation to release the ion with an open intracellular gate. Therefore, conformation of E148 could be correlated to the opening of the intracellular gate. Given the E148 is considered as the extracellular gate, there seems to be interaction between intracellular gate and extracellular gate, which is consistent with the X-link experiment linking residues 399 and 432.

Actually, such interaction has been implied in the studies of ClC-ec1 mutants. Y445A alone does not generate higher chloride flux than WT, even at pH 4.5, where the extracellular gate should be open much of the time. Also, E148Q/Y445A could not speed up the rate either. Only when both gates were removed in mutants E148A/Y445A, are the unitary Cl^- transport rates greatly increased (Jayaram et al 2008), implying the role of E148 in the opening of the intracellular gate. Besides, not only the extracellular gate could influence the intracellular gate, the conformation of the intracellular gate might also contribute to the opening of the extracellular gate. A mutation at the intracellular pore entrance of ClC-0, K519, influences the closing rate of the fast gate, which is similar to the extracellular gate of the ClC transporters (Chen et al 2003).

4.4 Conclusion:

In this work, conformational changes of F357 were identified to be essential for chloride ion permeation. Two conformations of F357 are correlated with inward facing and outward facing conformations of ClC-ec1, which constitute the alternating mechanism of chloride ion transport. The conformation of F357 is correlated to ion occupancy in the pore as well as the conformation of E148. Since the ion binding at Scen and Glu at the position of 148 are both essential for proton transport, the conformation of F357 could be correlated to proton transport as well. Therefore, the transport mechanism of ClC-ec1 is a modified version of the alternating mechanism, in which chloride ions permeate with the alternation between the outward facing and inward facing conformations, while the chloride ion binding during the permeation trigger the proton transport. Chloride ion binding at Scen and protonation of E148 seems to be interdependent. Which one should occur first and what kind of conformational changes the protein should experience are still open to answer.

4.5 Method:

4.5.1 System preparation

In order to explore the conformational change of the CLC structure that is restrained by X-link, two systems mimicking the experimental conditions were set up for simulations. Default protonation states of all residues in the forcefield are used. The molecular systems were assembled using the CHARMM-GUI web service. The crystal structure of CLC-ec1(PDB: 1ots) from OPM(Orientation of Proteins in Membranes database) was used for simulations under periodic boundary conditions in a NPT assemble with the temperature of 323.15K and the pressure of 1atm. The rectangular periodic system box contained two layers of bilayer composed of dimystoylphosphatidylcholine (DMPC) lipid molecules between protein molecules, water molecules 10 Å above and below the protein, and potassium/chloride ions to neutralize the systems and imitate a 150 mM KCL solution.

4.5.2 Molecular dynamic simulations

Simulations were carried out using CHARMM36 forcefield by NAMD {Phillips 2005} for 100ns with the following parameters. The cutoff for both the Lennard-Jones and Coulomb interactions was 12 Å. Non-bonded forces were calculated every step. The switching function begins to take effect at 10 Å. Non-bonded pair list is updated every 10 steps, which includes all the pairs with 16 Å. Long-ranged electrostatic interactions were treated every step by Particle Mesh Ewald(PME) method with the interpolation order of 6. Langevin dynamics was used on non-hydrogen atoms to maintain the temperature constant with damping coefficient of 1/ps while constant pressure was controlled by Langevin piston Nosé-Hoover method with the oscillation period of 50 fs and the oscilallation decay time of 25 fs. All bonds involving H are constrained to the nominal length in the parameter file using the SHAKE algorithm. The simulations last 100 ns with a timestep of 2 fs.

4.5.3 Free energy calculations

Free energy calculation is an important method to explore states and the transition of the states in the transporting cycle of channels and transporters. In our work, iPMF (Wojtas-Niziurski et al 2013), based on umbrella sampling method, was used to calculate the free energy landscape along certain reaction coordinates. All the calculations were listed in Table 1.

In order to understand the X-link effect on the ion permeation, monomer systems with and without X-link were set up by CHARMM (Brooks et al 2009). In both systems, two ions were put in the pore, and their z coordinates relative to Scen were used as two reaction coordinates. Starting with one ion at Sext and the other at Scen, 2D free energy landscapes were calcultated by iPMF, with 300ps' sampling in w/o xlink (PMF1) and xlink (PMF2)

Since conformational change of F357 was seen in the ion permeation, in the transporting cycle, different ion binding states should be correlated to different conformations of F357. In order to get insight of the favorable conformations of F357 in different ion binding states, we performed 1D free energy calculation based on 400ps' sampling with chi1 of F357 as the reaction coordinate in three systems with different ion occupancy: no ion binding (PMF3), one ion at Scen (PMF4), one ion at Sext (PMF5), and two ions at Sext and Scen separately (PMF6).

To investigate the effect of the conformation of F357 on the ion permeation, with z positive of two ions relative to Scen as the reaction coordinates, 2D free energy calculation were performed based on 300ps' sampling by iPMF with chi1 of F357 restrained to be -70 (PMF7) and -160 (PMF8).

4.5.4 Structural analysis

OpenStructure (Biasini et al 2010) is used to characterize the ion permeation and the conformational change observed in different systems.

The following timeseries were calculated: 1) z coordinates of the ion in the pore and Scen1, Scen2, Sint, defined as the center of mass of residue 356/357, 107/445, 107/108 separately; 2) distance between CA atoms of S107 and Y445, between CA atom of F357 and OH atom of Y445, between OE1 atom of E148 and N atom of A358; 3) chi1 of F357, E148.

The distribution of chi1/chi2 fo F357 in 100ns' molecular simulations were calculated.

F357chi1 in the sampling of PMF1 and PMF2 was calculated along the relative z of the higher ion with the lower ion at Scen (z=0.0) or along the relative z of the lower ion with the higher ion at around Sext (z=5.5).

The size of the intracellular gate and the ion coordination were calculated for the sampling of PMF7 and PMF8. In particular, the distance between CA of 107 and 445 was calculated to represent the size of the intracellular gate. The distance between ion and HN atom of 108 or 109 was calculated to examine the ion coordination. The calculation were all performed on the samplings along the relative z of the lower ion with the higher ion at Sext (z=5.0)

5 Conclusion

In this thesis, three allosteric conformational changes were identified: 1) In the Pgp/Sav systems, small conformational changes in NBD lead to rotation of helices in TMD, controlling the cavity of TMD to recruit and release allocrites; 2) In the ClC-ec1 system, conformation of helix O determines different interaction between the bottom of helix O and Y445, regulating the opening of the intracellular gate to stop and release chloride ions at Scen; 3) F357 of ClC-ec1 alternates in two conformations to mediate protein conformations to recruit and release chloride ions. All of these changes are common in the sense that a small change is enough to trigger larger and function-related conformational changes. This is consistent with the idea that small structural differences could underlie the specificity of channels and transporters. Since the fast gating and slow gating in ClC channels seems related to the opening of the extracellular gate and intracellular gate of ClC transporters due to similar locations of the important residues, studies of ClC channels and transporters should be carefully compared to identify the small but important distinction. One possibility is that they differ in the correlation between the extracellular gate and the intracellular gate, leading to or avoiding simultaneous opening of the two gates. Similar comparison should be also applied between Pgp/Sav and CFTR, the channel member in ABC family, to understand the difference in their coupling of ATP hydrolysis with allocrites transport.

6 Bibliography

Accardi, A. & Miller, C., 2004, Secondary active transport mediated by a prokaryotic homologue of ClC Cl- channels, *Nature*, 427(6977), pp. 803-7.

Accardi, A. & Pusch, M., 2003, Conformational changes in the pore of CLC-0, *The Journal of general physiology*, 122(3), pp. 277-93.

Accardi, A., Lobet, S., Williams, C., Miller, C. & Dutzler, R., 2006, Synergism between halide binding and proton transport in a CLC-type exchanger, *Journal of molecular biology*, 362(4), pp. 691-9.

Accardi, A., Walden, M., Nguitragool, W., Jayaram, H., Williams, C. & Miller, C., 2005, Separate ion pathways in a Cl-/H+ exchanger, *The Journal of general physiology*, 126(6), pp. 563-70.

Aleksandrov, A.A., Chang, X., Aleksandrov, L. & Riordan, J.R., 2000, The non-hydrolytic pathway of cystic fibrosis transmembrane conductance regulator ion channel gating, *The Journal of physiology*, 528 Pt 2, pp. 259-65.

Aller, S.G., Yu, J., Ward, A., Weng, Y., Chittaboina, S., Zhuo, R., Harrell, P.M., Trinh, Y.T., Zhang, Q., Urbatsch, I.L. & Chang, G., 2009, Structure of P-glycoprotein reveals a molecular basis for poly-specific drug binding, *Science (New York, N.Y.)*, 323(5922), pp. 1718-22.

Arkin, I.T., Xu, H., Jensen, M.Ø., Arbely, E., Bennett, E.R., Bowers, K.J., Chow, E., Dror, R.O., Eastwood, M.P., Flitman-Tene, R., Gregersen, B.A., Klepeis, J.L., Kolossváry, I., Shan, Y. & Shaw, D.E., 2007, Mechanism of Na+/H+ antiporting, *Science (New York, N.Y.)*, 317(5839), pp. 799-803.

Azzaria, M., Schurr, E. & Gros, P., 1989, Discrete mutations introduced in the predicted nucleotide-binding sites of the mdr1 gene abolish its ability to confer multidrug resistance, *Molecular and cellular biology*, 9(12), pp. 5289-97.

Bakos, E., Klein, I., Welker, E., Szabó, K., Müller, M., Sarkadi, B. & Váradi, A., 1997, Characterization of the human multidrug resistance protein containing mutations in the ATP-binding cassette signature region, *The Biochemical journal*, 323 (Pt 3), pp. 777-83.

Bell, S.P., Curran, P.K., Choi, S. & Mindell, J.A., 2006, Site-directed fluorescence studies of a prokaryotic ClC antiporter, *Biochemistry*, 45(22), pp. 6773-82.

Berger, H.A., Anderson, M.P., Gregory, R.J., Thompson, S., Howard, P.W., Maurer, R.A., Mulligan, R., Smith, A.E. & Welsh, M.J., 1991, Identification and regulation of the cystic fibrosis transmembrane conductance regulator-generated chloride channel, *The Journal of clinical investigation*, 88(4), pp. 1422-31.

Biasini, M., Mariani, V., Haas, J., Scheuber, S., Schenk, A.D., Schwede, T. & Philippsen, A., 2010, OpenStructure: a flexible software framework for computational structural biology, *Bioinformatics*, 26(20), pp. 2626-8.

Bisset, D., Corry, B. & Chung, S.H., 2005, The fast gating mechanism in ClC-0 channels, *Biophysical journal*, 89(1), pp. 179-86.

Boehr, D.D., Nussinov, R. & Wright, P.E., 2009, The role of dynamic conformational ensembles in biomolecular recognition, *Nature chemical biology*, 5(11), pp. 789-96.

Borbat, P.P., Surendhran, K., Bortolus, M., Zou, P., Freed, J.H. & Mchaourab, H.S., 2007, Conformational motion of the ABC transporter MsbA induced by ATP hydrolysis, *PLoS biology*, 5(10), p. e271.

Borgnia, M.J., Eytan, G.D. & Assaraf, Y.G., 1996, Competition of hydrophobic peptides, cytotoxic drugs, and chemosensitizers on a common P-glycoprotein pharmacophore as revealed by its ATPase activity, *The Journal of biological chemistry*, 271(6), pp. 3163-71.

Brandt, S. & Jentsch, T.J., 1995, ClC-6 and ClC-7 are two novel broadly expressed members of the CLC chloride channel family, *FEBS letters*, 377(1), pp. 15-20.

Brooks, B.R., Brooks, C.L., Mackerell, A.D., Nilsson, L., Petrella, R.J., Roux, B., Won, Y., Archontis, G., Bartels, C., Boresch, S., Caflisch, A., Caves, L., Cui, Q., Dinner, A.R., Feig, M., Fischer, S., Gao, J., Hodoscek, M., Im, W., Kuczera, K., Lazaridis, T., Ma, J., Ovchinnikov, V., Paci, E., Pastor, R.W., Post, C.B., Pu, J.Z., Schaefer, M., Tidor, B., Venable, R.M., Woodcock, H.L., Wu, X., Yang, W., York, D.M. & Karplus, M., 2009, CHARMM: the biomolecular simulation program, *Journal of computational chemistry*, 30(10), pp. 1545-614.

Buchaklian, A.H. & Klug, C.S., 2006, Characterization of the LSGGQ and H motifs from the Escherichia coli lipid A transporter MsbA, *Biochemistry*, 45(41), pp. 12539-46.

Bykova, E.A., Zhang, X.D., Chen, T.Y. & Zheng, J., 2006, Large movement in the C terminus of CLC-0 chloride channel during slow gating, *Nature structural & molecular biology*, 13(12), pp. 1115-9.

Chang, G., 2003, Multidrug resistance ABC transporters, *FEBS letters*, 555(1), pp. 102-5.

Chen, J., Sharma, S., Quiocho, F.A. & Davidson, A.L., 2001, Trapping the transition state of an ATP-binding cassette transporter: evidence for a concerted mechanism of maltose transport, *Proceedings of the National Academy of Sciences of the United States of America*, 98(4), pp. 1525-30.

Chen, M.F. & Chen, T.Y., 2003, Side-chain charge effects and conductance determinants in the pore of ClC-0 chloride channels, *The Journal of general physiology*, 122(2), pp. 133-45.

Chen, T.Y., 2003, Coupling gating with ion permeation in ClC channels, *Science's STKE : signal transduction knowledge environment*, 2003(188), p. pe23.

Chen, T.Y. & Hwang, T.C., 2008, CLC-0 and CFTR: chloride channels evolved from transporters, *Physiological reviews*, 88(2), pp. 351-87.

Chen, T.Y. & Miller, C., 1996, Nonequilibrium gating and voltage dependence of the ClC-0 Cl- channel, *The Journal of general physiology*, 108(4), pp. 237-50.

Chen, T.Y., Chen, M.F. & Lin, C.W., 2003, Electrostatic control and chloride regulation of the fast gating of ClC-0 chloride channels, *The Journal of general physiology*, 122(5), pp. 641-51.

Cheng, M.H., Mamonov, A.B., Dukes, J.W. & Coalson, R.D., 2007, Modeling the fast gating mechanism in the ClC-0 chloride channel, *The journal of physical chemistry. B*, 111(21), pp. 5956-65.

Cheng, S.H., Rich, D.P., Marshall, J., Gregory, R.J., Welsh, M.J. & Smith, A.E., 1991, Phosphorylation of the R domain by cAMP-dependent protein kinase regulates the CFTR chloride channel, *Cell*, 66(5), pp. 1027-36.

Chufan, E.E., Kapoor, K., Sim, H.M., Singh, S., Talele, T.T., Durell, S.R. & Ambudkar, S.V., 2013, Multiple transport-active binding sites are available for a single substrate on human P-glycoprotein (ABCB1), *PloS one*, 8(12), p. e82463.

Crisman, T.J., Qu, S., Kanner, B.I. & Forrest, L.R., 2009, Inward-facing conformation of glutamate transporters as revealed by their inverted-topology structural repeats, *Proceedings of the National Academy of Sciences of the United States of America*, 106(49), pp. 20752-7.

Csermely, P., Palotai, R. & Nussinov, R., 2010, Induced fit, conformational selection and independent dynamic segments: an extended view of binding events, *Trends in biochemical sciences*, 35(10), pp. 539-46.

Davidson, A.L. & Sharma, S., 1997, Mutation of a single MalK subunit severely impairs maltose transport activity in Escherichia coli, *Journal of bacteriology*, 179(17), pp. 5458-64.

Dawson, R.J. & Locher, K.P., 2006, Structure of a bacterial multidrug ABC transporter, *Nature*, 443(7108), pp. 180-5.

Dawson, R.J. & Locher, K.P., 2007, Structure of the multidrug ABC transporter Sav1866 from Staphylococcus aureus in complex with AMP-PNP, *FEBS letters*, 581(5), pp. 935-8.

Dean, M., Rzhetsky, A. & Allikmets, R., 2001, The human ATP-binding cassette (ABC) transporter superfamily, *Genome research*, 11(7), pp. 1156-66.

Devine, S.E., Ling, V. & Melera, P.W., 1992, Amino acid substitutions in the sixth transmembrane domain of P-glycoprotein alter multidrug resistance, *Proceedings of the National Academy of Sciences of the United States of America*, 89(10), pp. 4564-8.

Dey, S., Ramachandra, M., Pastan, I., Gottesman, M.M. & Ambudkar, S.V., 1997, Evidence for two nonidentical drug-interaction sites in the human P-glycoprotein, *Proceedings of the National Academy of Sciences of the United States of America*, 94(20), pp. 10594-9.

Doerrler, W.T., Reedy, M.C. & Raetz, C.R., 2001, An Escherichia coli mutant defective in lipid export, *The Journal of biological chemistry*, 276(15), pp. 11461-4.

Dutzler, R., Campbell, E.B. & MacKinnon, R., 2003, Gating the selectivity filter in ClC chloride channels, *Science (New York, N.Y.)*, 300(5616), pp. 108-12.

Dutzler, R., Campbell, E.B., Cadene, M., Chait, B.T. & MacKinnon, R., 2002, X-ray structure of a ClC chloride channel at 3.0 A reveals the molecular basis of anion selectivity, *Nature*, 415(6869), pp. 287-94.

Elvington, S.M., Liu, C.W. & Maduke, M.C., 2009, Substrate-driven conformational changes in ClC-ec1 observed by fluorine NMR, *The EMBO journal*, 28(20), pp. 3090-102.

Engh, A.M. & Maduke, M., 2005, Cysteine accessibility in ClC-0 supports conservation of the ClC intracellular vestibule, *The Journal of general physiology*, 125(6), pp. 601-17.

Ernst, R., Koch, J., Horn, C., Tampé, R. & Schmitt, L., 2006, Engineering ATPase activity in the isolated ABC cassette of human TAP1, *The Journal of biological chemistry*, 281(37), pp. 27471-80.

Estévez, R., Schroeder, B.C., Accardi, A., Jentsch, T.J. & Pusch, M., 2003, Conservation of chloride channel structure revealed by an inhibitor binding site in ClC-1, *Neuron*, 38(1), pp. 47-59.

Fairman, W.A., Vandenberg, R.J., Arriza, J.L., Kavanaugh, M.P. & Amara, S.G., 1995, An excitatory amino-acid transporter with properties of a ligand-gated chloride channel, *Nature*, 375(6532), pp. 599-603.

Faraldo-Gómez, J.D. & Roux, B., 2004, Electrostatics of ion stabilization in a ClC chloride channel homologue from Escherichia coli, *Journal of molecular biology*, 339(4), pp. 981-1000.

Fong, P., Rehfeldt, A. & Jentsch, T.J., 1998, Determinants of slow gating in ClC-0, the voltage-gated chloride channel of Torpedo marmorata, *The American journal of physiology*, 274(4 Pt 1), pp. C966-73.

Ford, J.M. & Hait, W.N., 1990, Pharmacology of drugs that alter multidrug resistance in cancer, *Pharmacological reviews*, 42(3), pp. 155-99.

Forrest, L.R., Zhang, Y.W., Jacobs, M.T., Gesmonde, J., Xie, L., Honig, B.H. & Rudnick, G., 2008, Mechanism for alternating access in neurotransmitter transporters, *Proceedings of the National Academy of Sciences of the United States of America*, 105(30), pp. 10338-43.

Gadsby, D.C., 2009, Ion channels versus ion pumps: the principal difference, in principle, *Nature reviews. Molecular cell biology*, 10(5), pp. 344-52.

Garrigues, A., Loiseau, N., Delaforge, M., Ferté, J., Garrigos, M., André, F. & Orlowski, S., 2002, Characterization of two pharmacophores on the multidrug transporter P-glycoprotein, *Molecular pharmacology*, 62(6), pp. 1288-98.

Geourjon, C., Orelle, C., Steinfels, E., Blanchet, C., Deléage, G., Di Pietro, A. & Jault, J.M., 2001, A common mechanism for ATP hydrolysis in ABC transporter and helicase superfamilies, *Trends in biochemical sciences*, 26(9), pp. 539-44.

Gervasio, F.L., Parrinello, M., Ceccarelli, M. & Klein, M.L., 2006, Exploring the gating mechanism in the ClC chloride channel via metadynamics, *Journal of molecular biology*, 361(2), pp. 390-8.

Goetz, B.A., Perozo, E. & Locher, K.P., 2009, Distinct gate conformations of the ABC transporter BtuCD revealed by electron spin resonance spectroscopy and chemical cross-linking, *FEBS letters*, 583(2), pp. 266-70.

Gradogna, A., Babini, E., Picollo, A. & Pusch, M., 2010, A regulatory calcium-binding site at the subunit interface of CLC-K kidney chloride channels, *The Journal of general physiology*, 136(3), pp. 311-23.

Gutmann, D.A., Ward, A., Urbatsch, I.L., Chang, G. & van Veen, H.W., 2010, Understanding polyspecificity of multidrug ABC transporters: closing in on the gaps in ABCB1, *Trends in biochemical sciences*, 35(1), pp. 36-42.

Günther, W., Piwon, N. & Jentsch, T.J., 2003, The ClC-5 chloride channel knock-out mouse - an animal model for Dent's disease, *Pflügers Archiv : European journal of physiology*, 445(4), pp. 456-62.

Han, W., Cheng, R.C., Maduke, M.C. & Tajkhorshid, E., 2014, Water access points and hydration pathways in CLC H+/Cl- transporters, *Proceedings of the National Academy of Sciences of the United States of America*, 111(5), pp. 1819-24.

He, L., Aleksandrov, A.A., Serohijos, A.W., Hegedus, T., Aleksandrov, L.A., Cui, L., Dokholyan, N.V. & Riordan, J.R., 2008, Multiple membrane-cytoplasmic domain contacts in the cystic fibrosis transmembrane conductance regulator (CFTR) mediate regulation of channel gating, *The Journal of biological chemistry*, 283(39), pp. 26383-90.

He, L., Denton, J., Nehrke, K. & Strange, K., 2006, Carboxy terminus splice variation alters ClC channel gating and extracellular cysteine reactivity, *Biophysical journal*, 90(10), pp. 3570-81.

Higgins, C.F. & Linton, K.J., 2004, The ATP switch model for ABC transporters, *Nature structural & molecular biology*, 11(10), pp. 918-26.

Hirsh, J.K. & Wu, C.H., 1997, Palytoxin-induced single-channel currents from the sodium pump synthesized by in vitro expression, *Toxicon : official journal of the International Society on Toxinology*, 35(2), pp. 169-76.

Hohl, M., Briand, C., Grütter, M.G. & Seeger, M.A., 2012, Crystal structure of a heterodimeric ABC transporter in its inward-facing conformation, *Nature structural & molecular biology*, 19(4), pp. 395-402.

Hollenstein, K., Dawson, R.J. & Locher, K.P., 2007, Structure and mechanism of ABC transporter proteins, *Current opinion in structural biology*, 17(4), pp. 412-8.

Hopfner, K.P., Karcher, A., Shin, D.S., Craig, L., Arthur, L.M., Carney, J.P. & Tainer, J.A., 2000, Structural biology of Rad50 ATPase: ATP-driven conformational control in DNA double-strand break repair and the ABC-ATPase superfamily, *Cell*, 101(7), pp. 789-800.

Humphrey, W., Dalke, A. & Schulten, K., 1996, VMD: visual molecular dynamics, *Journal of molecular graphics*, 14(1), pp. 33-8, 27-8.

Hung, L.W., Wang, I.X., Nikaido, K., Liu, P.Q., Ames, G.F. & Kim, S.H., 1998, Crystal structure of the ATP-binding subunit of an ABC transporter, *Nature*, 396(6712), pp. 703-7.

Hübner, C.A. & Jentsch, T.J., 2002, Ion channel diseases, *Human molecular genetics*, 11(20), pp. 2435-45.

Iyer, R., Iverson, T.M., Accardi, A. & Miller, C., 2002, A biological role for prokaryotic ClC chloride channels, *Nature*, 419(6908), pp. 715-8.

Janas, E., Hofacker, M., Chen, M., Gompf, S., van der Does, C. & Tampé, R., 2003, The ATP hydrolysis cycle of the nucleotide-binding domain of the mitochondrial ATP-binding cassette transporter Mdl1p, *The Journal of biological chemistry*, 278(29), pp. 26862-9.

Jayaram, H., Accardi, A., Wu, F., Williams, C. & Miller, C., 2008, Ion permeation through a Cl--selective channel designed from a CLC Cl-/H+ exchanger, *Proceedings of the National Academy of Sciences of the United States of America*, 105(32), pp. 11194-9.

Jentsch, T.J., 2008, CLC chloride channels and transporters: from genes to protein structure, pathology and physiology, *Critical reviews in biochemistry and molecular biology*, 43(1), pp. 3-36.

Jentsch, T.J., Friedrich, T., Schriever, A. & Yamada, H., 1999, The CLC chloride channel family, *Pflügers Archiv : European journal of physiology*, 437(6), pp. 783-95.

Jentsch, T.J., Steinmeyer, K. & Schwarz, G., 1990, Primary structure of Torpedo marmorata chloride channel isolated by expression cloning in Xenopus oocytes, *Nature*, 348(6301), pp. 510-4.

Jin, M.S., Oldham, M.L., Zhang, Q. & Chen, J., 2012, Crystal structure of the multidrug transporter P-glycoprotein from Caenorhabditis elegans, *Nature*, 490(7421), pp. 566-9.

Jones, P.M. & George, A.M., 2011, Molecular-dynamics simulations of the ATP/apo state of a multidrug ATP-binding cassette transporter provide a structural and mechanistic basis for the asymmetric occluded state, *Biophysical journal*, 100(12), pp. 3025-34.

Kaback, H.R., Smirnova, I., Kasho, V., Nie, Y. & Zhou, Y., 2011, The alternating access transport mechanism in LacY, *The Journal of membrane biology*, 239(1-2), pp. 85-93.

Karpowich, N., Martsinkevich, O., Millen, L., Yuan, Y.R., Dai, P.L., MacVey, K., Thomas, P.J. & Hunt, J.F., 2001, Crystal structures of the MJ1267 ATP binding cassette reveal an induced-fit effect at the ATPase active site of an ABC transporter, *Structure (London, England : 1993)*, 9(7), pp. 571-86.

Khare, D., Oldham, M.L., Orelle, C., Davidson, A.L. & Chen, J., 2009, Alternating access in maltose transporter mediated by rigid-body rotations, *Molecular cell*, 33(4), pp. 528-36.

Klein, I., Sarkadi, B. & Váradi, A., 1999, An inventory of the human ABC proteins, *Biochimica et biophysica acta*, 1461(2), pp. 237-62.

Kornak, U., Kasper, D., Bösl, M.R., Kaiser, E., Schweizer, M., Schulz, A., Friedrich, W., Delling, G. & Jentsch, T.J., 2001, Loss of the ClC-7 chloride channel leads to osteopetrosis in mice and man, *Cell*, 104(2), pp. 205-15.

Li-Blatter, X. & Seelig, A., 2010, Exploring the P-glycoprotein binding cavity with polyoxyethylene alkyl ethers, *Biophysical journal*, 99(11), pp. 3589-98.

Lim, H.H. & Miller, C., 2009, Intracellular proton-transfer mutants in a CLC Cl-/H+ exchanger, *The Journal of general physiology*, 133(2), pp. 131-8.

Lin, C.W. & Chen, T.Y., 2000, Cysteine modification of a putative pore residue in ClC-0: implication for the pore stoichiometry of ClC chloride channels, *The Journal of general physiology*, 116(4), pp. 535-46.

Lin, C.W. & Chen, T.Y., 2003, Probing the pore of ClC-0 by substituted cysteine accessibility method using methane thiosulfonate reagents, *The Journal of general physiology*, 122(2), pp. 147-59.

Litman, T., Druley, T.E., Stein, W.D. & Bates, S.E., 2001, From MDR to MXR: new understanding of multidrug resistance systems, their properties and clinical significance, *Cellular and molecular life sciences : CMLS*, 58(7), pp. 931-59.

Lísal, J. & Maduke, M., 2008, The ClC-0 chloride channel is a 'broken' Cl-/H+ antiporter, *Nature structural & molecular biology*, 15(8), pp. 805-10.

Locher, K.P., Lee, A.T. & Rees, D.C., 2002, The E. coli BtuCD structure: a framework for ABC transporter architecture and mechanism, *Science (New York, N.Y.)*, 296(5570), pp. 1091-8.

Loo, T.W. & Clarke, D.M., 1993, Functional consequences of phenylalanine mutations in the predicted transmembrane domain of P-glycoprotein, *The Journal of biological chemistry*, 268(27), pp. 19965-72.

Loo, T.W. & Clarke, D.M., 1994a, Mutations to amino acids located in predicted transmembrane segment 6 (TM6) modulate the activity and substrate specificity of human P-glycoprotein, *Biochemistry*, 33(47), pp. 14049-57.

Loo, T.W. & Clarke, D.M., 1994b, Reconstitution of drug-stimulated ATPase activity following co-expression of each half of human P-glycoprotein as separate polypeptides, *The Journal of biological chemistry*, 269(10), pp. 7750-5.

Loo, T.W. & Clarke, D.M., 1997, Drug-stimulated ATPase activity of human P-glycoprotein requires movement between transmembrane segments 6 and 12, *The Journal of biological chemistry*, 272(34), pp. 20986-9.

Loo, T.W. & Clarke, D.M., 2000, The packing of the transmembrane segments of human multidrug resistance P-glycoprotein is revealed by disulfide cross-linking analysis, *The Journal of biological chemistry*, 275(8), pp. 5253-6.

Loo, T.W. & Clarke, D.M., 2001a, Cross-linking of human multidrug resistance P-glycoprotein by the substrate, tris-(2-maleimidoethyl)amine, is altered by ATP hydrolysis. Evidence for rotation of a transmembrane helix, *The Journal of biological chemistry*, 276(34), pp. 31800-5.

Loo, T.W. & Clarke, D.M., 2001b, Determining the dimensions of the drug-binding domain of human P-glycoprotein using thiol cross-linking compounds as molecular rulers, *The Journal of biological chemistry*, 276(40), pp. 36877-80.

Loo, T.W. & Clarke, D.M., 2002, Vanadate trapping of nucleotide at the ATP-binding sites of human multidrug resistance P-glycoprotein exposes different residues to the drug-binding site, *Proceedings of the National Academy of Sciences of the United States of America*, 99(6), pp. 3511-6.

Loo, T.W. & Clarke, D.M., 2008, Mutational analysis of ABC proteins, *Archives of biochemistry and biophysics*, 476(1), pp. 51-64.

Loo, T.W., Bartlett, M.C. & Clarke, D.M., 2003a, Methanethiosulfonate derivatives of rhodamine and verapamil activate human P-glycoprotein at different sites, *The Journal of biological chemistry*, 278(50), pp. 50136-41.

Loo, T.W., Bartlett, M.C. & Clarke, D.M., 2003b, Simultaneous binding of two different drugs in the binding pocket of the human multidrug resistance P-glycoprotein, *The Journal of biological chemistry*, 278(41), pp. 39706-10.

Loo, T.W., Bartlett, M.C. & Clarke, D.M., 2003c, Substrate-induced conformational changes in the transmembrane segments of human P-glycoprotein. Direct evidence for the substrate-induced fit mechanism for drug binding, *The Journal of biological chemistry*, 278(16), pp. 13603-6.

Loo, T.W., Bartlett, M.C., Detty, M.R. & Clarke, D.M., 2012, The ATPase activity of the P-glycoprotein drug pump is highly activated when the N-terminal and central regions of the nucleotide-binding domains are linked closely together, *The Journal of biological chemistry*, 287(32), pp. 26806-16.

Lugo, M.R. & Sharom, F.J., 2005a, Interaction of LDS-751 and rhodamine 123 with P-glycoprotein: evidence for simultaneous binding of both drugs, *Biochemistry*, 44(42), pp. 14020-9.

Lugo, M.R. & Sharom, F.J., 2005b, Interaction of LDS-751 with P-glycoprotein and mapping of the location of the R drug binding site, *Biochemistry*, 44(2), pp. 643-55.

Ma, J.F., Grant, G. & Melera, P.W., 1997, Mutations in the sixth transmembrane domain of P-glycoprotein that alter the pattern of cross-resistance also alter sensitivity to cyclosporin A reversal, *Molecular pharmacology*, 51(6), pp. 922-30.

Maduke, M., Miller, C. & Mindell, J.A., 2000, A decade of CLC chloride channels: structure, mechanism, and many unsettled questions, *Annual review of biophysics and biomolecular structure*, 29, pp. 411-38.

Maegley, K.A., Admiraal, S.J. & Herschlag, D., 1996, Ras-catalyzed hydrolysis of GTP: a new perspective from model studies, *Proceedings of the National Academy of Sciences of the United States of America*, 93(16), pp. 8160-6.

Mao, L., Wang, Y., Liu, Y. & Hu, X., 2004, Molecular determinants for ATP-binding in proteins: a data mining and quantum chemical analysis, *Journal of molecular biology*, 336(3), pp. 787-807.

Martin, C., Berridge, G., Higgins, C.F., Mistry, P., Charlton, P. & Callaghan, R., 2000, Communication between multiple drug binding sites on P-glycoprotein, *Molecular pharmacology*, 58(3), pp. 624-32.

Martin, C., Higgins, C.F. & Callaghan, R., 2001, The vinblastine binding site adopts high- and low-affinity conformations during a transport cycle of P-glycoprotein, *Biochemistry*, 40(51), pp. 15733-42.

Matte, A., Tari, L.W. & Delbaere, L.T., 1998, How do kinases transfer phosphoryl groups? *Structure (London, England : 1993)*, 6(4), pp. 413-9.

Miller, C., 2006, ClC chloride channels viewed through a transporter lens, *Nature*, 440(7083), pp. 484-9.

Miloshevsky, G.V., Hassanein, A. & Jordan, P.C., 2010, Antiport mechanism for Cl(-)/H(+) in ClC-ec1 from normal-mode analysis, *Biophysical journal*, 98(6), pp. 999-1008.

Mohammad-Panah, R., Harrison, R., Dhani, S., Ackerley, C., Huan, L.J., Wang, Y. & Bear, C.E., 2003, The chloride channel ClC-4 contributes to endosomal acidification and trafficking, *The Journal of biological chemistry*, 278(31), pp. 29267-77.

Moody, J.E., Millen, L., Binns, D., Hunt, J.F. & Thomas, P.J., 2002, Cooperative, ATP-dependent association of the nucleotide binding cassettes during the catalytic cycle of ATP-binding cassette transporters, *The Journal of biological chemistry*, 277(24), pp. 21111-4.

Müller, M., Bakos, E., Welker, E., Váradi, A., Germann, U.A., Gottesman, M.M., Morse, B.S., Roninson, I.B. & Sarkadi, B., 1996, Altered drug-stimulated ATPase activity in mutants of the human multidrug resistance protein, *The Journal of biological chemistry*, 271(4), pp. 1877-83.

Naren, A.P., Cormet-Boyaka, E., Fu, J., Villain, M., Blalock, J.E., Quick, M.W. & Kirk, K.L., 1999, CFTR chloride channel regulation by an interdomain interaction, *Science*, 286(5439), pp. 544-8.

Nguitragool, W. & Miller, C., 2006, Uncoupling of a CLC Cl-/H+ exchange transporter by polyatomic anions, *Journal of molecular biology*, 362(4), pp. 682-90.

Nikaido, K. & Ames, G.F., 1999, One intact ATP-binding subunit is sufficient to support ATP hydrolysis and translocation in an ABC transporter, the histidine permease, *The Journal of biological chemistry*, 274(38), pp. 26727-35.

Oancea, G., O'Mara, M.L., Bennett, W.F., Tieleman, D.P., Abele, R. & Tampé, R., 2009, Structural arrangement of the transmission interface in the antigen ABC transport complex TAP, *Proceedings of the National Academy of Sciences of the United States of America*, 106(14), pp. 5551-6.

O'Neill, G.P., Grygorczyk, R., Adam, M. & Ford-Hutchinson, A.W., 1991, The nucleotide sequence of a voltage-gated chloride channel from the electric organ of Torpedo californica, *Biochimica et biophysica acta*, 1129(1), pp. 131-4.

Orelle, C., Alvarez, F.J., Oldham, M.L., Orelle, A., Wiley, T.E., Chen, J. & Davidson, A.L., 2010, Dynamics of alpha-helical subdomain rotation in the intact maltose ATP-binding cassette transporter, *Proceedings of the National Academy of Sciences of the United States of America*, 107(47), pp. 20293-8.

Orelle, C., Ayvaz, T., Everly, R.M., Klug, C.S. & Davidson, A.L., 2008, Both maltose-binding protein and ATP are required for nucleotide-binding domain closure in the intact maltose ABC transporter, *Proceedings of the National Academy of Sciences of the United States of America*, 105(35), pp. 12837-42.

Ostedgaard, L.S., Rich, D.P., DeBerg, L.G. & Welsh, M.J., 1997, Association of domains within the cystic fibrosis transmembrane conductance regulator, *Biochemistry*, 36(6), pp. 1287-94.

Oswald, C., Holland, I.B. & Schmitt, L., 2006, The motor domains of ABC-transporters. What can structures tell us? *Naunyn-Schmiedeberg's archives of pharmacology*, 372(6), pp. 385-99.

Pagant, S., Brovman, E.Y., Halliday, J.J. & Miller, E.A., 2008, Mapping of interdomain interfaces required for the functional architecture of Yor1p, a eukaryotic ATP-binding cassette (ABC) transporter, *The Journal of biological chemistry*, 283(39), pp. 26444-51.

Phillips, S., Brammer, A.E., Rodriguez, L., Lim, H.H., Stary-Weinzinger, A. & Matulef, K., 2012, Surprises from an unusual CLC homolog, *Biophysical journal*, 103(9), pp. L44-6.

Picollo, A. & Pusch, M., 2005, Chloride/proton antiporter activity of mammalian CLC proteins ClC-4 and ClC-5, *Nature*, 436(7049), pp. 420-3.

Picollo, A., Malvezzi, M., Houtman, J.C. & Accardi, A., 2009, Basis of substrate binding and conservation of selectivity in the CLC family of channels and transporters, *Nature structural & molecular biology*, 16(12), pp. 1294-301.

Picollo, A., Xu, Y., Johner, N., Bernèche, S. & Accardi, A., 2012, Synergistic substrate binding determines the stoichiometry of transport of a prokaryotic H(+)/Cl(-) exchanger, *Nature structural & molecular biology*, 19(5), pp. 525-31, S1.

Pohl, A., Devaux, P.F. & Herrmann, A., 2005, Function of prokaryotic and eukaryotic ABC proteins in lipid transport, *Biochimica et biophysica acta*, 1733(1), pp. 29-52.

Procko, E., O'Mara, M.L., Bennett, W.F., Tieleman, D.P. & Gaudet, R., 2009, The mechanism of ABC transporters: general lessons from structural and functional studies of an antigenic peptide transporter, *FASEB journal : official publication of the Federation of American Societies for Experimental Biology*, 23(5), pp. 1287-302.

Pusch, M., Ludewig, U. & Jentsch, T.J., 1997, Temperature dependence of fast and slow gating relaxations of ClC-0 chloride channels, *The Journal of general physiology*, 109(1), pp. 105-16.

Pusch, M., Ludewig, U., Rehfeldt, A. & Jentsch, T.J., 1995, Gating of the voltage-dependent chloride channel CIC-0 by the permeant anion, *Nature*, 373(6514), pp. 527-31.

Radestock, S. & Forrest, L.R., 2011, The alternating-access mechanism of MFS transporters arises from inverted-topology repeats, *Journal of molecular biology*, 407(5), pp. 698-715.

Ramjeesingh, M., Li, C., She, Y.M. & Bear, C.E., 2006, Evaluation of the membrane-spanning domain of ClC-2, *The Biochemical journal*, 396(3), pp. 449-60.

Redondo, J., Fiedler, B. & Scheiner-Bobis, G., 1996, Palytoxin-induced Na+ influx into yeast cells expressing the mammalian sodium pump is due to the formation of a channel within the enzyme, *Molecular pharmacology*, 49(1), pp. 49-57.

Rich, D.P., Gregory, R.J., Anderson, M.P., Manavalan, P., Smith, A.E. & Welsh, M.J., 1991, Effect of deleting the R domain on CFTR-generated chloride channels, *Science*, 253(5016), pp. 205-7.

Richard, E.A. & Miller, C., 1990, Steady-state coupling of ion-channel conformations to a transmembrane ion gradient, *Science*, 247(4947), pp. 1208-10.

Riordan, J.R., Rommens, J.M., Kerem, B., Alon, N., Rozmahel, R., Grzelczak, Z., Zielenski, J., Lok, S., Plavsic, N. & Chou, J.L., 1989, Identification of the cystic fibrosis gene: cloning and characterization of complementary DNA, *Science*, 245(4922), pp. 1066-73.

Robertson, J.L., Kolmakova-Partensky, L. & Miller, C., 2010, Design, function and structure of a monomeric ClC transporter, *Nature*, 468(7325), pp. 844-7.

Rosenberg, M.F., Velarde, G., Ford, R.C., Martin, C., Berridge, G., Kerr, I.D., Callaghan, R., Schmidlin, A., Wooding, C., Linton, K.J. & Higgins, C.F., 2001, Repacking of the transmembrane domains of P-glycoprotein during the transport ATPase cycle, *The EMBO journal*, 20(20), pp. 5615-25.

Rothnie, A., Storm, J., Campbell, J., Linton, K.J., Kerr, I.D. & Callaghan, R., 2004, The topography of transmembrane segment six is altered during the catalytic cycle of P-glycoprotein, *The Journal of biological chemistry*, 279(33), pp. 34913-21.

Ryan, R.M. & Mindell, J.A., 2007, The uncoupled chloride conductance of a bacterial glutamate transporter homolog, *Nature structural & molecular biology*, 14(5), pp. 365-71.

Sarkadi, B., Müller, M., Homolya, L., Holló, Z., Seprödi, J., Germann, U.A., Gottesman, M.M., Price, E.M. & Boucher, R.C., 1994, Interaction of bioactive hydrophobic peptides with the human multidrug transporter, *FASEB journal : official publication of the Federation of American Societies for Experimental Biology*, 8(10), pp. 766-70.

Scheiner-Bobis, G., Meyer zu Heringdorf, D., Christ, M. & Habermann, E., 1994, Palytoxin induces K+ efflux from yeast cells expressing the mammalian sodium pump, *Molecular pharmacology*, 45(6), pp. 1132-6.

Seeger, M.A. & van Veen, H.W., 2009, Molecular basis of multidrug transport by ABC transporters, *Biochimica et biophysica acta*, 1794(5), pp. 725-37.

Seelig, A., 1998a, A general pattern for substrate recognition by P-glycoprotein, *European journal of biochemistry / FEBS*, 251(1-2), pp. 252-61.

Seelig, A., 1998b, How does P-glycoprotein recognize its substrates? *International journal of clinical pharmacology and therapeutics*, 36(1), pp. 50-4.

Senior, A.E., al-Shawi, M.K. & Urbatsch, I.L., 1995, The catalytic cycle of P-glycoprotein, *FEBS letters*, 377(3), pp. 285-9.

Serohijos, A.W., Hegedus, T., Aleksandrov, A.A., He, L., Cui, L., Dokholyan, N.V. & Riordan, J.R., 2008, Phenylalanine-508 mediates a cytoplasmic-membrane domain contact in the CFTR 3D structure crucial to assembly and channel function, *Proceedings of the National Academy of Sciences of the United States of America*, 105(9), pp. 3256-61.

Shapiro, A.B. & Ling, V., 1997, Positively cooperative sites for drug transport by P-glycoprotein with distinct drug specificities, *European journal of biochemistry / FEBS*, 250(1), pp. 130-7.

Shapiro, A.B., Fox, K., Lam, P. & Ling, V., 1999, Stimulation of P-glycoprotein-mediated drug transport by prazosin and progesterone. Evidence for a third drug-binding site, *European journal of biochemistry / FEBS*, 259(3), pp. 841-50.

Sharom, F.J., 1997, The P-glycoprotein efflux pump: how does it transport drugs? *The Journal of membrane biology*, 160(3), pp. 161-75.

Sharom, F.J., DiDiodato, G., Yu, X. & Ashbourne, K.J., 1995, Interaction of the P-glycoprotein multidrug transporter with peptides and ionophores, *The Journal of biological chemistry*, 270(17), pp. 10334-41.

Shintre, C.A., Pike, A.C., Li, Q., Kim, J.I., Barr, A.J., Goubin, S., Shrestha, L., Yang, J., Berridge, G., Ross, J., Stansfeld, P.J., Sansom, M.S., Edwards, A.M., Bountra, C., Marsden, B.D., von Delft, F., Bullock, A.N., Gileadi, O., Burgess-Brown, N.A. & Carpenter, E.P., 2013, Structures of ABCB10, a human ATP-binding cassette transporter in apo- and nucleotide-bound states, *Proceedings of the National Academy of Sciences of the United States of America*, 110(24), pp. 9710-5.

Smart, O.S., Neduvelil, J.G., Wang, X., Wallace, B.A. & Sansom, M.S., 1996, HOLE: a program for the analysis of the pore dimensions of ion channel structural models, *Journal of molecular graphics*, 14(6), pp. 354-60, 376.

Smith, P.C., Karpowich, N., Millen, L., Moody, J.E., Rosen, J., Thomas, P.J. & Hunt, J.F., 2002, ATP binding to the motor domain from an ABC transporter drives formation of a nucleotide sandwich dimer, *Molecular cell*, 10(1), pp. 139-49.

Song, J. & Melera, P.W., 2001, Further characterization of the sixth transmembrane domain of Pgp1 by site-directed mutagenesis, *Cancer chemotherapy and pharmacology*, 48(5), pp. 339-46.

Stobrawa, S.M., Breiderhoff, T., Takamori, S., Engel, D., Schweizer, M., Zdebik, A.A., Bösl, M.R., Ruether, K., Jahn, H., Draguhn, A., Jahn, R. & Jentsch, T.J., 2001, Disruption of ClC-3, a chloride channel expressed on synaptic vesicles, leads to a loss of the hippocampus, *Neuron*, 29(1), pp. 185-96.

Storm, J., Modok, S., O'Mara, M.L., Tieleman, D.P., Kerr, I.D. & Callaghan, R., 2008, Cytosolic region of TM6 in P-glycoprotein: topographical analysis and functional perturbation by site directed labeling, *Biochemistry*, 47(12), pp. 3615-24.

St-Pierre, J.F., Bunker, A., Róg, T., Karttunen, M. & Mousseau, N., 2012, Molecular dynamics simulations of the bacterial ABC transporter SAV1866 in the closed form, *The journal of physical chemistry. B*, 116(9), pp. 2934-42.

Tan, B., Piwnica-Worms, D. & Ratner, L., 2000, Multidrug resistance transporters and modulation, *Current opinion in oncology*, 12(5), pp. 450-8.

Tombline, G., Bartholomew, L., Gimi, K., Tyndall, G.A. & Senior, A.E., 2004a, Synergy between conserved ABC signature Ser residues in P-glycoprotein catalysis, *The Journal of biological chemistry*, 279(7), pp. 5363-73.

Tombline, G., Bartholomew, L.A., Tyndall, G.A., Gimi, K., Urbatsch, I.L. & Senior, A.E., 2004b, Properties of P-glycoprotein with mutations in the "catalytic carboxylate" glutamate residues, *The Journal of biological chemistry*, 279(45), pp. 46518-26.

Tombline, G., Bartholomew, L.A., Urbatsch, I.L. & Senior, A.E., 2004c, Combined mutation of catalytic glutamate residues in the two nucleotide binding domains

of P-glycoprotein generates a conformation that binds ATP and ADP tightly, *The Journal of biological chemistry*, 279(30), pp. 31212-20.

Tzingounis, A.V. & Wadiche, J.I., 2007, Glutamate transporters: confining runaway excitation by shaping synaptic transmission, *Nature reviews. Neuroscience*, 8(12), pp. 935-47.

Urbatsch, I.L., Gimi, K., Wilke-Mounts, S. & Senior, A.E., 2000a, Investigation of the role of glutamine-471 and glutamine-1114 in the two catalytic sites of P-glycoprotein, *Biochemistry*, 39(39), pp. 11921-7.

Urbatsch, I.L., Julien, M., Carrier, I., Rousseau, M.E., Cayrol, R. & Gros, P., 2000b, Mutational analysis of conserved carboxylate residues in the nucleotide binding sites of P-glycoprotein, *Biochemistry*, 39(46), pp. 14138-49.

Vandenberg, R.J., Huang, S. & Ryan, R.M., 2008, Slips, leaks and channels in glutamate transporters, *Channels (Austin, Tex.)*, 2(1), pp. 51-8.

van Helvoort, A., Smith, A.J., Sprong, H., Fritzsche, I., Schinkel, A.H., Borst, P. & van Meer, G., 1996, MDR1 P-glycoprotein is a lipid translocase of broad specificity, while MDR3 P-glycoprotein specifically translocates phosphatidylcholine, *Cell*, 87(3), pp. 507-17.

Velamakanni, S., Yao, Y., Gutmann, D.A. & van Veen, H.W., 2008, Multidrug transport by the ABC transporter Sav1866 from Staphylococcus aureus, *Biochemistry*, 47(35), pp. 9300-8.

Verdon, G., Albers, S.V., Dijkstra, B.W., Driessen, A.J. & Thunnissen, A.M., 2003, Crystal structures of the ATPase subunit of the glucose ABC transporter from Sulfolobus solfataricus: nucleotide-free and nucleotide-bound conformations, *Journal of molecular biology*, 330(2), pp. 343-58.

Vergani, P., Nairn, A.C. & Gadsby, D.C., 2003, On the mechanism of MgATP-dependent gating of CFTR Cl- channels, *The Journal of general physiology*, 121(1), pp. 17-36.

Verhalen, B. & Wilkens, S., 2011, P-glycoprotein retains drug-stimulated ATPase activity upon covalent linkage of the two nucleotide binding domains at their C-terminal ends, *The Journal of biological chemistry*, 286(12), pp. 10476-82.

Verhalen, B., Ernst, S., Börsch, M. & Wilkens, S., 2012, Dynamic ligand-induced conformational rearrangements in P-glycoprotein as probed by fluorescence resonance energy transfer spectroscopy, *The Journal of biological chemistry*, 287(2), pp. 1112-27.

Wadiche, J.I. & Kavanaugh, M.P., 1998, Macroscopic and microscopic properties of a cloned glutamate transporter/chloride channel, *The Journal of neuroscience : the official journal of the Society for Neuroscience*, 18(19), pp. 7650-61.

Walden, M., Accardi, A., Wu, F., Xu, C., Williams, C. & Miller, C., 2007, Uncoupling and turnover in a Cl-/H+ exchange transporter, *The Journal of general physiology*, 129(4), pp. 317-29.

Wang, C., Karpowich, N., Hunt, J.F., Rance, M. & Palmer, A.G., 2004, Dynamics of ATP-binding cassette contribute to allosteric control, nucleotide binding and energy transduction in ABC transporters, *Journal of molecular biology*, 342(2), pp. 525-37.

Ward, A., Reyes, C.L., Yu, J., Roth, C.B. & Chang, G., 2007, Flexibility in the ABC transporter MsbA: Alternating access with a twist, *Proceedings of the National Academy of Sciences of the United States of America*, 104(48), pp. 19005-10.

Wellhauser, L., Luna-Chavez, C., D'Antonio, C., Tainer, J. & Bear, C.E., 2011, ATP induces conformational changes in the carboxyl-terminal region of ClC-5, *The Journal of biological chemistry*, 286(8), pp. 6733-41.

Wojtas-Niziurski, W., Meng, Y., Roux, B. & Bernèche, S., 2013, Self-Learning Adaptive Umbrella Sampling Method for the Determination of Free Energy Landscapes in Multiple Dimensions, *Journal of chemical theory and computation*, 9(4), pp. 1885-95.

Wu, W., Rychkov, G.Y., Hughes, B.P. & Bretag, A.H., 2006, Functional complementation of truncated human skeletal-muscle chloride channel (hClC-1) using carboxyl tail fragments, *The Biochemical journal*, 395(1), pp. 89-97.

Yamada, T., Bhate, M.P. & Strange, K., 2013, Regulatory phosphorylation induces extracellular conformational changes in a CLC anion channel, *Biophysical journal*, 104(9), pp. 1893-904.

Yang, R., Hou, Y.X., Campbell, C.A., Palaniyandi, K., Zhao, Q., Bordner, A.J. & Chang, X.B., 2011, Glutamine residues in Q-loops of multidrug resistance protein MRP1 contribute to ATP binding via interaction with metal cofactor, *Biochimica et biophysica acta*, 1808(7), pp. 1790-6.

Yin, J., Kuang, Z., Mahankali, U. & Beck, T.L., 2004, Ion transit pathways and gating in ClC chloride channels, *Proteins*, 57(2), pp. 414-21.

Zaitseva, J., Jenewein, S., Jumpertz, T., Holland, I.B. & Schmitt, L., 2005, H662 is the linchpin of ATP hydrolysis in the nucleotide-binding domain of the ABC transporter HlyB, *The EMBO journal*, 24(11), pp. 1901-10.

Zhou, Z., White, K.A., Polissi, A., Georgopoulos, C. & Raetz, C.R., 1998, Function of Escherichia coli MsbA, an essential ABC family transporter, in lipid A and phospholipid biosynthesis, *The Journal of biological chemistry*, 273(20), pp. 12466-75.

Zolnerciks, J.K., Wooding, C. & Linton, K.J., 2007, Evidence for a Sav1866-like architecture for the human multidrug transporter P-glycoprotein, *FASEB journal : official publication of the Federation of American Societies for Experimental Biology*, 21(14), pp. 3937-48.